Fermentation-induced gelation of pea protein: molecular interactions and rheological properties

vorgelegt von
M.Sc.
Martina Stephanie Klost
ORCID: 0000-0001-7131-6406

an der Fakultät III – Prozesswissenschaften
der Technischen Universität Berlin
zur Erlangung des akademischen Grades

Doktorin der Ingenieurswissenschaften
– Dr.-Ing. –

genehmigte Dissertation

Promotionsausschuss:
Vorsitzende: Prof. Dr. Claudia Fleck
Gutachter: Prof. Dr. Stephan Drusch
Gutachter: Prof. Dr. Leonard Sagis
Gutachterin: Prof. Dr. Anja Maria Wagemans

Tag der wissenschaftlichen Aussprache: 20. Januar 2021

Berlin 2021

Dedicated to all those, who would have been pleased
but are not with me anymore.

Kurzfassung

Bedingt durch die steigende Lebenserwartung nimmt auch der Anteil nicht übertragbarer, sogenannter altersbedingter Krankheiten zu. Neben einer ausreichenden Aufnahme von Ballaststoffen und ungesättigten Fettsäuren ist der Verzehr von pflanzlichen Proteinen ein vielversprechender Ansatz, diesen Krankheiten entgegenzuwirken. Um die gewünschten Effekte zu erzielen, ist es notwendig, Produkte mit hohem Proteingehalt zu entwickeln, die gleichzeitig eine hohe Verbraucherakzeptanz aufweisen und das Potential haben, mit weiteren ernährungsphysiologisch wünschenswerten Komponenten angereichert zu werden. Eine Produktkategorie, die diese Anforderungen erfüllt, sind joghurtartige Gele. Während es in diesem Bereich bereits eine große Auswahl an Produkten auf der Basis von Sojaprotein gibt, sind Produkte aus Erbsenprotein noch weitestgehend unterrepräsentiert, obwohl die Erbse deutschlandweit die höchsten Erntemengen aller Proteinpflanzen abwirft. Darüber hinaus gibt es bislang noch keinerlei Literaturangaben zur fermentativen Gelbildung von Erbsenprotein. Vor diesem Hintergrund war das Ziel dieser Arbeit, die physiko-chemischen Eigenschaften von Erbsenprotein und Erbsenproteinhydrolysaten zu charakterisieren, um die zugrunde liegenden Mechanismen ihrer Gelbildungseigenschaften in fermentativ hergestellten Gelen und an der Öl-Wasser-Grenzfläche zu verstehen und anschließend zu verwenden, um sowohl die Textur- als auch den Nährstoffgehalt anpassen zu können.

Die Ergebnisse zeigten die Fähigkeit von Erbsenprotein, sowohl durch Fermentation als auch an der Öl-Wasser-Grenzfläche Netzwerkstrukturen auszubilden. Bei der fermentativen Gelbildung geschah dies in einem zweistufigen Prozess: (1) Ausbildung einer porösen Netzwerkstruktur durch elektrostatische Interaktionen zwischen dem Legumin-β und dem Vicilin, (2) Kondensation weiterer Legumin-Aggregate über hydrophobe Wechselwirkungen nahe am isoelektrischen Punkt des Legumins. Durch eine enzymatische Hydrolyse mit Trypsin wurden die elektrostatischen Wechselwirkungen zwischen dem Legumin-β und dem Vicilin verstärkt und alle bedeutenden Proteinfraktionen in die Netzwerkstruktur integriert. Diese Ergebnisse wurden auf Proteinnetzwerke an der Öl-Wasser-Grenzfläche übertragen, wo der Anstieg der Gelstärke durch eine Hydrolyse mit Trypsin und die Abnahme der Desorption des Proteins von der Grenzfläche ebenfalls auf eine vollständigere Einbindung aller Proteinfraktionen in das Netzwerk hindeuten. Nachfolgend wurden die Erkenntnisse zum Verhalten des Erbsenproteins an der Grenzfläche genutzt, um die fermentativ gebildeten Gele mit ernährungsphysiologisch wertvollem Öl mit einem hohen Anteil an ungesättigten Fettsäuren anzureichern. Eine zusätzliche Anreicherung mit Ballaststoffen führte zu einem Anstieg des komplexen Schubmoduls |G*| und wurde auf eine Zunahme der relativen Proteinkonzentration zurückgeführt. Der Einfluss der Proteinkonzentration auf die rheologischen Eigenschaften von fermentativ gebildeten Erbsenproteingelen wurde im Weiteren durch eine gezielte Variation des Verhältnisses zwischen löslichen und unlöslichen Proteinfraktionen bei gleichbleibendem absoluten Proteingehalt eingesetzt, um rheologische Eigenschaften zu erzielen, die von joghurtartig zu nahezu pastös reichten.

Abstract

In the context of increasing life expectancy, the consumption of plant-derived proteins – along with a sufficient intake of dietary fibre and unsaturated fatty acids – can contribute to the prevention of age-related non-communicable diseases. In this context, it is important to create products with high protein contents and the potential for further fortification that will be well accepted by consumers. One type of products that meets these requirements are yoghurt-type gels. While a wide range of soy products already exists on the market, pea protein, the most harvested protein crop in Germany, is vastly underutilised and no literature exists on the fermentation-induced gelation of this raw material. Therefore, in this thesis physico-chemical properties of pea protein and pea protein hydrolysates were characterised and connected to fermentation-induced and interfacial gelation of pea protein in order to understand the underlying mechanisms and to subsequently customise texture and nutritional properties.

Results showed the general ability of pea protein to form interfacial and fermentation-induced network structures. Fermentation-induced bulk gelation was found to be a two-step process that involved the formation of an overall percolating network structure via electrostatic interactions between the legumin-β and vicilin fractions, followed by condensation of smaller legumin aggregates that further stabilised the primary network structure via hydrophobic interactions at pH values close to the isoelectric point of legumin. Enzymatic hydrolysis with trypsin was found to enhance the electrostatic interactions between legumin-β and vicilin thus incorporating all major protein fractions into the gel structure. These results were transferred to interfacial networks at the oil-water interface, where tryptic hydrolysis led to increased gel strength and a decrease of protein desorption from the interface, thus also indicating a more complete incorporation of all protein fractions into the interfacial network structure. As a result, knowledge on interfacial behaviour of pea protein at the oil-water interface could be applied to fortify fermentation-induced bulk gels with nutritionally valuable oil high in unsaturated fatty acids. Additional nutritional fortification with dietary fibre led to an increase in the complex shear modulus |G*| which was ascribed to the increase in the relative protein concentration owing to water immobilisation by the fibre. The influence of protein concentration on rheological properties was subsequently utilised to customise the storage modulus in unfortified fermentation-induced bulk gels with constant protein content by influencing the ratio of soluble to insoluble protein fractions. Results ranged from rheological properties close to commercial milk-based yoghurts to very thick gels, and contributed to the general understanding of fermentation-induced gelation properties of pea protein.

Table of contents

Kurzfassung i
Abstract iii
Table of contents iv
List of figures vi
List of tables x
List of abbreviations and symbols xii
Motivation and Objectives 1
Theoretical background 7
Composition and molecular structure of pea protein 7
Specific cleaving behaviour of selected enzymes as a prerequisite for enzymatic hydrolysis of pea protein 11
Characterisation of molecular and physico-chemical properties of proteins 12
Protein solubility and aggregation behaviour 14
Gelation properties of proteins in general – and pea protein and pea protein hydrolysates specifically – in bulk and at the oil-water interface 14
Manuscript I: 19
Functionalisation of pea protein by tryptic hydrolysis – characterisation of interfacial and functional properties 19
Abstract 20
I 1 Introduction 20
I 2 Materials and methods 21
I 3 Results and Discussion 24
I 4 Conclusions 29
Manuscript II: 31
Structure formation and rheological properties of pea protein-based gels 31
Abstract 32
II 1 Introduction 32
II 2 Materials and methods 34
II 3 Results and Discussion 38
II 4 Conclusions 46

Manuscript III: 49
Enzymatic hydrolysis of pea protein: Interactions and protein fractions involved in fermentation induced gels and their influence on rheological properties 49
Abstract 50
III 1 Introduction 50
III 2 Materials and methods 53
III 3 Results and Discussion 56
III 4 Conclusions 64
Manuscript IV: 67
Effect of protein aggregation on rheological properties of pea protein gels 67
Abstract 68
IV 1 Introduction 68
IV 2 Materials and methods 70
IV 3 Results and discussion 75
IV 4 Conclusions 86
General discussion 89
Characterisation of molecular and physico-chemical properties of pea protein and pea protein hydrolysates 89
Elucidation and understanding of gelation kinetics and gel network properties of pea protein and pea protein hydrolysates based on molecular interactions in bulk and at the oil-water interface. 91
Application of the obtained knowledge on molecular, physico-chemical and gelation properties of pea protein and pea protein hydrolysates towards the modification of texture and nutritional characteristics of fermentation-induced pea protein gels 94
Concluding remarks and outlook 97
Acknowledgements 99
References 101
Appendix 120
Supplementary material to Manuscript II 120
Supplementary material to Manuscript IV 124
Unpublished data from Manuscript III 126

List of figures

Fig 1 Pea protein fractions and their specific molecular parameters as derived from literature (Bown et al., 1988; Croy et al., 1979; Croy, Gatehouse, Evans, et al., 1980; Croy, Gatehouse, Tyler, et al., 1980; Gatehouse et al., 1981, 1982, 1983; Gruen et al., 1987; Higgins et al., 1986; Lycett et al., 1983) 7

Fig 2 Amino acid sequence of legumin divided into signal peptide (black), legumin α (blue) and legumin β (red) including disulphide bonds (arrows) and amino acids susceptible to tryptic hydrolysis (printed in bold) or hydrolysis by Alcalase® (printed in italics). (https://www.Uniprot.Org/Uniprot/P02857, n.d.) 8

Fig 3 Amino acid sequence of vicilin divided into signal peptide (black), α-fraction (grey), β-fraction (blue) and γ-fraction (red) including disulphide bonds (arrows) and amino acids susceptible to tryptic hydrolysis (printed in bold) or hydrolysis by Alcalase® (printed in italics). (https://www.Uniprot.Org/Uniprot/P13918, n.d.) 9

Fig 4 Amino acid sequence of convicilin, amino acids susceptible to tryptic hydrolysis are printed in bold and amino acids susceptible to hydrolysis by Alcalase® are printed in italics (https://www.Uniprot.Org/Uniprot/P13915, n.d.). 10

Fig 5 Relationship between intrinsic and extrinsic factors relevant to this thesis and selected functional properties of pea protein (schematic drawing) 12

Fig I 1 molecular weight distribution of PPC and PPH DH2 and DH 4 as shown in a) SDS-page and b) SEC-chromatography 24

Fig I 2 solubility profiles of pea protein concentrate and corresponding hydrolysates in dependence of pH-value 25

Fig I 3 ζ-potential profiles of pea protein concentrate and corresponding hydrolysates in dependence of pH-value 25

Fig I 4 a) oil-droplet size distribution and absolute values of ζ-potential and b) selected microscopic pictures for PPC 27

Fig I 5 oil-droplet size distribution and absolute values of ζ-potential for a) DH 2 and b) DH 4 27

Fig I 6 a) |Gi*|12h, b) E*|30min, c) | tan δ12h and d) slope of the frequency sweeps from dilatational experiments 28

Fig II 1 change in intrinsic fluorescence (a) and complex viscosity (|η*|) (b) induced by heating 10% pea protein to 60 and 80 °C. (|η*| closed line, T dashed line) 38

Fig II 2 development of pH (a) and complex shear modulus |G*| (b) over time and |G*| over pH (c) during the fermentation process of samples containing oil and fibre. Development of the parameters (closed lines) is shown alongside their first derivations (dashed lines). Curves for all samples are provided in supplementary material (Appendix Fig A 1, Fig A 2 and Fig A 3) 39

Fig II 3 SEM images of fermented pea protein gels. SEM of pea protein only at 300-fold (a) and 3000-fold (b) magnification, SEM of pea protein supplemented with fibre at 300-fold (c) and supplemented with oil at 3000-fold (d) magnification. 42

Fig II 4 rheological properties of fermented pea protein gels after 24-30 h storage (6 °C). Thixotropy test (a), amplitude sweep (b) and frequency sweep (c) of samples containing oil and fibre (■ G', □ G'', ▲ |η*|). Curves for all samples are provided in supplementary material (Appendix Fig A 5, Fig A 6 and Fig A 7) 44

Fig III 1 pea protein hydrolysates obtained by enzymatic hydrolysis with Protamex®, trypsin and Alcalase® determined by SDS-PAGE under reducing conditions. 56

Fig III 2 Gel solubility of gels prepared from pea protein and pea protein hydrolysates obtained by enzymatic hydrolysis with Protamex® and trypsin in different solvents. (H_2O=distilled water, PG=propylene glycol, NaCl=sodium chloride, DTT= dithiothreitol, SDS= sodium dodecyl sulfate). Error bars represent the standard deviations of triplicate determinations. 58

Fig III 3 Molecular weight distribution of supernatants from gel solubility experiments in H_2O, NaCl and SDS of gels from pea protein (a) and pea protein hydrolysates obtained by enzymatic hydrolysis with Protamex® (b) and trypsin (c) determined by SDS-PAGE under reducing conditions. (con = convicilin, vic = vicilin, leg = legumin) 59

Fig III 5 Storage modulus G' and loss modulus G'' from Frequency- (a) and amplitude- (b) sweeps of fully set of gels prepared from pea protein and pea protein hydrolysates obtained by enzymatic hydrolysis with Protamex® and trypsin 62

Fig III 6 Lissajous plots of fully set of gels prepared from pea protein and pea protein hydrolysates obtained by enzymatic hydrolysis with Protamex® and trypsin: (a) elastic curves of stress τ versus strain γ, (b) viscous curves of stress τ versus shear rate γ. 63

Fig III 7 Shear stiffening ratio (S-factor) (a) and shear thickening ratio (T-factor) (b) of gels prepared from pea protein and pea protein hydrolysates obtained by enzymatic hydrolysis with Protamex® and trypsin. 63

Fig IV 1 flow chart of experimental setup 71

Fig IV 2 SDS-PAGE under reducing and non-reducing conditions (a) and SEC (b) of pea protein heated at pH 6 to 8. 78

Fig IV 3 CLSM micrographs of fermentation induced pea protein gels made from pea protein slurry pre-treated at pH 6.0 to 8.0. pH values during heating are noted in the upper left-hand corner of the micrographs. 81

Fig IV 4 amplitude sweeps of fermentation induced pea protein gels made from pea protein pre-treated at pH 6.0 to 8.0 at intercycle strain amplitudes γ0 between 0.1% and 1010% and a frequency of 1 s-1. (a) top row: storage and loss modulus G' and G'' over, γ0, (a) middle row: dissipation ratio φ over γ0, (a) bottom row: stiffening ratio (S-factor) over γ0, (b): elastic Lissajous plots, (c) elastic stress. 83

Fig A 1 development of pH (a) over time during the fermentation process of samples containing protein only (a), protein and oil (b), protein and fibre (c) and protein, oil and fibre (d). Development of the parameters (closed lines) is shown alongside their first derivations (dashed lines). 120

Fig A 2 development of complex shear modulus |G*| over time during the fermentation process of samples containing protein only (a), protein and oil (b), protein and fibre (c) and protein, oil and fibre (d). Development of the parameters (closed lines) is shown alongside their first derivations (dashed lines). 121

Fig A 3 development of |G*| over pH during the fermentation process of samples containing protein only (a), protein and oil (b), protein and fibre (c) and protein, oil and fibre (d). Development of the parameters (closed lines) is shown alongside their first derivations (dashed lines). 121

Fig A 4 correlation between relative protein concentration and d|G*|/dtmax as well as |G*| at different times of fermentation and resting. 122

Fig A 5 Thixotropy test of fermented of samples containing protein only (a), protein and oil (b), protein and fibre (c) and protein, oil and fibre (d)after 24-30 h storage (6 °C)., (■ G', □ G''). 122

Fig A 6 amplitude sweeps of fermented of samples containing protein only (a), protein and oil (b), protein and fibre (c) and protein, oil and fibre (d)after 24-30 h storage (6 °C)., (■ G', □ G''). 123

Fig A 7 frequency sweeps of fermented of samples containing protein only (a), protein and oil (b), protein and fibre (c) and protein, oil and fibre (d)after 24-30 h storage (6 °C)., (■ G', □ G'' ▲ |η*|)..... 123

Fig A 8 SEM images of samples containing oil and fibre at 300-fold (a) and 3000-fold (b) magnification..... 124

Fig A 9 molecular weight profile of pea protein (black) and pea protein hydrolysed with Protamex® under different pH conditions (blue: pH 8.0, grey: pH 7.5, red: pH 7.0) and storage moduli of the corresponding fermentation induced gels..... 124

Fig A 10 pH-drop (a) and increase of G' (b) during fermentation of pea protein preheated at different pH-values..... 124

Fig A 11 G' and G'' in frequency sweeps pH 6.0 (a), pH 6.5 (b), pH 7.0 (c), pH 7.5 (d), pH 8.0 (e)..... 125

Fig A 12 protein solubility of untreated, unhydrolysed pea protein and pea protein hydrolysed with different enzymes (Protamex®, trypsin® and Alcalase®)..... 126

Fig A 13 ζ-potential of untreated or unhydrolysed pea protein and pea protein hydrolysed with different enzymes (Protamex®, trypsin® and Alcalase®)..... 126

List of tables

Table 1: harvest yield of protein crops in Germany in 2019 1

Table II 1 composition of the samples (content in 100 g sample), the water retention capacity of the fibre, the calculated available water and the relative protein content of all samples 35

Table II 2 maximum values for d|G*|/dt and dpH/dt and the corresponding values for time and pH. pH values at maximum and minimum values for d|G*|/dpH. 40

Table II 3 complex shear modulus |G*| at d|G*|/dtmax, at the end of the fermentation-process (18 h) and after 24-30 h storage at 6 °C. Loss factor tan δ at the end of the fermentation-process (18 h) and after 24-30 h storage at 6 °C. 40

Table II 4 Data from amplitude sweeps (deformation γ0 at the end of the linear viscoelastic regime and at the yield point. G'. G'' at the yield point) and thixotropy measurements (difference in G' and G'' after intense shearing). All measured after 24-30 h storage at 6 °C. 45

Table II 5 Data from frequency sweeps (slopes of logG', logG'' and log|η*| versus logω). 45

Table III 1 specific molecular parameters of pea globular proteins derived from literature 52

Table III 2 Characteristics of gels prepared from pea protein and pea protein hydrolysates obtained by enzymatic hydrolysis with Protamex®, trypsin and Alcalase®: storage modulus G',end and loss factor tanδ,end (f = 1 Hz and γ0 = 0.1%) at the end of fermenation, syneresis of fully set of gels. 58

Table IV 1 types of aggregates formed upon heating of mixtures of soy 11S and 7S: types of interactions involved in aggregate formation and composition of aggregates (corresponding pea proteins are: 11S → Legumin, 7Sαα' → Convicilin, 7Sβ→ Vicilin) .69

Table IV 2 ζ-potential and protein solubility before heating, protein solubility of heated, homogenised and lyophilised protein at the original pH value and at pH 8 simulating the beginning of fermentation and red shift during heating of the protein. 76

Table IV 3 correlation matrix for results that showed significant differences in Tables IV 2 & IV 4 77

Table IV 4 pH, storage modulus G' and loss factor tan δ at the end of fermentation, G', recovery from thixotropy test, slope dlogG'/dlogω from frequency sweeps and loss of water after 24 hours of gel storage. 80

List of abbreviations and symbols

$\|E^*\|$	Interfacial dilatational modulus
$\|G^*\|$	Complex shear modulus
$\|G_i^*\|$	Complex interfacial shear modulus
$\|\eta^*\|$	Complex viscosity
B	Volume of base consumption during hydrolysis
DH	Degree of hydrolysis
DTT	Dithiothreitol
E'	Elastic dilatational modulus
E''	Viscous dilatational modulus
E_D	Dissipated energy per cycle
$E_{D,PP}$	Dissipated energy per cycle in the perfect plastic system corresponding to E_D
f	Frequency
Fig	Figure
FKZ	Förderkennzeichen (grant number)
G'	Storage modulus
G''	Loss modulus
G'_L	Storage modulus for large intracycle strain
G'_M	Storage modulus for minimum intracycle strain
HCl	Hydrochloric acid
LVE	Linear viscoelastic regime
h_{tot}	Total number of peptide bonds in the substrate for hydrolysis
MCT-oil	Medium-chain triglycerides oil
mp	Mass of protein used for hydrolysis

NaCl	Sodium chloride
NaOH	Sodium hydroxide
N_b	Molarity of base used for hydrolysis
P	Protein
PF	Protein and oat fibre
PG	Propylene glycol
pI	Isoelectric point
PO	Protein and rapeseed oil
POF	Protein, rapeseed oil and oat fiber
PPC	Pea protein concentrate
PPH	Pea protein hydrolysate
SDS	Sodium Dodecyl Sulfate
SEC	Size exclusion chromatography
SEM	Scan electron microscopy
α	Average degree of dissociation of the α-NH groups in the substrate for hydrolysis
γ	Intracycle shear strain
γ_o	Intercycle shear strain
$\dot{\gamma}$	Shear rate
ΔG^0	Gibbs free energy
η'_L	Real contribution to complex viscosity for large intracycle shear rate
η'_M	Real contribution to complex viscosity for minimum intracycle shear rate
τ	Shear stress
τ'	Elastic stress
φ	Dissipation ratio
ψ	Surface potential
ω	Angular frequency

Motivation and Objectives

Increased consumption of plant-derived proteins can contribute to tackling two of the key challenges of our times: (1) increase in age-related non-communicable diseases caused by increasing life expectancy and (2) environmental changes and associated challenges like an increasing demand for sustainable raw materials. Consequently, in the last few decades, interest in plant-derived proteins has steadily increased and the corresponding market is continuously growing (European Commission, 2018). With growth rates of 14% and 11% respectively, the market for meat and cheese substitutes in particular is rapidly gaining importance and corresponding products can no longer be considered niche products (European Commission, 2018). As a result, the range of respective products increases and research in the field is extended to previously under-utilised raw materials such as lentils (e.g. Boye et al., 2010; Karaca, Low, et al., 2011; Ma et al., 2011), lupine (e.g. Berghout et al., 2015; Hickisch et al., 2016; Makri et al., 2005), beans (other than soy beans) (e.g. Karaca, Low, et al., 2011; Makri et al., 2005), oat (e.g. Brückner-Gühmann et al., 2018; Brückner-Gühmann, Banovic, et al., 2019; Brückner-Gühmann, Benthin, et al., 2019; Brückner-Gühmann et al., 2019; Yang et al., 2017), quinoa (e.g. Kaspchak et al., 2017; Mäkinen et al., 2015, 2016; Ruiz et al., 2016; Zannini et al., 2018), canola (e.g. J. H. J. Kim et al., 2016; Tan et al., 2014; Yang et al., 2014), sunflower (e.g. Conde et al., 2005), pumpkin (e.g. Bučko et al., 2015), chickpea (e.g. Clemente et al., 1999; Karaca, Low, et al., 2011; Karaca, Nickerson, et al., 2011; Ma et al., 2011) and pea (e.g. Barac et al., 2015; Ben-Harb et al., 2018; Karaca, Low, et al., 2011; Sun & Arntfield, 2012; Tamm et al., 2016). Moreover, enhancing the utilisation of regionally grown protein crops is in line with the "German protein crop strategy" as well as with the "European Soya Declaration" (BMEL, 2020).

Within protein crops, peas are by far the legume with the highest harvest yield in Germany (Table 1) and therefore a source of plant protein well worth investigating with regard to the manufacture of plant protein-based products to accommodate the increased interest in the consumption of these proteins.

Table 1: harvest yield of protein crops in Germany in 2019 (Destatis, 2020)

Legume	Pea	Faba bean	Sweet lupin	Soya beans
Harvest [1000 t]	228.2	159.5	25.6	84.1

So far, pea protein has sometimes been used as an ingredient in niche products like vegetarian and vegan spreads, and pea protein hydrolysates can be found in vegan sweets. However, commercial food based on pea protein is still an exception and – despite the investigation of various pea protein raw materials in the past 20 years – only very few products in everyday use are based on pea protein. So far, investigations into pea protein have covered raw materials ranging from commercial products (e.g. Ben-

Harb et al., 2018; Karamac et al., 1998, 2018; Peters et al., 2017; Tamm et al., 2016) to isoelectric precipitated (e.g. Boye et al., 2010; Karaca, Low, et al., 2011; Stone et al., 2015), ultrafiltrated (e.g. Boye et al., 2010) and salt-extracted pea protein isolates (e.g. Karaca, Low, et al., 2011; Stone et al., 2015; Sun & Arntfield, 2010, 2011b) and have focused on various objectives and functional properties. Moreover, some studies investigate pea protein as a whole, while others only focus on individual protein fractions (e.g. Bora et al., 1994; O'Kane et al., 2004c). Additionally, literature describes enzymatic hydrolysis for the customisation of various functional properties of proteins in general, and pea protein specifically (e.g. Barac et al., 2012; Karamac et al., 1998; Schwenke et al., 2001; Sijtsma et al., 1998; Soral-Smietana et al., 1998; Tamm et al., 2016). Generally, an influence of extraction method, pea protein fraction and enzymatic hydrolysis on functional properties of pea protein in emulsions, foams and gels can be deduced from those studies.

Emulsions are the dispersed system investigated most extensively (e.g. Aluko et al., 2009; Amine et al., 2014; Barac et al., 2010; Chang et al., 2015; Gharsallaoui et al., 2009; Karaca, Low, et al., 2011; Ladjal-Ettoumi et al., 2016; Liang & Tang, 2013; W. Peng et al., 2016; Sosulski & McCurdy, 1987; Stone et al., 2015; Tamm et al., 2016; Tsoukala et al., 2006). During the formation of emulsions, pea proteins have been described to unfold at the oil-water interface (Gharsallaoui et al., 2009) which is a prerequisite for globular proteins to be able to form two-dimensional interfacial networks (Mezzenga & Fischer, 2013), thereby stabilising oil droplets in an aqueous phase. Literature suggests an influence of pH on the stability of pea protein-based emulsions (e.g. Amine et al., 2014; Chang et al., 2015; Ladjal-Ettoumi et al., 2016; Liang & Tang, 2013) and on the strength of corresponding interfacial films at the oil-water interface (e.g. Amine et al., 2014; Chang et al., 2015; Gharsallaoui et al., 2009). In addition, an influence of the extraction method on emulsifying properties of pea protein was described by some authors (e.g. Karaca, Low, et al., 2011). One commercial application that exploits these emulsifying properties is the production of pea-based milk alternatives, where rapeseed oil or sunflower oil is emulsified into the pea protein base for texture and/or nutritional purposes. In this context, the first two brands of pea protein-based milk alternatives ("Princess and the Pea" and "Vly Foods") were only recently launched in the German market, while "Ripple" has been present for a few years in the US market. This development can be considered as a first step towards the "mainstream" utilisation of pea protein.

However, with protein contents between 0.1 and 2% (e.g. Barac et al., 2010; Sosulski & McCurdy, 1987; Stone et al., 2015), emulsions do not generally contain high amounts of protein, and even pea protein-based milk alternatives only reach protein contents between 2.1 and 5.2% according to manufacturers' declarations. Consequently, in order to obtain potential health benefits from the consumption of plant-derived proteins, a larger variety of corresponding products, as well as products with higher protein contents is required. A promising approach for the incorporation of larger amounts of plant-derived proteins into the everyday diet is the utilisation of pea protein gels, which generally contain protein concentrations above 6 to 20% (e.g. O'Kane et al., 2005; Shand et al., 2007; Sun & Arntfield, 2010). In this context, acid-induced gels are a group of products with a high potential for market success. Yoghurt, for example, is already associated with high protein foods by consumers and is well accepted by them (Banovic et al., 2018).

However, literature on acid-induced gelation of pea protein is very limited, despite the fact that a thorough understanding of gel properties, gelation kinetics and mechanisms – including involved protein fractions and relevant types of interactions – would be a prerequisite for the development and customisation of corresponding products.

The existing studies on acid-induced gelation of pea protein can be divided into two categories: (1) investigation of milk-based yoghurt fortified with pea protein (e.g. Denkova et al., 2015; Yousseef et al., 2016; Zare et al., 2013) and (2) pea protein acidified via use of glucono-δ-lactone (Ben-Harb et al., 2018; Mession et al., 2015). However, category (1) deviates from fermentation-induced pea protein gels with regard to sample composition, and category (2) with regard to the acidification method. Therefore, results from these studies need to be carefully evaluated concerning their applicability to specific details of mechanisms in fermentation-induced gelation and resulting gel properties, because – as stated above – it is these details that are required as a basis for the systematic development of pea protein-based yoghurt alternatives. In this context, the mixed protein systems in category (1) may be interesting from a nutritional point of view, but do not contribute much to the required understanding of the mechanisms in fermentation-induced pea protein gels, owing to competitive effects between milk and pea proteins. With regard to category (2), the most extensive study on gelation kinetics was carried out by Mession et al. They compared glucono-δ-lactone-induced gelation and gel properties of mixed and individual pea protein fractions and proposed the interactions within the gel to be of a physical nature (Mession et al., 2015). However, they did not investigate these types of interactions any further, nor did they give detailed information on the involvement of the different protein fractions if mixed pea protein was used. Moreover, as previously shown for soy protein, acidification velocity differs between samples acidified with glucono-δ-lactone and those acidified via fermentation (Grygorczyk & Corredig, 2013). For soy protein, this led to differences in gelation kinetics owing to additional time for protein rearrangements – and therefore changes in the susceptibility of individual protein fractions to interact with each other – even though final gel properties were similar for both acidification methods (Grygorczyk & Corredig, 2013). In conclusion, the existing studies on acidification of pea protein via glucono-δ-lactone may allow for a general characterisation of gel properties in acid-induced pea protein gels. However, owing to a lack of details on the gelation mechanism and the diverging acidification method, they are insufficient for the required in-depth understanding of fermentation-induced gelation of pea protein.

In addition, no research exists on the influence of additional ingredients such as oil or dietary fibre on the acid-induced gelation of pea protein in general and in the fermentation induced-gelation in particular. However, it is a prerequisite for the prospective development and customisation of formulations to understand if and how these components interfere with the formation of the pea protein network or if and how they may interact with the protein network. Based on the general ability of pea protein to stabilise oil in water emulsions (e.g. Aluko et al., 2009; Amine et al., 2014; Barac et al., 2010; Chang et al., 2015; Gharsallaoui et al., 2009; Karaca, Low, et al., 2011; Ladjal-Ettoumi et al., 2016; Liang & Tang, 2013; W. Peng et al., 2016; Sosulski & McCurdy, 1987; Stone et al., 2015; Tamm et al., 2016; Tsoukala et al., 2006) fermentation-induced gelation of pea protein fortified with oil may result in emulsion gels. These kinds of gels were previously

described for glucono-δ-lactone-induced gelation of soy (Gu et al., 2009; Li et al., 2012; Tang et al., 2011) and pea protein emulsions (Ben-Harb et al., 2018). However, similar to the effects described above, the different acidification velocity in fermentation-induced gels is also expected to influence the gelation behaviour in pea protein-based emulsion gels. When it comes to fortification with dietary fibre, literature is even less conclusive. Approaches to enrich milk-based yoghurts have been described for fibres of various origins (Aportela-Palacios et al., 2005; Damian & Olteanu, 2014; Espírito-Santo et al., 2013; Fernández García & McGregor, 1997; Kieserling et al., 2019; Sah et al., 2016; Sanz et al., 2008; Sendra et al., 2010). In those studies, results concerning textural properties of the investigated yoghurts differed depending on various properties of the fibres, such as particle size or ratio of soluble to insoluble fibre. Moreover, information on protein fibre interactions in gel systems is entirely missing even for regular milk-yoghurts, let alone plant-derived yoghurt alternatives, and therefore needs to be investigated as a foundation for scientifically based product development.

Taking into account knowledge of the functional properties of pea protein and fermentation-induced gelation of other plant-derived proteins from literature, **the overall aim of this thesis is to investigate and understand the mechanism – and therefore the molecular interactions – behind fermentation-induced gelation of pea protein, to identify the protein fractions involved and to examine the influence of fortification with further ingredients such as dietary fibre and oil on the gelation process and gel properties.** To approach this overall aim, three specific research objectives and corresponding expectations were defined:

Objective 1:
Characterisation of molecular and physico-chemical properties of pea protein and pea protein hydrolysates as a basis on which molecular interactions can be anticipated and discussed.

In this context, it is generally acknowledged that molecular and physico-chemical properties of pea protein – such as molecular weight distribution, hydrophobicity, surface electrical properties (measured as ζ-potential) and protein solubility – will be influenced by various processing parameters such as enzymatic hydrolysis, pH value and temperature. More specifically, enzymatic hydrolysis will increase the protein solubility owing to the emergence of smaller peptides with higher hydratability, while pH values close to the isoelectric point (pI) lead to low electrostatic repulsion which, in turn, decreases the solubility of the protein owing to pronounced protein-protein aggregation. Heating will lead to the unfolding of the protein and therefore to an increase in hydrophobicity and a decrease in solubility owing to the increased exposure of hydrophobic patches. However, it is expected that the extent of these effects will differ depending on the type of selected enzyme and the selected processing parameters and therefore requires thorough and customised investigation in order to subsequently address the following objectives.

Objective 2:

Elucidation of the involvement of various molecular interactions and individual protein fractions in fermentation-induced bulk gelation, understanding of their impact on corresponding gel network properties and the investigation of emerging parallels between bulk gelation behaviour and interfacial network formation.

The gelation of pea proteins depends on various intrinsic and extrinsic factors and always requires protein-protein interactions to occur. In acid-induced bulk gelation the pH gradient can be considered to be the driving force for gelation. More precisely, if the decreasing pH value approaches the pI, surface electrical properties of the protein will decrease, thus increasing the susceptibility of individual protein molecules to interact with each other via various mechanisms. These mechanisms can be electrostatic in nature or may be promoted by lack of electrostatic repulsion at pH values close to the pI. In the latter case interactions can involve hydrophobic interactions, hydrogen bonds and/or disulphide bonds.

Owing to different molecular properties such as molecular weight, subunit structure, molecular flexibility and pI, it is expected that individual pea protein fractions will be affected differently by changes in pH and therefore contribute to the gel network structures to different extents, or via different mechanisms. Enzymatic hydrolysis can be used to further clarify the influence of different protein fractions, as – depending on the applied enzyme – different protein fractions will be degraded to different extents and previously buried functional groups and hydrophobic patches will become available, thus enhancing or decreasing the requirements for network formation.

It is further hypothesised, that – despite differences in the processing steps preceding the respective (gel) network formation and the variations in network forming kinetics – interfacial networks and their viscoelastic properties will show similarities to those obtained by fermentation-induced gelation in bulk gels owing to the presence of identical protein fractions in the respective aqueous phases.

Objective 3:

Application of the obtained knowledge on molecular, physico-chemical and gelation properties of pea protein and pea protein hydrolysates towards the modification of texture characteristics of the corresponding gels and towards understanding the impact of additional ingredients on the gel network properties.

With regard to the modification of texture properties and the fortification of fermentation-induced pea protein gels with oil, it is expected that knowledge on factors that influence the underlying mechanisms of gelation behaviour in bulk or at the oil-water interface can be utilised to select specific processing parameters or sample compositions that allow the customisation of texture properties and lead to the stabilisation of incorporated oil in fermentation-induced pea protein gels. Additionally, it is expected, that the incorporation of dietary fibre will decrease the amount of available water, thus increasing the relative protein content and therefore strengthening the gel network. However, added dietary fibre may also act as an inactive filler and therefore be incompatible with the protein network and impair its formation.

These specific research objectives were addressed by combining the results from the following published work, which is included in this thesis as manuscripts I to IV:

- Manuscript I: **Klost, M., & Drusch, S. (2019a). Functionalisation of pea protein by tryptic hydrolysis – Characterisation of interfacial and functional properties.** ***Food Hydrocolloids*****,** ***86*****, 134–140.** **https://doi.org/10.1016/j.foodhyd.2018.03.013** addresses Objective 1 by characterising the molecular weight distribution, the protein solubility and the surface electrical properties and contributes to Objective 2 by examining the influence of tryptic hydrolysis of pea protein on interfacial gelation at the oil-water interface. Additionally, Manuscript I is a preliminary step to the addition of oil into fermentation-induced bulk gels in Objective 3.
- Manuscript II: **Klost, M., & Drusch, S. (2019b). Structure formation and rheological properties of pea protein-based gels.** ***Food Hydrocolloids*****,** ***94*****, 622–630.** **https://doi.org/10.1016/j.foodhyd.2019.03.030** contributes to Objective 1 by characterising the heat-induced unfolding behaviour via intrinsic fluorescence measurements. Furthermore, Manuscript II investigates the gelation kinetics of fermentation-induced bulk gels and includes a basic characterisation of the corresponding gel properties as a contribution to Objective 2. With regard to Objective 3 it covers the impact of dietary fibre and oil on fermentation-induced bulk gels.
- Data from Manuscript III: **Klost, M., Giménez-Ribes, G., & Drusch, S. (2020). Enzymatic hydrolysis of pea protein: Interactions and protein fractions involved in fermentation induced gels and their influence on rheological properties.** ***Food Hydrocolloids*****,** ***105*****, 105793.** **https://doi.org/10.1016/j.foodhyd.2020.105793** covers the impact of hydrolysis with various enzymes on molecular weight distribution, ζ-potential and protein solubility in Objective 1. Moreover, Manuscript III addresses Objective 2 by focusing on the protein fractions and types of interactions involved in the formation of the network structure of fermentation-induced bulk gels and contributes fundamental knowledge of gel properties to Objective 3.
- Manuscript IV: **Klost, M., Brzeski, C., & Drusch, S. (2020). Effect of protein aggregation on rheological properties of pea protein gels.** ***Food Hydrocolloids*****,** ***108*****, 106036.** **https://doi.org/10.1016/j.foodhyd.2020.106036** contains detailed investigations of molecular weight distribution, intrinsic fluorescence, surface electrical properties, protein solubility and rheological gel properties in dependence of the pH value and therefore also contributes to Objectives 1 and 2. Additionally, it applies knowledge obtained in Manuscripts II and III to the customisation of texture properties in Objective 3.

Theoretical background

This section gives an overview of the composition and molecular structure of pea protein and the specific cleaving behaviour of selected enzymes as a prerequisite for enzymatic hydrolysis applied throughout this thesis. In addition, it summarises the current state of knowledge of proteins in general and – where available – on pea protein specifically, regarding physico-chemical properties such as solubility, surface electrical and hydrophobic properties alongside gelation behaviour in bulk and at the interface, and therefore forms the basis required to address the specific research Objectives 1 to 3.

Composition and molecular structure of pea protein

Peas *(Pisum sativum)* belong to the legume family (Leguminosae). Pea meal was previously described as containing 39.2% starch, 27.9% protein, 8.04% total sugars (composed of 5.88% total oligosaccharides (2.76% verbascose, 2.31% stachyose, 0.81% raffinose), 2.04% sucrose, 0.12% glucose), 3.0% ash and 1.7% fibre (Bhatty & Christison, 1984). The protein fraction can be further subdivided into 65 to 80% globulins and 20 to 35% albumins (Schroeder, 1982) (Fig 1).

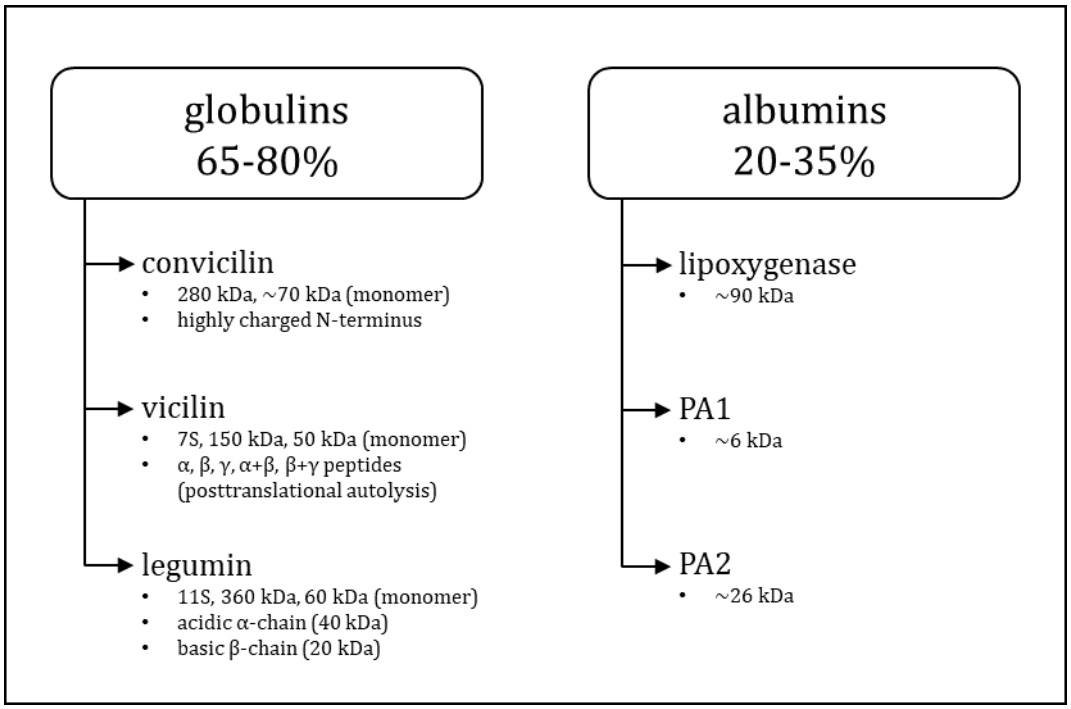

Fig 1 Pea protein fractions and their specific molecular parameters as derived from literature (Bown et al., 1988; Croy et al., 1979; Croy, Gatehouse, Evans, et al., 1980; Croy, Gatehouse, Tyler, et al., 1980; Gatehouse et al., 1981, 1982, 1983; Gruen et al., 1987; Higgins et al., 1986; Lycett et al., 1983)

Out of the various pea-protein fractions, techno-functional properties – such as the ability to stabilise emulsions and foams and to form gels – are mainly ascribed to the globulin fractions in literature. Therefore, only these fractions will be regarded in the following sections. Similar to many other plant-derived proteins, pea globulins can be divided into an 11S and a 7S fraction. In pea protein, legumin is the 11S fraction. Legumin assumes its native hexameric state at pH 7 to 9 (Gueguen et al., 1988), which is distinctly above its pI, (pH 4.8 (Danielsson, 1950)) but begins to dissociate into monomeric, dimeric and trimeric forms at pH values above pH 9 and below pH 3.35 (Gueguen et al., 1988), and no research describes the quaternary structure at pH values approaching the pI where aggregation occurs. Legumin hexamers have a molecular weight of approximately 360 kDa (Boulter, 1983) with each monomer accounting for 60 kDa (Boulter, 1983; Croy, Gatehouse, Evans, et al., 1980).

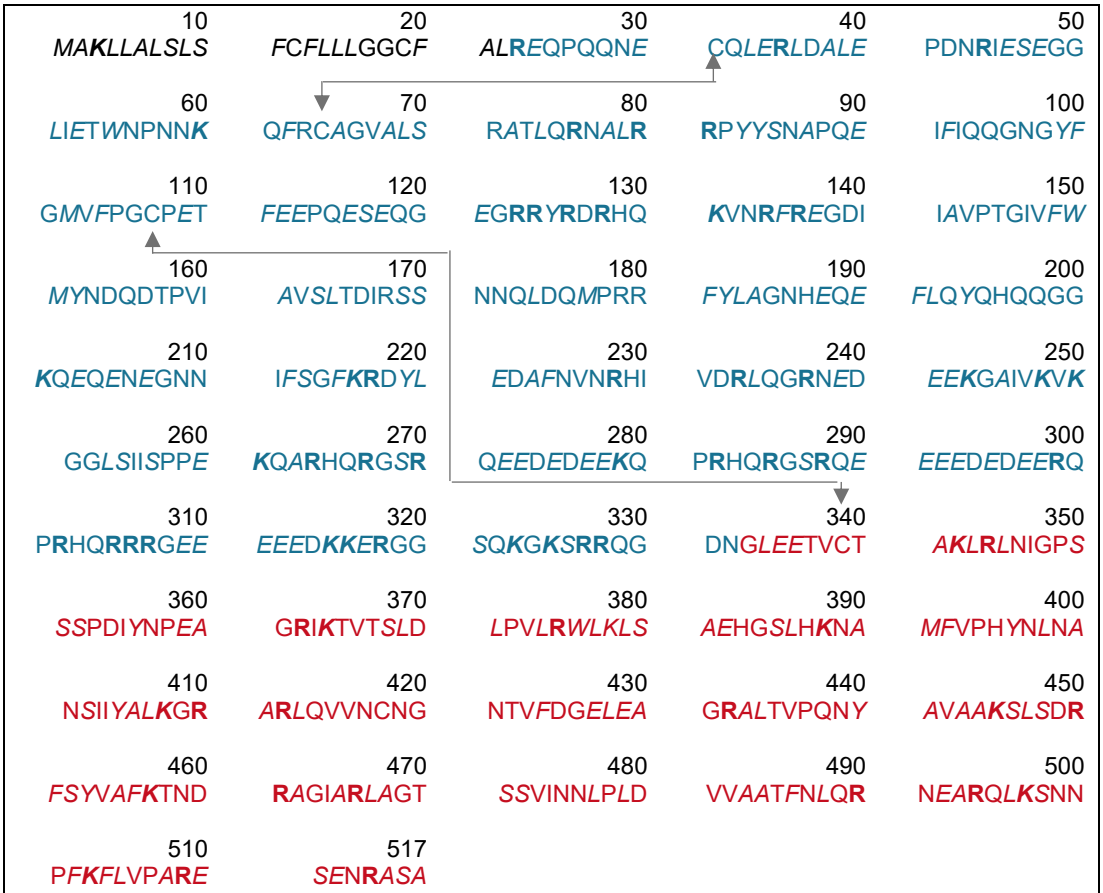

signal peptide, legumin α, legumin β ↔ disulphide bond

A=alanine, **R=arginine**, N=asparagine, D=aspartic acid, B asparagine or aspartic acid, C=cysteine, E=glutamic acid, Q=glutamine, Z=glutamine or glutamic acid, G=glycine, H=histidine, I=isoleucine, L=leucine, **K=lysine**, M=methionine, F= phenylalanine, P=proline, S=serine, T=threonine, W=tryptophan, Y=tyrosine, V=valine

Fig 2 Amino acid sequence of legumin divided into signal peptide (black), legumin α (blue) and legumin β (red) including disulphide bonds (arrows) and amino acids susceptible to tryptic hydrolysis (printed in bold) or hydrolysis by Alcalase® (printed in italics). (https://www.Uniprot.Org/Uniprot/P02857, n.d.)

The secondary structure comprises a mixture of 41% β-sheets, 16% α-helices and some β-turns (Subirade et al., 1994), and the tertiary structure can be divided into a 40 kDa acidic α-chain (marked in blue) with a pI between pH 4 and pH 6 (Croy et al., 1979) starting after the signal peptide at the 23rd amino acid and a 20 kDa basic β-chain (marked in red) with a pI > pH 9 (Croy et al., 1979) starting at the 333rd amino acid that are covalently connected (Croy, Gatehouse, Evans, et al., 1980) by a disulphide bond between the 107th and the 339th amino acid (Fig 2). The acidic α-chain contains a higher proportion of hydrophilic amino acids, whereas the basic β-chain is more hydrophobic. This leads to an overall conformation where the β-chain is located on the inside of the molecule and the α-chain on the outside in an aqueous environment (Karaca, Low, et al., 2011). With seven cysteine and five methionine residues – as counted from the amino acid sequence in Fig 2 – legumin contains the most sulphur groups of the three pea globulins and is therefore most likely to be involved in the formation of disulphide bonds.

10	20	30	40	50
*MAA*TT*M**K**ASF*	P*LLMLM*GI*SF*	*LAS*VCV*SS*R*S*	DPQNP*FIF**K**S*	N*K*FQT*LFENE*
60	70	80	90	100
NGHI**R***LLQ**K**F*	DQ**R***S**K**IF*EN*L*	QNY**R***LLEY**K**S*	***K***PHTI*FL*PQH	TDADYI*L*VV*L*
110	120	130	140	150
*SG**K**AIL*TV*L**K***	PDD**R**N*SF*N*LE*	**R**GDTI***K***L*PA*G	TI*AYL*VN**R**DD	N*EEL**R**VLDLA*
160	170	180	190	200
IPVN**R**PGQ*L*Q	*SFLLS*GNQNQ	QN*YLSGFS**K***N	I*LEASF*NTD*Y*	*EEIE**K**VLLEE*
210	220	230	240	250
H*E**K**E*TQH**RR**S*	***LK***D***KR***QQS*QE*	*E*NVIV***K****L*S**R**G	QI*EELS**K**NA**K***	*STS**KK**SVSSE*
260	270	280	290	300
*SEPFNL**R**S**R***G	PI*YSNEFG**K**F*	*FE*ITP*E**K***NPQ	*LQDLDIFVNS*	VE*I**K**EGSLLL*
310	320	330	340	350
PH*YNS**R**A*IVI	VTVN*EG**K**GD*F*	*EL*VGQ**R**N*E*NQ	Q*EQ**RK**EDD*EE*	*EEQGEEE*IN***K***
360	370	380	390	400
QVQN*Y**KA**K**LS*	*SGDVFV*IP*AG*	HPV*AV**K**ASS*N	*LDLLGFGINA*	*E*NNQ**R**N*FLAG*
410	420	430	440	450
D*E*DNVISQIQ	**R**PV***K****ELAF*PG	*SAQEVDRILE*	NQ***K***QSH*FADA*	QPQQ**R***E***R**G*S***R***
459				
*E*T**R**D**R***LSS*V				

signal peptide, α fraction, β fraction, γ fraction

A=alanine, **R=arginine**, N=asparagine, D=aspartic acid, B asparagine or aspartic acid, C=cysteine, E=glutamic acid, Q=glutamine, Z=glutamine or glutamic acid, G=glycine, H=histidine, I=isoleucine, L=leucine, **K=lysine**, M=methionine, F= phenylalanine, P=proline, S=serine, T=threonine, W=tryptophan, Y=tyrosine, V=valine

Fig 3 Amino acid sequence of vicilin divided into signal peptide (black), α-fraction (grey), β-fraction (blue) and γ-fraction (red) including disulphide bonds (arrows) and amino acids susceptible to tryptic hydrolysis (printed in bold) or hydrolysis by Alcalase® (printed in italics). (https://www.Uniprot.Org/Uniprot/P13918, n.d.)

The 7S fraction in pea protein is called vicilin. Vicilin is a trimeric protein of approximately 150 kDa that consists of three 50 kDa monomers. The pI is at pH 5.5 (Danielsson, 1950). In contrast to legumin, vicilin is prone to post-translational autolysis that occurs mainly at two preferred cleavage sites (Gatehouse et al., 1982) as marked in Fig 3 (derived from (Herbst, 2015)) and leads to the formation of so-called α, β and γ fractions alongside α-β and β-γ fractions. However, despite the post-translational hydrolysis of vicilin, its overall molecular weight is not altered indicating continuous association even after cleavage (Gatehouse et al., 1981). Vicilin contains no cysteine residues (Croy, Gatehouse, Tyler, et al., 1980) and is therefore unlikely to form disulphide bonds.

10	20	30	40	50
MATTV**K**S**R**FP	LLLFLGIIFL	ASVCVTYANY	DEGSET**R**VPG	Q**R**ER**R**GRQEGE
60	70	80	90	100
KEE**K**RHGEW**R**	PSYE**K**EEHEE	EKQ**K**Y**R**YQ**R**E	**KK**EQ**K**EVQPG	**R**ER**R**WE**R**EEDE
110	120	130	140	150
EQVEEEW**R**GS	Q**RR**EDPEE**R**A	**R**LRHR**E**E**R**T**K**	**R**D**RR**HQ**R**EGE	EEE**R**SSESQE
160	170	180	190	200
H**R**NPFLF**K**SN	**K**FLTLFENEN	GHI**RR**LQ**R**FD	**KR**SDLFENLQ	NY**R**LVEY**R**A**K**
210	220	230	240	250
PHTIFLPQHI	DADLILVVLN	G**K**AILTVLSP	NDRNSYNLE**R**	GDTI**K**IPAGT
260	270	280	290	300
TSYLVNQDDE	EDL**R**VVDFVI	PVN**R**PG**K**FEA	FGLSEN**K**NQY	L**R**GFS**K**NILE
310	320	330	340	350
ASLNT**K**YETI	EKVLLEEQE**K**	**K**PQQL**R**D**RK**R	TQQGEE**R**DAI	I**K**VS**R**EQIEE
360	370	380	390	400
L**RK**LA**K**SSS**K**	**K**SLPSEFEPF	NL**R**SH**K**PEYS	N**K**FG**K**LFEIT	PE**KK**YPQLQD
410	420	430	440	450
LDILVSCVEI	N**K**GALMLPHY	NS**R**AIVVLLV	NEG**K**GNLELL	GL**K**NEQQE**R**E
460	470	480	490	500
D**RK**E**R**NNEVQ	**R**YEA**R**LSPGD	VVIIPAGHPV	AISASSNLNL	LGFGIN**AK**NN
510	520	530	540	550
Q**R**NFLSGSDD	NVISQIENPV	**K**ELTFPGSSQ	EVN**R**LI**K**NQ**K**	QSHFASAEPE
560	570	571		
Q**K**EEESQR**KR**	SPLSSVLDSF	Y		

A=alanine, **R=arginine**, N=asparagine, D=aspartic acid, B asparagine or aspartic acid, C=cysteine, E=glutamic acid, Q=glutamine, Z=glutamine or glutamic acid, G=glycine, H=histidine, I=isoleucine, L=leucine, **K=lysine**, M=methionine, F= phenylalanine, P=proline, S=serine, T=threonine, W=tryptophan, Y=tyrosine, V=valine

Fig 4 Amino acid sequence of convicilin, amino acids susceptible to tryptic hydrolysis are printed in bold and amino acids susceptible to hydrolysis by Alcalase® are printed in italics (https://www.Uniprot.Org/Uniprot/P13915, n.d.).

The third pea globulin, convicilin, has similarities to vicilin (Fig 4) and was previously also described as the α-subunit of the pea vicilin family (O'Kane et al., 2004a). In this context the term α-subunit is derived from the corresponding terminology of soy

proteins and should not be confused with the autolytically generated α fragment of vicilin. Convicilin monomers have a molecular weight between 70 and 78 kDa (Adal et al., 2017; Croy, Gatehouse, Tyler, et al., 1980) and a pI at pH 5.6 to pH 5.8 (Croy, Gatehouse, Tyler, et al., 1980). There is uncertainty about the quaternary structure which has been described as tetrameric by Croy et al. but as trimeric by Tzitzikas et al. (Croy, Gatehouse, Tyler, et al., 1980; Tzitzikas et al., 2006). In contrast to vicilin, convicilin contains a highly charged N-terminus (Bown et al., 1988) and some cysteine residues (Croy, Gatehouse, Tyler, et al., 1980), but no post-translational autolysis has been described for convicilin despite the genetic similarities of the two.

Specific cleaving behaviour of selected enzymes as a prerequisite for enzymatic hydrolysis of pea protein

Enzymatic hydrolysis describes the cleavage of peptide-bonds in protein molecules via the application of proteolytic enzymes. It leads to changes in the molecular and physico-chemical properties of proteins and can subsequently be used to customise functional properties such as bulk gelation or interfacial stabilisation of emulsions and foams. In order to obtain peptides eligible for the desired application, enzymes with suitable cleavage behaviour need to be selected and an appropriate degree of hydrolysis needs to be applied.

In literature, various enzymes are covered and applied to modify proteins. Out of these, cleavage behaviour of trypsin (EC 3.4.21.4) – a serine endopeptidase – has been described most extensively. It has a very high cleavage specificity, only cleaving at the N-terminus of lysine and arginine. Potential cleavage sites for trypsin in the different pea protein fractions (i.e. lysine and arginine) are marked in bold in Fig 2 to Fig 4. Legumin is first attacked at the C-terminus of the legumin-α chain by tryptic hydrolysis (Braudo et al., 2006). Considering the amino acid sequence in this region (Fig 2, amino acids ~300 to 330), the high density of susceptible amino acids (printed in bold) leads to the generation of a variety of small peptides with a high density of charged side chains. Moreover, as a result of cleavage at the C-terminus of the legumin-α chain, the entire molecule obtains a higher degree of flexibility and the basic legumin-β chain becomes exposed. At very limited tryptic hydrolysis, from this pattern of attack, legumin-T, a very ordered structure (Plumb & Lambert, 1990) with a nearly intact tertiary structure and improved techno-functionality (Krause & Schwenke, 1995; Ochiai et al., 1982) remains where cleavage had mostly taken place at the C-terminus of the legumin-α chain. Tryptic hydrolysis of vicilin starts in the areas already prone to post-translational autolysis (N-terminus of amino acids 208 and 351, Fig 4), since these areas are likely to be located at the molecule's surface because they have a high density of polar amino acids (Gatehouse et al., 1983). To date, the effect of tryptic hydrolysis on convicilin has not been described in detail. Tamm et al. noted that convicilin was degraded by trypsin with an increasing degree of hydrolysis, but did not refer to specific cleavage kinetics (Tamm et al., 2016). However, it is likely that tryptic hydrolysis of convicilin starts at the highly charged N-terminus, as this area is likely to be exposed to the aqueous phase and shows an amino acid composition similar to the sequence found close to the C-terminus of the legumin-α chain (Bown et al., 1988) where hydrolysis of legumin starts, as described above.

Other enzymes of interest have received less attention in the past. In this context, cleavage behaviour of Protamex® a *Bacillus ssp.* protease complex consisting of subtilisin (EC 3.4.21.62) – a serine endopeptidase– and a neutral metallo-endopeptidase (EC 3.4.24.28) is less well described in general and has only been investigated in one reference on pea protein so far. In that reference, it was found to cleave some of the vicilin and most of the convicilin fractions of pea protein, depending on the hydrolysis time (García Arteaga et al., 2020). Additionally, Garcia-Mora et al. compared the effect of hydrolysis with Protamex®, Alcalase® and other enzymes on lentil protein. They found only a slight decrease in the major protein fractions upon hydrolysis with Protamex® while upon hydrolysis with Alcalase® (EC 3.4.21.62) – a serine endopeptidase – all native protein fractions were drastically reduced (Garcia-Mora et al., 2015). This is in agreement with other literature, that assigns a low specificity with preferred cleavage at aromatic (phenylalanine, tryptophan and tyrosine), acidic (glutamic acid), sulphur-containing (methionine), aliphatic (leucine, alanine), hydroxyl (serine) and basic (lysine) residues (Doucet et al., 2003), depicted in italics in Fig 2 to Fig 4 to Alcalase®.

Characterisation of molecular and physico-chemical properties of proteins

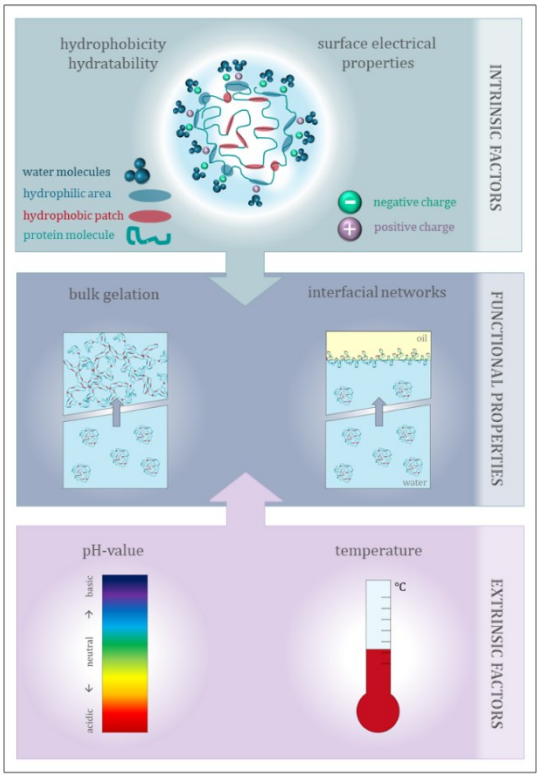

Fig 5 Relationship between intrinsic and extrinsic factors relevant to this thesis and selected functional properties of pea protein (schematic drawing).

As schematically shown in Fig 5, functional properties of proteins, such as the ability to form gels, depend on a wide range of intrinsic factors like molecular and physico-chemical characteristics, such as surface electrical properties and hydrophobicity, and can additionally be influenced by external conditions. The relevance of these parameters is described in literature for a wide range of proteins alongside the applied methods for their determination and will be summarised in the following section.

Surface electrical properties

Owing to their molecular structure – including sidechains carrying various functional groups such as carboxyl groups and amino groups – the net charge of dispersed proteins depends strongly on environmental conditions such as ionic strength and pH value. While the addition of ions may screen charges in general, the adjustment of pH i.e. the shift in the balance between hydrogen (H^+) and hydroxyl (OH^-) ions leads to different ratios of protonated to dissociated carboxyl groups ($COOH/COO^-$) and amino groups (NH_3^+/NH_2)

respectively, thus influencing the overall net charge. At the pI, the net charge of a protein is zero, below it is positive and above it is negative. When considering the surface electrical properties, the electrical potential at the surface of a particle or molecule (surface potential ψ) cannot be determined directly (Bhattacharjee, 2016). However, the dispersion of a charged particle influences the distribution of ions in the solvent and leads to the development of an electrical double layer around the protein caused by the increased concentration of counterions at the protein surface (Bhattacharjee, 2016). This electrical double layer has been extensively described and shown in schematic figures by various authors (e.g. Bhattacharjee, 2016; Cano-Sarmiento et al., 2018; Lin et al., 2003) and – depending on the chosen model – can be further divided into an inner layer called the "Stern Layer" comprising strongly bound counterions, and a diffuse outer layer (Bhattacharjee, 2016).

If an external electrical field is applied, the dispersed particle, the strongly bound "Stern layer" and possibly part of the diffuse layer, begin to move in this electrical field, while the rest of the dispersion/solution does not follow, thus generating a potential at the boundary between the moving particle and surrounding medium. This boundary is called the "slipping plane" and the generated potential is referred to as ζ-potential (Bhattacharjee, 2016; Genovese & Lozano, 2001), which can be easily measured in a standard procedure available in many laboratories. However, the diameter of the double layer strongly depends on external parameters (high ionic strength for example causes compression of the double layer), and the ratio between the surface potential ψ and the ζ-potential depends on the thickness of the double layer. Therefore, the ζ-potential always needs to be regarded as a description of the surface potential in a specific environment (Lin et al., 2003). Besides the direct influence of environmental parameters like pH and ionic strength on surface electrostatic properties of protein, these parameters may also influence the conformation of proteins and, in turn, have an impact on the surface electrical properties, as not all chargeable groups will be located at the molecule's surface and may therefore not be available for charge generation (Bowen et al., 1998).

Hydrophobic properties

Hydrophobic properties, as measured by intrinsic fluorescence, are less affected by changes in pH as this may lead to aggregation but not necessarily to any intramolecular rearrangement. Therefore, despite influencing the volume of individual protein particles, possible aggregation of protein will not considerably influence the type of exposed amino acids and patches. On the other hand, a temperature-increase i.e. heating (especially above the denaturation temperature) causes proteins to unfold. If heat is applied, the energy in the protein slurry increases which, in turn, leads to a decrease in the stabilising effects of non-polar group hydration and enthalpy of intramolecular interactions on the native conformation of the protein (Khechinashvili et al., 1995). If intramolecular interactions become insufficient and entropic effects gain importance, the protein begins to unfold (Khechinashvili et al., 1995) and previously buried hydrophobic patches become exposed (Guo & Ono, 2006). This exposure of hydrophobic patches can be measured as red shift in intrinsic fluorescence measurements, which is caused by the decrease in quenching of tryptophan-related fluorescence by adjoining groups (Cairoli et al., 1994)

and the transition of the tryptophan residues to a more polar environment (Miriani et al., 2011).

Protein solubility and aggregation behaviour

Protein solubility generally depends on the availability of hydratable groups on the surface of a particle or molecule. In an aqueous environment, globular proteins will generally bury more hydrophobic patches in their interior, while hydrophilic areas are more exposed to the surroundings (Mezzenga & Fischer, 2013). The approachability of protein by water molecules further depends on the environmental pH. pH values away from the pI lead to higher net charges that, in turn, lead to increased electrostatic repulsion between individual molecules and therefore an increased approachability. If protein net-charge decreases to ζ-potentials below |20| mV (Piorkowski & McClements, 2014) the electrostatic repulsion between individual protein molecules may become insufficient and aggregation begins to occur. Larger aggregates, in turn, carry fewer accessible hydratable groups per mass protein and, additionally, their volume increases, both promoting sedimentation and reducing solubility. Another factor that influences aggregation and therefore protein solubility is temperature. As described above, heating of proteins leads to conformational changes and increase in exposed hydrophobic patches which, in turn, may lead to protein aggregation. Depending on the interacting protein fractions the resulting aggregates may be soluble or insoluble. For soy protein, it was previously shown that basic subunits of the 11S fraction and the β subunits of 7S fraction form soluble aggregates via electrostatic interactions (Petruccelli & Añón, 1995) or disulphide bonds (Damodaran & Kinsella, 1982; German et al., 1982). Further, soluble aggregates were described as forming between αα' subunits of 7S and αα' subunits of 7S as well as between αα' subunits of 7S and 11S acidic subunits via disulphide bonds and between αα' subunits of 7S and β subunits of 7S as well as between β subunits of 7S and β subunits of 7S via non covalent bonds (Yamagishi et al., 1983). Also for soy proteins insoluble aggregates were formed between 11S acidic and 11S basic subunits as well as between αα' subunits of 7S and 11S acidic and basic subunits via disulphide bonds and between β subunits of 7S and β subunits of 7S as well as between 11 basic subunits and 11S basic subunits via non covalent bonds (German et al., 1982; Yamagishi et al., 1983). Consequently, the type of formed aggregates – and more precisely the ratio of soluble to insoluble aggregates – may influence the overall solubility of pea protein after thermal treatment.

Gelation properties of proteins in general – and pea protein and pea protein hydrolysates specifically – in bulk and at the oil-water interface

Gelation and/or aggregation properties of proteins are a prerequisite not only in the formation of bulk gels, but also in the stabilisation of oil-water and air-water interfaces in emulsions and foams via the development of interfacial protein layers. In general, gelation involves the formation of a protein network via molecular interactions. As schematically shown in Fig 5, gelation in the conventional perception, is based on the

formation of a space-spanning, three-dimensional network in a bulk system (Ross-Murphy, 1995), while in emulsions and foams, these networks are two-dimensional and enclose either oil droplets or air bubbles, respectively.

However, the underlying mechanisms in the gelation process show some similarities and can be divided into two steps: (1) Unfolding of the protein molecules in aqueous environment (usually either at an oil-water or air-water interface or in bulk via heat) and (2) Aggregation / intermolecular interaction. However, while in acid-induced gelation these are usually two separate processes, in interfacial and heat-induced gelation they often merge or directly succeed each other. When it comes to unfolding at the interface or via heat, a negative correlation between the surface activity of proteins at the air-water interface and the Gibbs free energy ΔG^0 of thermal denaturation has been described, indicating similarities between interfacial and thermal denaturation of proteins (Razumovsky & Damodaran, 1999).

Interfacial network formation

In the case of interfacial unfolding and network formation, protein molecules migrate to the interface driven by a difference between the chemical potential of the protein in the bulk phase and the surface chemical potential of the protein and – once they overcome the energy barrier caused by the balance of interactions between the periphery of the native protein and the interface – adsorb to the interface (Dickinson, 2011). Other authors describe adsorption at oil-water interfaces as not involving an energy barrier and to be driven by van der Waals and hydrophobic interactions between protein and interface, electrostatic interactions between the protein and its image charge, and overlapping of electrical double layers of the protein and the interface (Sengupta et al., 1999). In either case, adsorption of proteins to the interface affects the interfacial tension by reducing the mole fraction of interfacial water molecules or by decreasing their activity coefficient. The former occurs if protein molecules replace water molecules at the interface, while the latter is caused by interaction between the water molecules and the protein molecules. However, Damodaran and Rao also found that adsorption of the protein to the interface is not sufficient to cause major changes in the activity of surface water molecules (Damodaran & Rao, 2001). Nevertheless, if a critical surface protein concentration is reached, the subsequent protein unfolding and molecular reorientation alongside protein aggregation will be responsible for decreased water activity at the interface via increase of the effective area covered by the protein (Damodaran & Rao, 2001; Rao & Damodaran, 2000). In more detail, the interfacial aggregation is promoted by the exposure of previously buried hydrophobic sites towards the less polar phase (Dickinson, 2011). This structural rearrangement affects the secondary and tertiary structures of the protein, as previously shown for β-lactoglobulin at the hexadecane-water interface (Zhai et al., 2010), and leads to interactions – ranging from hydrogen bonding and hydrophobic interactions to disulphide bonds – between the closely packed protein molecules at the interface and thus to the formation of very thin viscoelastic interfacial films (Murray & Dickinson, 1996).

Heat and acid-induced gelation in bulk

Regardless of the following gelation process (heat or acid-induced), unfolding of the protein in bulk is generally induced by heating a protein slurry and follows the

mechanism described above in the section on hydrophobic properties. As described above in the section on protein solubility and aggregation behaviour, the heat-induced conformational changes then subsequently lead to the formation of soluble and insoluble aggregates. The formation of soluble aggregates, in particular, is a prerequisite for the formation of a continuous, space-spanning network (Ringgenberg et al., 2013). Aggregation is then followed by the arrangement of these aggregates into a three-dimensional network. For globular proteins, the microstructure of these networks is most commonly described as particulate or fibrillar, depending on the processing conditions such as pH and ionic strength as described in a review by Foegeding (Foegeding, 2006). However, Nieto-Nieto et al and Yang et al have also described the formation of polymer or percolating (i.e. porous, mesh-like) gel structures in heat and acid-induced oat protein gels (Nieto-Nieto et al., 2014; Yang et al., 2017).

In heat-induced gelation, network formation is generally achieved during the cooling step, and has been ascribed to the formation of hydrophobic interactions, hydrogen bonds and electrostatic interactions (O'Kane et al., 2004c; Sun & Arntfield, 2012). There is a range of studies describing various aspects of heat-induced gelation of pea protein, covering aspects from involved protein fractions and the ability of individual protein fractions to form gels, as well as applied extraction methods to varying environmental conditions during gelation (e.g. Bora et al., 1994; O'Kane, 2004; O'Kane et al., 2004b, 2004c, 2004a, 2005; Sun & Arntfield, 2010, 2011a, 2011b, 2012). Generally, the protein concentration was described as having a linear influence on gel strength determined as gel peak force from compression experiments (Bora et al., 1994) and the cooling rate influences the gel strength, i.e. slower rates lead to stronger gels in pea protein (O'Kane et al., 2005) and legumin gels (O'Kane et al., 2004c). This was caused by the formation of disulphide bonds in legumin gels (O'Kane et al., 2004c), whereas in pea protein gels depending on the pea cultivar, the formation of disulphide bonds or a convicilin content above a critical value may inhibit this effect (O'Kane et al., 2005).

For acid-induced gelation the heating step is succeeded by acidification. Most commonly, acidification is achieved via the addition of glucono-δ-lactone or via fermentation. While there is extensive literature on fermentation-induced gelation of soy protein (i.e. towards soy protein-based yoghurt alternatives) (e.g. Cheng et al., 1990; Chumchuere & Robinson, 1999; Donkor et al., 2007; Grygorczyk & Corredig, 2013; Hu et al., 2013; S.-Y. Lee et al., 1990; X. Peng & Guo, 2015; H. L. Wang et al., 1974; Yazici et al., 1997), literature on other sources of protein such as e.g. quinoa (Zannini et al., 2018), lupine (Hickisch et al., 2016) and oat (Brückner-Gühmann, Banovic, et al., 2019; Brückner-Gühmann et al., 2019; Yang et al., 2017) is scarce and so far none exists on the fermentation-induced gelation of pea protein.

In general, the gelation process via fermentation is induced by a gradual decrease of pH which results in a corresponding neutralisation of negatively charged side chains of the protein. A decrease in net charge, in turn, changes the balance between repulsive electrostatic interactions and attractive van der Waals interactions (Mezzenga & Fischer, 2013), thus promoting attractive interactions via hydrophobic effects (Guo & Ono, 2006; Kohyama et al., 1995). Consequently, acid-induced gelation is generally believed to be based on non-covalent interactions, however, pre-gelation aggregation during the

heating step may involve disulphide bonds as derived from studies on soy protein, where various soluble disulphide bound aggregates were formed as described above in the section on protein solubility and aggregation behaviour, thus disulphide bonds may indirectly contribute to the network properties.

Influence of enzymatic hydrolysis on bulk and interfacial network formation

Enzymatic hydrolysis can be applied to modify the network-forming properties of proteins, both in bulk and at the interface. Generally, molecular, physico-chemical and functional properties of hydrolysed proteins depend on the size, charge and polar/non-polar properties of the generated peptides. Enzymatic hydrolysis of plant proteins was previously described for various combinations of protein source, enzyme and dispersed system to address a wide range of research objectives. Nevertheless, so far there have only been a few studies on the enzymatic hydrolysis of pea protein (Barac et al., 2011, 2012; Braudo et al., 2006; Humiski & Aluko, 2007; Karamac et al., 1998, 2018; Schwenke et al., 2001; Tamm et al., 2016) and even fewer consider emulsification properties of pea protein hydrolysates (Barac et al., 2011, 2012; Humiski & Aluko, 2007; Tamm et al., 2016). Out of these only Tamm et al pay closer attention to the interfacial properties of these hydrolysates and so far, no one has investigated the bulk gelation of pea protein hydrolysates.

Humiski and Aluko found the emulsifying properties of pea protein hydrolysates obtained by hydrolysis with trypsin, Alcalase®, Flavourzyme®, papain or chymotrypsin to depend on the balance between charge and peptide size but ascribed more importance to a high level of charge (Humiski & Aluko, 2007). In two studies Barac et al. investigated functional properties of hydrolysates obtained by hydrolysis of protein from two different pea genotypes with papain, chymosin and a commercial protease (*Streptomyces griseus protease*) at various degrees of hydrolysis and pH values between pH 3 and pH 8 and found an increased solubility at pH values close to pI, and various influences on emulsification behaviour depending on pH, degree of hydrolysis and applied enzyme (Barac et al., 2011, 2012). Besides describing the emulsifying and antioxidative properties of tryptic and Alcalase® generated pea protein hydrolysates with different degrees of hydrolysis, Tamm et al. investigated the interfacial properties of these hydrolysates at pH 8 and found tryptic hydrolysates to form stronger, more elastic interfacial films, and to decrease oil droplet size and lipid oxidation. Alcalase® had an adverse effect (Tamm et al., 2016).

Since no literature exists on the bulk gelation behaviour of pea protein hydrolysates, investigations on other plant-derived proteins are considered to describe the impact of hydrolysis with various enzymes (Alcalase®, Flavourzyme®, Protamex®, papain, trypsin) on their gelation behaviour in bulk. In a study on oat protein hydrolysates, Nieto-Nieto et al. hydrolysed with Flavourzyme®, Alcalase®, pepsin and trypsin, and found improved gel strength in heat-induced oat protein hydrolysate gels upon applying Flavourzyme® and trypsin, and impaired gelation properties in Alcalase® and pepsin hydrolysates (Nieto-Nieto et al., 2014). According to Meinlschmidt et al., hydrolysis of soy protein with Alcalase® reduced the gelation properties (increase in least gelling concentration) but hydrolysis with papain or a mixture of papain and Flavourzyme® increased the gelation properties (decrease in least gelling concentration) (Meinlschmidt et al.,

2016). Protamex® was shown to reduce the storage modulus G‘ of heat-induced gluten gels (J. Wang et al., 2006).

Manuscript I[1]:

Functionalisation of pea protein by tryptic hydrolysis – characterisation of interfacial and functional properties

Food Hydrocolloids (2019), 86, 134–140.
https://doi.org/10.1016/j.foodhyd.2018.03.013

Authors

Martina Klost [a*]

Stephan Drusch [a]

[a] Technische Universität Berlin, Department of Food Technology and Food Material Science, Königin-Luise-Str. 22, 14195 Berlin, Germany

[1] *Isoelectric point was abbreviated as IEP in the original publication but was changed to pI in this thesis to ensure consistent nomenclature with regard to the other manuscripts.*

Abstract

With regard to applications in dispersed systems (i.e. emulsions), improving the poor solubility of pea protein in the pH-range applicable to foods (pH 3 to pH 7) is a prerequisite. To achieve this, a pea protein concentrate was produced on a lab scale using alkaline extraction and subsequent enzymatic hydrolysis to degrees of 2 and 4%. Solubility was improved and interfacial properties were influenced. All samples led to the formation of emulsions but displayed a tendency towards wider oil-droplet size distributions at pH close to the isoelectric point. Using microscopy, this increase could be attributed to the formation of aggregates, which in turn can be ascribed to lack of repulsion caused by the low absolute values of ζ-potentials. The same lack of repulsion led to stronger and more elastic interfacial films at pH 4 and 5 than at pH 7. Moreover, film strength increased significantly with increasing degree of hydrolysis. Dilatational experiments imply that hydrolysis enhances in-plane structural rearrangements. Thus, it is concluded that tryptic hydrolysis has the potential to improve the overall stability of emulsions.

Keywords: pea protein; hydrolysis; emulsion; interfacial properties

I 1 Introduction

Emulsions generally are thermodynamically and kinetically unstable systems (McClements, 2016). Gravimetrical separation, as in creaming or sedimentation and droplet aggregation, are the most common mechanisms of emulsion instability and often occur in combination (McClements, 2007). Aggregation can be divided into flocculation and coalescence. In flocculation individual oil-droplets form aggregates, without merging with each other, while coalescence describes the fusion of two adjoining oil-droplets (McClements, 2016). Lack of repulsion can lead to aggregation, and the resultant increase in particle-size can thus support creaming (Fennema, 2017). Additionally, the close proximity of oil-droplets in flocculated and/or creamed emulsions may in turn enhance the tendency to coalesce (McClements, 2007). Therefore, in order to prevent destabilisation of emulsions by creaming and flocculation, electrostatic and steric interactions need to be mainly repulsive (McClements, 2004). Furthermore, the ability of interfacial membranes to resist deformation is a key countermeasure to coalescence. One means to promote low deformability are oil-droplet sizes <1 μm (Robins et al., 2002). Another means is to attain highly elastic interfacial films, which should be composed of molecules that show low tendencies to detach from or to be compressed at the interface (Yarranton et al., 2007), making them able to counteract a decrease of the surface to volume ratio during potential oil-droplet fusion.

In order to be able to incorporate proteins in dispersed food systems, the protein needs to be able to dissolve in the continuous phase. Plant-derived proteins in general and pea protein specifically display low solubilities at pH-values relevant to food systems. Pea protein consists mainly of globular proteins (approx. 60% (Gueguen & Barbot, 1988)) that can be divided into legumin, vicilin and convicilin fractions. The first is a hexameric 11 S fraction (~360 kDa), consisting of six subunits (~60 kDa), each a combination of an acidic α-chain (~40 kDa) and a basic β-chain (20 kDa) (Croy et al., 1979; Croy, Gatehouse, Evans, et al., 1980). The second is a trimeric 7 S fraction (~180 kDa), consisting of three subunits (~50 kDa) (Gatehouse et al., 1981), and the

third a tetrameric fraction (~290±40 kDa) consisting of four subunits (~71 KDa) (Croy, Gatehouse, Tyler, et al., 1980). One possible approach to improve protein solubility is controlled enzymatic hydrolysis (Barac et al., 2011; Soral-Smietana et al., 1998). As the change in peptide profile and size cannot only increase solubility, but can also influence other functional properties (Barac et al., 2011; Tamm et al., 2016), hydrolysis may be used to tailor functionalities such as interfacial properties, which in turn can influence the emulsifying behaviour (Avramenko et al., 2013; Henning et al., 1997; Krause & Schwenke, 1995). Close attention has to be paid to the enzyme selection, the hydrolysis parameters, and the degree of hydrolysis applied since functional properties can also be impaired under certain conditions (Avramenko et al., 2013; Barac et al., 2011; Tsumura et al., 2005). For studies on faba-bean (Henning et al., 1997; Krause & Schwenke, 1995) and soy-proteins (Ochiai et al., 1982), an improvement in emulsifying properties was connected to the emergence of legumin-T. As for emulsifying properties of pea protein hydrolysates, only little research is available. Barac et al., (2012) used papain and a commercial protease, in combination with different pea genotypes, and found an overall tendency toward improved emulsifying properties after hydrolysis. Humiski & Aluko, (2007) compared the effect of different enzymes on the emulsifying properties of pea protein hydrolysates and identified the smallest oil-droplet size when using trypsin. Tamm, et al. (2016) reported that oil-droplet size decreased for emulsions stabilised with tryptic hydrolysates of a commercial pea protein but increased for alcalase hydrolysates. So far, only Tamm, et al. (2016) looked into the interfacial properties of pea protein hydrolysates and described an increase in the elastic proportions up to DH 4. However, these authors only chose parameters away from both the pI and the pH range relevant to food applications.

The current study therefore aims to estimate the suitability of trypsin hydrolysis of pea protein for emulsion stabilisation in the context of molecular structure and interactions at a pH region relevant to food applications. It is expected that enzymatic hydrolysis will improve the solubility of pea protein, will positively influence interfacial properties of the protein, and will consequently lead to an increase in emulsion stability without affecting the oil-droplet size.

I 2 Materials and methods

I 2.1 *Materials*

Dried peas were supplied by Emsland-Stärke GmbH (Emlichheim, Germany), Cremer Oleo (Hamburg, Germany) provided MCT-oil. All materials and chemicals for SDS page were purchased from BioRad Laboratiories GmbH (München, Germany) and all other lab chemicals were purchased from Carl Roth GmbH + Co.KG (Karlsruhe, Germany), Merck and Sigma Aldrich (both Life Science bei Merck, Darmstadt, Germany) and of analytical grade.

I 2.2 Methods

Unless stated differently, all further experiments were carried out as a single determination for the pea protein concentrate (PPC) as well as for each pea protein hydrolysate (PPH), leading to a determination in duplicate for DH 2 and DH 4, respectively.

I 2.3 Pea protein concentrate (PPC) preparation and hydrolysis

PPC was produced on lab scale: dry peas were ground and the flour then dispersed in 0.0375 M NaOH. After 2.5 h of extraction at room temperature, the sample was centrifuged (5000 g, 20 °C for 30 minutes) followed by lyophilisation of the supernatant. Enzymatic hydrolysis was conducted as described by Tamm, et al. (2015) with modifications. In brief, PPC was dissolved in distilled water and the pH value adjusted (0.1 M HCl / 1 M HCl). Tryptic hydrolysis (Trypsin from bovine pancreas, Sigma (cat#T8003, EC:3.4.21.4, ~10000 BAEE units/mg Protein)) was conducted at pH 8 and 45 °C using the pH-stat method and a h_{tot}-value of 7.2 meqv/g protein. According to the pH-stat method, the DH was set by calculation and use of the amount of NaOH required to achieve the desired DH. The enzyme to substrate ratio was 1:1620 for DH 2 and 1:810 for DH 4. Hydrolysis was stopped by heating samples at 75 °C for 30 minutes, cooling on ice to room temperature (approx. 20 minutes), and then lyophilizing. Pea protein hydrolysates (PPH) were attained at degrees of hydrolysis of 2 and 4% (DH 2 and DH 4); PPC may occasionally be referred to as DH 0. Hydrolysis was carried out in duplicate for each degree of hydrolysis.

I 2.4 Solubility

50 g of a solution containing 5% protein were prepared in distilled water and the pH-value was subsequently adjusted to pH 8, 7, 6, 5, 4 and 3 using 0.1 M / 1 M HCl. Two aliquots of 2 ml were taken at each pH, one of which was measured directly, while the other one was first centrifuged at 13000 g for 15 minutes before determining the protein content in the supernatant (Method according to Dumas (Dumatherm N64+, Gerhardt, Königswinter, Germany), protein conversion factor 6.25). Solubility was calculated as percentage retained after centrifugation.

I 2.5 Molecular weight distribution

SDS-PAGE was carried out on 4-15% Criterion™ TGX™ Precast Midi Protein Gel according to the BioRad Bulletin 4110001. 10 µl of sample (0.1%in sample-buffer, non reducing conditions (Biorad 2xLaemmli Sample, Cat# 161-0737)) were applied to the gel alongside lanes of the molecular weight marker (5µl, Thermo Fisher PageRuler™ Prestained Protein Ladder, 10 to 180 kDa, Cat# 26616). Running buffer was Biorad 10xTris/Glycine/SDS Cat# 161-0732. Photographs of the gel were then transformed to peaks using an image processing program (image J). The molecular weights of the individual bands were calculated using a calibration slope obtained via standardised measurements of the marker bands and matched to individual protein-fractions based on values given in literature. Size exclusion chromatography (SEC) was performed at room temperature (HPLC ÄKTAbasicTM 10 system, Amersham Biosciences, Uppsala, Sweden)

with samples of 1% protein in 0.1 M phosphate buffer. Samples were filtered and passed over a Superdex 200 Increase 10/300 GL (GE healthcare GmbH, Solingen, Germany) column using 0.1 M phosphate buffer as the eluent and an UV detector at 280 nm for detection. Evaluation took place via a set of standards ((GE healthcare GmbH, Solingen, Germany): feritin (440 kDa), aldolase (158 kDa), conalbumin (75 kDa), ovalbumin (44 kDA), carbonic anhydrase (29 kDa), ribonuclease (13.7 kDa), aprotinin (6.5 kDa)) and the calculation of molecular weights based on the calibration-substances. Both methods were carried out once for the concentrate and once for each degree of hydrolysis at selected pH-values.

I 2.6 ζ-potential

For the determination of the ζ-potential, solutions of 0.3% protein were prepared in distilled water, the pH was adjusted to pH 3, 4, 5, 6 and 7 (0.1 HCl/ 1 M HCl), and the ζ-potential was measured in triplicate (Zetasizer Nano-ZS, Malvern Instruments GmbH, Germany).

I 2.7 Emulsifying properties

For emulsifying experiments, 300 g of protein solutions were prepared in distilled water. The protein content was calculated under consideration of solubility results, aiming at contents of soluble protein > 1.05%. The pH was adjusted to 3, 4, 5, 6 and 7 (0.1 HCl/ 1 M HCl) followed by centrifugation (10000g, 20 min., 20 °C), determination of the protein content and dilution of the supernatant to 1.05% protein. Pre-emulsification was carried out in a mixture of 10 g purified MCT-oil and 190 g protein-solution at 21500 rpm for 90 s using an Ultra-Turrax (T25 basic, IKA, Germany) followed by high pressure homogenisation (Panda Plus, Niro Soavi, Germany) at 300 bar and 3 passes. Within five minutes of emulsifying the oil-droplet size distribution (D10, D50, D90 and Span) of the emulsion was measured (Horiba, Retsch Technology GmbH, Haan, Germany). For further examination, microscopic pictures of the emulsions were taken.

I 2.8 Interfacial properties

All experiments were carried out with 0.25% protein solutions from the supernatants of the centrifugation step at pH 4, 5 and 7 (adjusted with 0.1 HCl/ 1 M HCl) at the MCT-oil-water interface. Oscillatory shear-measurements were performed using a rheometer (Physica MCR 301 / 102, Anton Paar GmbH, Ostfildern, Germany) equipped with a biconical disk geometry. Formation of an interfacial film was monitored over 12 h at 20 °C (deformation 0.1%, frequency 1 Hz). For evaluation, the dynamic complex interfacial shear modulus $|G_i^*|$ was calculated using the Rheoplus software. Oscillatory dilatational measurements were performed using a pendant drop tensiometer (OCA 20 Dataphysics GmbH, Germany) with an oscillation drop generator (ODG20, Dataphysics). After interfacial aging of 30 minutes, a frequency sweep was performed ($\Delta A/A$=3%, f=0.01 Hz – 1 Hz). From this sweep at the lowest frequency the complex dilatational modulus |E*| was calculated by the SCA 20 software.

I 3 Results and Discussion

I 3.1 Characterisation of tryptic digestion

All fractions at DH 0 showed typical patterns in SDS-PAGE (Fig I 1a) and SEC (Fig I 1b) chromatograms. In the SDS-PAGE profile, beside a wide range of peaks at lower molecular weights, the main storage proteins legumin (~60 kDa) (Croy, Gatehouse, Evans, et al., 1980), convicilin (~70 kDa) (Croy, Gatehouse, Tyler, et al., 1980) and vicilin (~50 kDa) (Gatehouse et al., 1981) could be seen in their monomeric forms. SEC showed the typical quaternary conformation of those proteins: hexameric (~380 kDa (Danielsson, 1948) (331 kDa) (Croy et al., 1979) (390kDa)) for legumin and trimeric (~160 kDa (Danielsson, 1948) (186 kDa)) for vicilin. Convicilin could not clearly be identified in SEC. The fractions of smaller molecular weights observed in both the SDS-PAGE and SEC profiles cannot as easily be matched to specific protein fractions, they are likely to be the different vicilin fractions (Gatehouse et al., 1981) as well as of pea albumin and trypsin inhibitors (Ma et al., 2017).

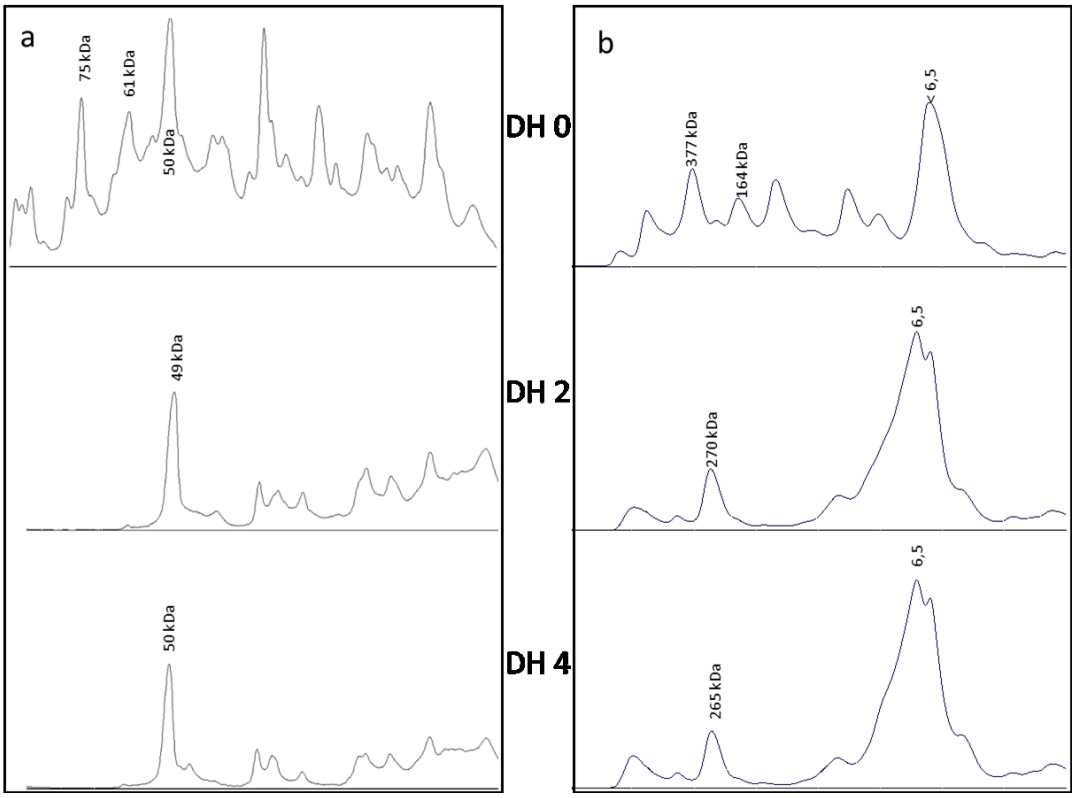

Fig I 1 molecular weight distribution of PPC and PPH DH2 and DH 4 as shown in a) SDS-page and b) SEC-chromatography, both at pH 7

After hydrolysis, DH2 and DH4 led to similar molecular weight patterns: convicilin, legumin and vicilin were no longer detectable in the SDS-PAGE profile. Instead a variety of smaller peptides as well as one prominent peak at ~47 kDa appeared. In SEC, one peak remained at ~265 kDa, whereas all other structures were reduced to significantly smaller peptides. Gatehouse, Lycett, Delauney, & Croy, (1983) described the first enzymatic attacks on vicilin as usually occurring at two potential sides, which display a high

density of polar amino acids and are therefore likely to be located at the molecule's surface. As can be seen from SEC, the quaternary structure of vicilin was lost with hydrolysis. As the convicilin peak (SDS-PAGE) fully disappeared, it is concluded that convicilin was fully digested to small peptides.

Tryptic attack on pea legumin starts at the C-terminus of the α-chain, (Braudo, et al. 2006) and thus exposes the hydrophobic β-chain and generates a variety of small peptides carrying a high density of charged side chains. It is also known that with limited hydrolysis legumin-T, a very ordered structure (M=200±50 kDa (Plumb et al., 1989)) with a nearly intact tertiary structure and improved techno-functional properties (Krause & Schwenke, 1995; Ochiai et al. 1982) remains. The improvement in functionality is attributed to the more flexible structure of the α-chain and the increased availability of hydrophobic patches from the β-chain combined with the otherwise nearly intact structure (Schwenke, 2001). The appearance of peaks at ~47 kDa (SDS-Page) and ~265 kDa (SEC) after hydrolysis leads to the conclusion that in this study legumin-T was produced.

I 3.2 Solubility, electrostatic properties and emulsification

Hydrolysis led to a significant increase in solubility from 30% (DH 0) to approximately 60% (DH 4, pH 5) at pH 4 to 6 (Fig I 2). This was caused by the increased amount of terminal carboxyl- and amino-groups (Panyam & Kilara, 1996) with these results supported by the findings of Soral-Smietana, et al. (1998). An impaired solubility at pH 3 and 7 for the hydrolysed samples is in accordance with the findings of Barać et al. (2011); Tsoukala, Papalamprou, Makri, Doxastakis, & Braudo, (2006) and Tsumura et al. (2005). All authors relate this to the increased exposure of interior hydrophobic residues, which can cause aggregation, insolubility and sedimentation of individual peptide fractions. The small peptides from hydrolysis of legumin are likely to aggregate and therefore to be responsible for the decrease in solubility and seem to have had an impact on the electrostatic properties of the hydrolysates (Fig I 3) as well.

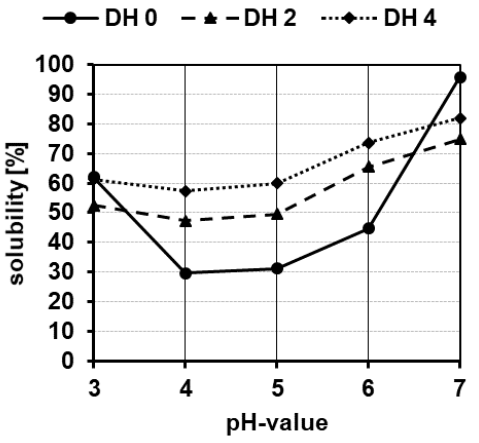

Fig I 2 solubility profiles of pea protein concentrate and corresponding hydrolysates in dependence of pH-value

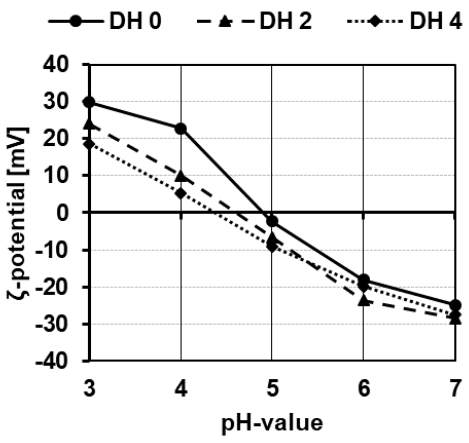

Fig I 3 ζ-potential profiles of pea protein concentrate and corresponding hydrolysates in dependence of pH-value

With increasing degree of hydrolysis, a shift in ζ-potential could be observed (Fig I 3), moving the pI from pH 4.91 (DH 0) to pH 4.60 (DH 2) and pH 4.37 (DH 4), respectively. Ochiai, et al. (1982) described a similar effect when investigating tryptic hydrolysis of soybean proteins. In the present study it is concluded, that the fractions involved in the aggregation and decrease of solubility at pH-values away from the isoelectric point must consist of more basic than acidic amino acids. Trypsin hydrolysis was carried out at pH 8 and cleavage occurred at the C-terminus of basic amino acids (Braudo et al. 2006). Therefore, it is likely that small, mainly basic peptides from legumin may be close to their isoelectric points and aggregate. This, in turn, would lead to a larger fraction of acidic amino acids in the soluble peptides. The more acidic amino acids a polypeptide contains, the more protons required to bind to all dissociated carboxyl-groups, thus leading to a decrease in the isoelectric point.

In visual assessment of emulsions, creaming was observed close to the isoelectric point. Fig I 4a shows the oil-droplet size distribution of freshly formed emulsions stabilised with PPC and the corresponding absolute values of the ζ-potentials. Where oil-droplet size was bimodal, this is depicted by two stacked boxes above each other representing the D10, D50 and D90 of each peak. It is apparent that low ζ-potentials and therefore low electrostatic repulsion led to wider oil-droplet distributions and bimodality. As all these factors implied a possible formation of aggregates from individual small oil-droplets, microscopic pictures of the emulsions were taken (Fig I 4b) for confirmation. Thus, creaming was concluded to be caused by aggregation.

Hydrolysate-stabilised emulsions displayed a similar behaviour at DH 2 (Fig I 5a), while at DH 4 an increase in aggregation at pH 7 and an overall increased oil-droplet size was determined (Fig I 5b). Where oil-droplet size distributions were wide or bimodal, microscopic pictures again showed aggregation of small, individual oil-droplets rather than an increase in the size of single droplets. While for DH 0 and DH 2, the increase in measured oil-droplet-size and the tendency to aggregate could be attributed to the lack of electrostatic repulsion, whereas, the increased tendency of DH 4 samples to aggregate at pH 7 was most likely due to hydrophobic interactions resulting from increasing amounts of exposed hydrophobic patches with continued hydrolysis. This is in accordance with Henning, et al. (1997) and Krause & Schwenke, (1995) who also described an initial improvement of emulsifying properties, followed by a decline when hydrolysis was carried out too extensively. A sufficient resistance to coalescence at all considered pH-values was indicated by the formation of oil-droplets <1 µm, as deduced from the microscopic pictures in combination with the size of the smaller oil-droplets in bimodal distributions (Robins, et al 2002). As even a few minutes after emulsification, no monomodal distributions could be found, aggregation was presumed to occur almost immediately. However, the initial formation of small oil-droplets at all pH-values pointed to the general ability of the protein and its hydrolysates to rapidly form stable interfacial films.

It can be summarised that lack of electrostatic repulsion played a key role in this study in the formation of flocs. However, the formation of individual oil-droplets with sizes <1µm implied a low tendency to coalescence. Particularly in flocculated emulsions, the risk of subsequent coalescence is enhanced. Therefore, the interfacial properties of

PPC and PPH were examined in order to further estimate the stability of emulsions attained with either sample.

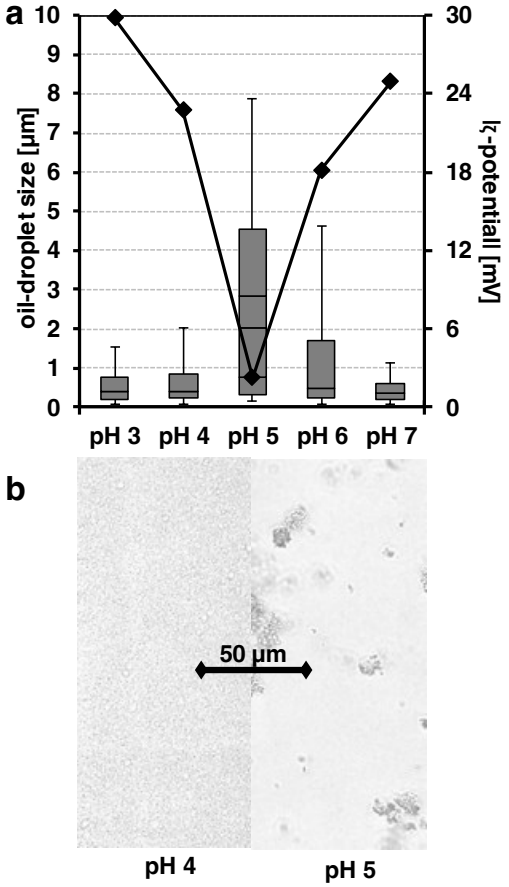

Fig I 4 a) oil-droplet size distribution and absolute values of ζ-potential and b) selected microscopic pictures for PPC

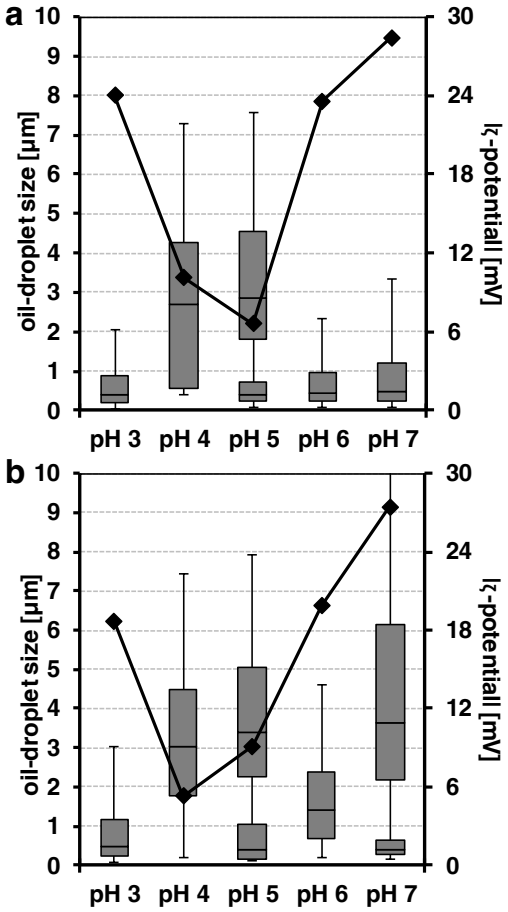

Fig I 5 oil-droplet size distribution and absolute values of ζ-potential for a) DH 2 and b) DH 4

I 3.3 Interfacial rheology

Charge, molecular size and the availability of hydrophobic patches can influence a protein's interfacial properties (Chang et al., 2015). While lack of electrostatic repulsion leads to aggregation in emulsions and is therefore unwanted, it plays a key role in the formation of interfacial films by enhancing the formation of interactions between individual protein molecules in the interface (i.e. via hydrophobic interactions), in turn leading to stronger interfacial films (Fennema, 2017). The complex interfacial shear modulus $|G_i^*|_{12h}$ decreased with increasing pH and decreasing degree of hydrolysis, indicating stronger intermolecular interactions at lower pH-values and with increasing DH (Fig I 6a). The influence of both DH and pH was found to be significant. In the present study, the interfacial dilatational modulus |E*| (Fig I 6b) showed a similar but less pronounced tendency as $|G_i^*|$, leading to the conclusion that intermolecular interactions were accompanied by additional effects specific to area changes. While the elastic proportions of PPC-films decreased with increasing pH, no significant influence on the loss factor tan δ (Fig I 6c) of either PPH could be found, implying that despite the lower

viscoelasticity of interfacial films at higher pH values, the ratio between elastic and viscous parts was not affected. These results were in accordance with the findings derived from the slopes of the dilatational frequency sweep (Fig I 6d). At slopes <0.1, mainly in-plane structural rearrangements (Wan et al., 2016) could be assumed for all hydrolysed samples. As a value of 0.5 would indicate desorption of molecules from the interface and their interchange with the bulk, a mix of in-plane rearrangements and desorption needed to be considered for PPC.

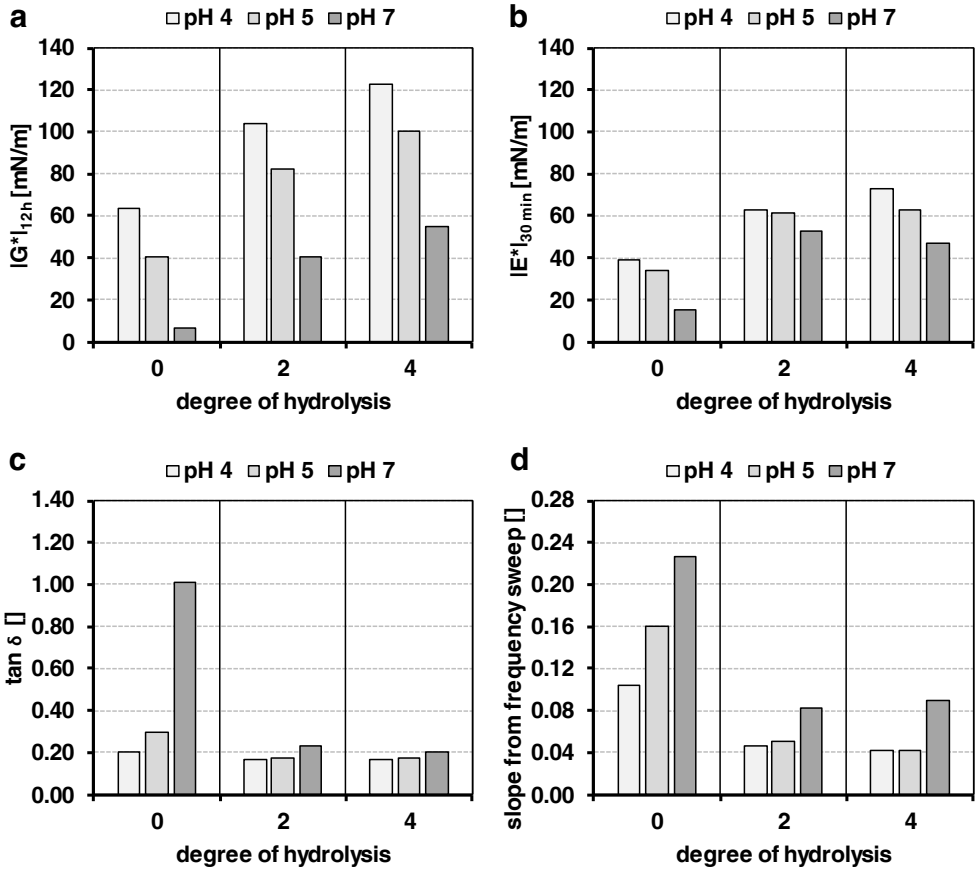

Fig I 6 a) |G_i|12h, b) E*|30min, c) | tan δ12h and d) slope of the frequency sweeps from dilatational experiments*

It was hypothesised, that different interactions must dominate in hydrolysed and unhydrolysed samples, but throughout the considered pH-values, interactions in all hydrolysed samples must be similar in nature. Both, hydrophobic and electrostatic interactions can influence film formation. Assuming an increasing hydrophobicity after hydrolysis (Braudo et al. 2006), especially at pH 7, the ratio between charge and hydrophobicity will shift. In PPC at pH 7, electrostatic repulsion was strong but hydrophobic attraction would have been low, changing to low electrostatic repulsion with low hydrophobicity at pH 5 and higher hydrophobicity and strong electrostatic repulsion at pH 4. Consequently, an overall dominance of electrostatic repulsion with increasing pH occurred. In contrast, the increased hydrophobicity attained through hydrolysis led to a decline in the influence of the pH on the balance between electrostatic and hydrophobic interactions, thus interfacial films of the PPHs demonstrated similar viscoelastic behaviour over a wide pH range.

In summary, interfacial films formed by PPHs, in comparison to PPC, displayed an increase in film strength while maintaining a high proportion of elastic properties independent of pH Moreover, PPH are estimated to be less susceptible to protein interchange between interface and bulk.

I 4 Conclusions

The downside of conditions where electrostatic repulsion is low is that creaming, due to aggregation of small individual oil-droplets, is favoured. The upside is that these very same conditions are highly beneficial in improving parameters that indicate stable interfacial films. In this study, samples at DH 2 combined a small oil-droplet size, high elastic proportions of the interfacial film and a low tendency for the desorption of protein molecules from the interface and therefore are likely to resist coalescence. Generally, aggregation in a dispersed system is considered to be detrimental. However, in the past decade, research has started to focus on exploitation of this property by using aggregates for creating turbidity in non-alcoholic beverages, heteroaggregates for simulating creaminess in low calorie foods and encapsulation of bioactives. In this context, tryptic hydrolysates of the present study represent a biomaterial with improved functionality.

Acknowledgements:
The authors gratefully acknowledge the skill-full experimental work of Marina Eichhorn, Sarah Gleisenberg and Karla Kern.

Funding:
This work was supported by the "Competence Cluster Nutrition Research" funded by the Federal Ministry of Education and Research, Germany (FKZ: 01EA1408C)

CRediT authorship contribution statement:[2]
M.Klost: Conceptualization, Writing – original draft, Writing – review & editing, Formal analysis, investigation, Data curation, Visualization. S. Drusch: Supervision, Writing - review & editing, Funding acquisition, Resources

[2] This was not part of the original manuscript, but was added upon writing this thesis to clearly state the contributions of each author

Manuscript II[3]:

Structure formation and rheological properties of pea protein-based gels

Food Hydrocolloids (2019), 94, 622–630.
https://doi.org/10.1016/j.foodhyd.2019.03.030

Authors

Martina Klost [a,b*]

Stephan Drusch [a,b]

[a] Technische Universität Berlin, Department of Food Technology and Food Material Science, Königin-Luise-Str. 22, 14195 Berlin, Germany

[b] NutriAct – Competence Cluster Nutrition Research Berlin-Potsdam

[3] Isoelectric point was abbreviated as IEP in the original publication but was changed to pI in this thesis and intercycle strain / deformation was abbreviated as γ in the original publication but was changed to γ_0 in this thesis to ensure consistent nomenclature with regard to the other manuscripts.

Abstract

Nutritional recommendations for the elderly, but also the general public, include incorporation of plant proteins in the diet, an increase in the intake of Ω-3 fatty acids and an increase in intake of dietary fibre. Protein structure and structuring behaviour of plant proteins differ from that of milk proteins. Therefore, the aim of the presented study was to characterise the structuring process and resulting structure of yoghurt-style gels containing 10% pea protein with and without addition of nutritionally recommended ingredients like rapeseed-oil and/or commercial oat fibre. Rheological measurements were combined with microscopy for sample characterisation. Generally, all studied formulations were able to form acid-induced gels via fermentation. The acidification led to a two-phase gelation process resulting in thick gels that showed mainly weak rheological behaviour. Supplementation with oil and/or fibre resulted in an increase of the relative concentration of pea protein in the aqueous phase and led to a strong increase in the complex shear modulus |G*| as well as the maximum structuring velocity d|G*|/dt. These effects need to be considered when tailoring yoghurt-style gels with high consumer acceptance.

Keywords: plant protein, gelation, fermentation, rheology, oat fibre, rapeseed-oil

II 1 Introduction

In the light of steadily increasing life expectancy in developed countries, improvement of health and well-being in general and healthy aging in particular are key challenges. It is known, that plant proteins may be beneficial in the prevention of chronic degenerative diseases (Krajcovicova-Kudlackova et al., 2005). Additionally the demand for an increased fibre intake as well as the benefits that derive from the intake of unsaturated fatty acids (European Food Safety Authority & EFSA, 2010b, 2010a) are to be considered when designing products to support healthy ageing. A suitable product-category for incorporation of the required amounts of protein, oil and fibre are yoghurt-type gels. Yoghurt is associated with protein-rich food and has a high consumer acceptance (Banovic et al., 2018). Traditionally, yoghurt is based on dairy ingredients. The casein fraction of milk possesses a unique micellar structure, which leads to a specific gelation behaviour. (W. J. Lee & Lucey, 2010). The gel structure forms at the isoelectric point (pI) of casein during acidification of milk (W. J. Lee & Lucey, 2010) and dairy-based yoghurt gels are particulate on a microscopic scale (Lucey & Singh, 1997).

When partly or fully substituting dairy proteins during yoghurt processing the underlying mechanisms for gel formation are similar. There has already been extensive research on many aspects of a variety of plant-derived proteins. Besides cereal and oil seed proteins, pulse proteins have been in focus in the past. Within the pulse family interest in pea is increasing due to its ability to easily grow all over the world and an easily removable hull (Day, 2013). Molecular interactions during gel formation are mainly non-covalent in nature and may include hydrogen bonding, electrostatic and hydrophobic interactions (Kohyama et al., 1995). However, due to differences in protein structure and course of fermentation plant protein-based systems may show very different structuring behaviour. Several studies focused on partial replacement of dairy proteins in yoghurt

and the impact on yoghurt structure (Yousseef et al., 2016; Zare et al., 2013) and taste (Denkova et al., 2015; Yousseef et al., 2016). In contrast, the structuring behaviour and gel properties upon fermentation of pea protein alone have not been investigated in detail. The few studies covering pea protein used glucono-δ-lactone for acidification (Ben-Harb et al., 2018; Mession et al., 2015). However it is well described in literature that kinetics of acidification and structure formation during microbial fermentation may differ from kinetics when using glucono-δ-lactone (Grygorczyk & Corredig, 2013).

It is widely accepted, that proteins need to undergo some heat induced unfolding and pre-aggregation in order to be able to form gels by acidification. Therefore, studies generally employ a heating step above the denaturation temperature of the protein to ensure sufficient network formation during acidification. However, there are studies that report incomplete unfolding of globular proteins even above the denaturation temperature (Hirose, 1993) and structural changes below the denaturation temperature (Miriani et al., 2011), where proteins may assume a molten globule state. N. Chen, Zhao, Chassenieux, & Nicolai, 2016 described a strong time dependence for the formation of self-similar aggregates in soy globulins at a wide range of temperatures (50 to 95 °C). The same authors also described the ability of native soy globulins to form self-assembled aggregates and found this ability to be concentration- and charge-dependent (N. Chen et al., 2016a). Moreover, hydrophobic interactions between exposed groups have been described to lead to aggregation between globular protein molecules while still in the molten globule state (Ochenduszko & Buckin, 2010). It is therefore likely that pea protein in concentrated suspensions will be able to pre-aggregate to a certain extend below the denaturation temperature.

Structure formation may additionally be affected by supplementation with other food constituents. When considering the literature on yoghurt supplementation with various fibres it becomes obvious, that textural properties are affected in various ways as shown for orange fibre (Sendra et al., 2010), passionfruit fibre (Espírito-Santo et al., 2013), asparagus fibre (Sanz et al., 2008), pea fibre (Damian & Olteanu, 2014), soy, rice, oat, corn, sugar beet fibre (Fernández García & McGregor, 1997), wheat bran fibre (Aportela-Palacios et al., 2005) and fibre rich pineapple peel (Sah et al., 2016). Since commercial fibre may vary in the ratio of soluble and insoluble constituents, particle size and resulting functional properties, little is known about the general mechanisms behind these effects. Insoluble particles may act as active or inactive fillers. While inactive fillers have little chemical affinity for the matrix, active fillers normally interact strongly with the gel (J. Chen & Dickinson, 1998) and influence water-holding, microstructural and rheological properties (Gu et al., 2009; Keogh & O'Kennedy, 1998; Tang et al., 2011). The ability of fillers to interact with the gel matrix – making them active or inactive –depends on the filler particles surface properties (Dickinson & Chen, 1999). To our knowledge, so far there is no literature available on fibre-protein-interactions in protein-based gels or on the categorisation of fibres into active or inactive fillers. The oat fibre used in this study contained a minimum of 90% insoluble fibre of which 75% are cellulose. The remaining part most likely consists of hemicelluloses and lignin. Cellulose, hemicelluloses and lignin are described to be mostly non-ionic. While cellulose and hemicelluloses carry hydroxyl-groups at their surface, making them hydrophilic, lignin is more hydrophobic. Molecular properties similar to cellulose and hemicelluloses can be observed in intact

starch granules (α(1-4)-linked D-glucose). From literature it is known, that crosslinked waxy maize starch does not directly interact with milk proteins in acidified milk gels (Azim et al., 2010).

The supplementation of acid-induced protein gels with oil has previously been described in the context of filled emulsion gels by various authors (Ben-Harb et al., 2018; Dickinson, 2012; Gu et al., 2009; Li et al., 2012; Tang et al., 2011). Gel systems that contain emulsified oil droplets are known as emulsion gels. Dickinson, 2012 distinguishes between emulsion-filled protein gels and protein-stabilised emulsion gels based on the dominating network structure. Literature usually considers protein-stabilised oil-droplets as active fillers due to their affinity to the gel matrix (Dickinson, 2012) with their role in the gel network strongly depending on the interactions between interfacial and bulk proteins (Tang et al., 2011). Active fillers are known to decrease tan δ (Dickinson & Chen, 1999; Gu et al., 2009) and may increase the storage modulus G' (Ben-Harb et al., 2018; Dickinson & Chen, 1999).

The presented study aims to investigate the structuring process during fermentative gelation of pea protein and the properties of the gel as well as the effect of supplementation with nutritionally favourable food ingredients like rapeseed oil and/or oat fibre. The experimental design, ingredient choices and sample compositions of this study are therefore motivated by nutritional recommendations for the ageing population: increased intake of plant protein, dietary fibre and unsaturated fatty acids.

II 2 Materials and methods

Within this study, different samples were formulated which contained pea protein (P), or pea protein in combination with rapeseed oil (PO), oat fibre (PF) or both (POF). For the characterisation of structure formation and gel properties, rheological measurements were performed during and after the fermentation process. Conclusions drawn on the structure were supported by microscopy.

Dried peas were supplied by Emsland-Stärke GmbH (Emlichheim, Germany), ADM WILD Europe GmbH&Co.KG (Hamburg, Germany) provided rapeseed oil and Herbafood Ingredients GmbH (Werder (Havel), Germany) the oat fibre Herbacel Classic Plus HF 04. The oat fibre contains 68% cellulose (as determined by determination of glucose content after Seaman-Hydrolysis) and a minimum total of 90% insoluble fibre according to the manufacturer's specification. Soluble fibre content accounts for a maximum of 5.6% with negligible amounts of pectic substances (galacturonic acid content below 0.5% as determined by m-hydroxydiphenyl method). All lab chemicals were purchased from Carl Roth GmbH + Co.KG (Karlsruhe, Germany), Merck and Sigma Aldrich (both Life Science at Merck, Darmstadt, Germany) and were of analytical grade. Yoghurt culture containing *Lactobacillus delbrueckii* ssp. bulgaricus and *Streptococcus thermophilus* (YC-X11 Yo-Flex®) was provided by Chr. Hansen Holding A/S (Hoersholm, Denmark).

Pea protein was produced on lab scale as previously described in more detail (Klost & Drusch, 2019a). Briefly, dry peas were ground and the flour was dispersed in 0.0375 M NaOH leading to an initial pH value of approximately 8.7 which dropped to just above pH 8 during the extraction time. After 2.5 h of extraction at room temperature, the sample

was centrifuged (5000 g, 20 °C for 30 minutes) and the supernatant was lyophilized. The resulting protein powder had a protein-content of 53.8%, 3.5% water, 1.6% starch, 7% sucrose, 4% fat and ~17% raffinose family sugars, calculated as stachyose.

II 2.1 Characterisation of pea protein in solution

Unfolding and pre-aggregation of protein molecules is generally acknowledged as a prerequisite for acid-induced gelation of proteins. Therefore, the pea protein solution was characterised prior to fermentation via intrinsic fluorescence and temperature-sweep rheology to determine protein unfolding and pre-aggregation in the protein solutions during the applied heat treatment.

In intrinsic fluorescence measurements, a protein-solution (0.1% (w/w), pH 6.5) was exited at a fixed wavelength (290 nm) and the emission-wavelength was scanned between 300 and 400 nm (Cary Eclipse Fluorescence Spectrophotometer (Agilent Technologies, Victoria, Australia)). The wavelength at maximum emission was then used to characterise structural changes as a red shift in the maximum emission wavelength generally indicates protein unfolding. Additionally, protein solutions (10% (w/w), pH 6.5) were swept in a rheometer (MCR 502, Anton Paar, Austria (couette system CC 27) (f = 1Hz, deformation γ_0 = 0.1%)) to determine aggregation via increase in viscosity.

Both experiments were conducted at the same heating regime: heating from 20 to 60 °C with a heating rate of 1 K/min followed by a holding time of 60 minutes at 60 °C and subsequent heating from 60 to 80 °C (rate 1 K/min) and further 15 minutes of holding. In the rheometer values of temperature T and complex viscosity |η*| were taken at regular intervals. Scans in the fluorescence Spectrophotometer were performed before heating, after holding at 60 °C and after holding at 80°C. The experiments were carried out in duplicate.

II 2.2 Relative protein concentration depending on sample composition and water retention capacity of supplements

Table II 1 composition of the samples (content in 100 g sample), the water retention capacity of the fibre, the calculated available water and the relative protein content of all samples

Sample	Pea protein [g]	HCl 0.025 M [g]	Oil [g]	Fibre [g]	Water retention capacity [g water/ g fibre]	Available water [g]	Relative protein content [%]
P	18.53	81.47	-	-	-	81.47	10.83
PO	18.53	77.47	4	-	-	77.47	11.27
PF	18.53	78.47	-	3	5.2	57.67	13.96
POF	18.53	74.47	4	3	5.2	53.67	14.64

(Samples: P = pea protein, PO = pea protein and rapeseed-oil, PF = pea protein and fibre, POF = pea protein, rapeseed-oil and fibre)

Table II 1 shows the composition of all samples. The protein-concentration in all samples was kept constant at 10% (w/w). Consequently, the total amount of water in the samples decreased with increasing supplementation. Additionally, the water retention

capacity of the fibre (5.2 g water/g fibre) decreases the availability of water even further. The relative protein concentration in the samples is considered to be the concentration that can be calculated when the amount of protein is only related to the amount of available water instead of the net weight of the sample. Calculated values are given in Table II 1.

II 2.3 Sample preparation, fermentation and analysis of structure formation

Pea protein was dissolved in 0.025 M HCl to achieve a final protein concentration of 10% (w/w) and a pH of approximately 6.5. The suspension was mixed by rotor-stator homogenisation (Ultraturrax T25 basic, IKA, Germany, 90 s, 21500 rpm). In case of fibre supplementation, 3% (w/w) fibre were suspended in the 0,025 M HCl, and passed through a high-pressure homogeniser (Panda Plus, Niro Soavi, Germany) at 7.5 MPa. Pea-protein was then dissolved in the fibre-dispersion. The protein or protein-fibre dispersion was heated to 60 °C for 60 min for pasteurisation adjusted from (Krämer, 1997) who described low temperature pasteurisation at 65°C and 30 minutes. Heating was followed by cooling at room temperature for 15 min. The pasteurisation-temperature was chosen just below the denaturation temperature of the pea protein in order to not overly damage the protein structure while achieving some unfolding to induce gelation via fermentation later. Afterwards, the samples where passed through a high-pressure homogeniser (Panda Plus, Niro Soavi, Germany) at 3 MPa. In case of supplementation with rapeseed-oil, 4 % (w/w) oil was added prior to homogenising. Starter culture (YC-X11 Yo-Flex®) was added, and after 10 minutes of stirring the blend was fermented in a water bath at 43 °C for 18 h, while constantly tracking the pH-value (SI Analytics Lab 865, Xylem, USA).

Gels and gelation processes can be monitored by rheology. During gelation the cross-over of storage modulus G' and loss modulus G'' (loss-factor tan δ = 1) can be considered as "gel-point" (Morris et al., 2012) and the structuring velocity can be used to estimate the end of the structuring process. Therefore, approximately 20 mL of the mix were fermented in a rheometer for 18 hours (Rheometers were Physica UDS and MCR 502, Anton Paar, Austria (couette system Z 3 DIN and CC 27 respectively) (f = 1Hz, deformation γ_0 = 0.1%). At least one repetition for each experiment was performed in each rheometer) in order to study structure formation. |G*| and tan δ were chosen for the rheological characterisation of the structuring process. They are defined as

$$|G*| = G' + i \cdot G'' \qquad \text{(II 1)}$$

and

$$\tan\delta = \frac{G''}{G'} \qquad \text{(II 2)}$$

For the characterisation of maximum structuring velocity the first derivative of |G*| (d |G*|/dt) was calculated (Grosso & Rao, 1998) using the software Origin 9.0, OriginLab, USA .All samples were prepared in triplicate and stored at 6 °C for 24 – 30 h after fermentation.

II 2.4 Rheology of fully set gels

Rheology classifies gels into strong and weak gels. Strong and weak gels behave differently in texture and rheology-experiments. A strong gel is characterised by low dependence of G' and G'' on frequency, values of G' that exceed G'' by at least one order of magnitude and linear relation between log |η*| and log ω with a slope close to -1 (Morris et al., 2012). Additionally, strong gels remain strain independent up to deformations of 25%, but will rupture and be irreversibly destroyed under larger deformations (Ross-Murphy & Shatwell, 1993). In contrast, weak gels may begin to flow at an increase of frequency and deformation, but are able to restructure afterwards (Ross-Murphy & Shatwell, 1993).

In the present study, all rheology tests of fully set gels after 24-30 hours were performed at the Physica UDS, Anton Paar, Austria. $|G^*|_{24\text{-}30\,h}$ and $\tan\delta_{24\text{-}30\,h}$ (γ_0 = 0.1 % and 1 Hz) were measured after sample-resting at 6 °C in beakers. Prior to measurement, the samples were carefully spooned into the rheometer cup. Frequency sweeps were carried out at a constant deformation of γ_0 = 0.1% and frequencies ranging from 0.01 to 10 Hz. For evaluation, the slopes of logG', logG'' and log |η*| over log ω = 2πf were calculated in order to characterise gel behaviour. Amplitude sweeps were carried out at a frequency of 1 Hz and amplitudes from γ_0 = 0.1% to γ_0 = 5000%. The deformation at the end of the linear viscoelastic regime (LVE) was calculated as the largest deformation where |G*| deviates from the original value by less than 5% (Mezger, 2006). The yield point is the point where tan δ becomes >1 (*DIN Technical Report No. 143*, 2005) and the deformation at this point was used for further evaluation. For thixotropy tests according to *DIN SPEC 91143-2*, 2012, oscillation at γ_0 = 0.1% and f = 1 Hz was applied for 100 s, followed by shearing at a rate of γ = 200 s^{-1} for 2 min and another 10 min of oscillation. The loss of structure was calculated as

$$\Delta G' = \left|100\% - \frac{G'_{end}\cdot 100\%}{G'_{start}}\right| \qquad \text{(II 3)}$$

and

$$\Delta G'' = \left|100\% - \frac{G''_{end}\cdot 100\%}{G''_{start}}\right| \qquad \text{(II 4)}$$

II 2.5 Scanning electron microscopy (SEM)

After storage for 24 h at 6 °C, approx. 3 g of fermented sample were filled into 20 mL plastic beakers, frozen by immersing the beaker into liquid nitrogen and stored at -20 °C prior to lyophilisation. Lyophilised samples were carefully broken into pieces and the breakage site was gold sputtered in a sputter coater SCD 030 (Balzers, Wiesbaden-Nordenstadt, Germany). The microstructure was analysed by SEM at the Center for Electron Microscopy (ZELMI), Technische Universität Berlin, Berlin, Germany by the S-2700 scanning electron microscope (Hitachi, Tokyo, Japan); magnification was 300x and 3000x. SEM was carried out once for each formulation.

II 2.6 Statistic evaluation

All fermentation and rheology experiments were carried out in triplicate and evaluated using a one factorial ANOVA followed by a post hoc test (Tukey) to determine

differences between samples with different formulations (Origin 9.0, OriginLab, USA). Normal distribution was tested by Kolmogorov-Smirnov-Test.

II 3 Results and Discussion

II 3.1 Characterisation of pea protein – unfolding and aggregation behaviour upon heating

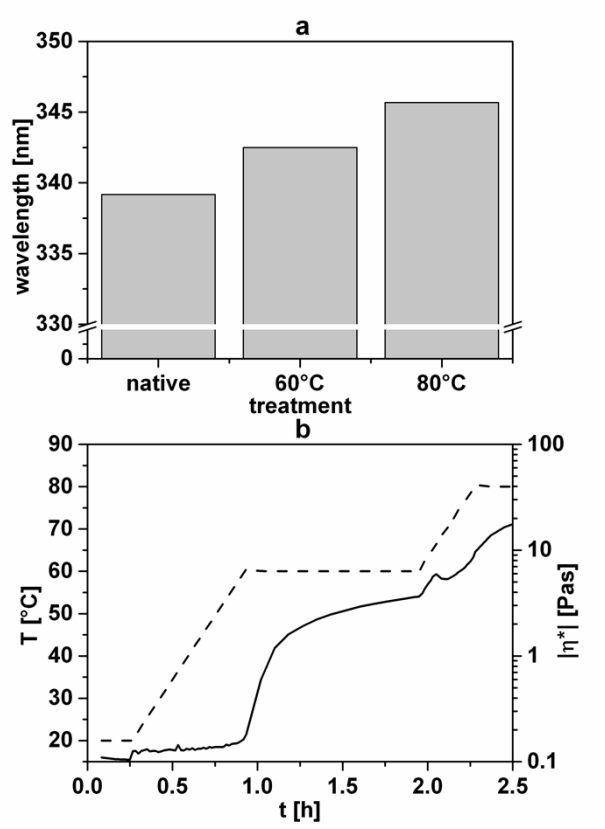

Fig II 1 change in intrinsic fluorescence (a) and complex viscosity (|η|) (b) induced by heating 10% pea protein to 60 and 80 °C. (|η*| closed line, T dashed line)*

Upon heating of diluted pea protein solution to 60 °C followed by holding for 60 minutes, in intrinsic fluorescence measurements a red shift of approximately 3 nm occurred. Further heating to 80°C led to a further shift of additional 3 nm (Fig II 1a). Even though the red shift is more pronounced at 80 °C, it becomes obvious, that with the applied heating regime the pea protein used in this study already undergoes considerable unfolding and exposure of previously buried hydrophobic regions, which will enable it to form intermolecular interactions, despite not being heated beyond the denaturation temperature. This is also supported by the results from rheological temperature sweep (Fig II 1b). In this experiment a 10% (w/w) protein-solution was heated to 60 °C, held for 60 minutes and then heated to 80 °C and held for an additional 15 minutes. Just below 60 °C the complex viscosity |η*| began to increase from approximately 1.3 Pas to 3.7 Pas at the end of the holding time at 60°C where G' exceeded G'' by almost an order of magnitude. |η*| reached a local maximum at of 5.9 Pas at 66 °C and then continued to increase to 18.3 Pas after holding for 15 minutes at 80 °C. Considering data from intrinsic fluorescence and rheological temperature sweeps, we propose some unfolding of the protein at 60 °C accompanied by intermolecular interactions, which leads to an increase in viscosity. As heat-induced aggregation has been described to be a prerequisite for acid-induced gelation, we expect the heat treatment applied to be sufficient for use in further experiments. However, from the data it also becomes obvious, that unfolding and pre-aggregation would be more pronounced in samples that were heated above the denaturation temperature. However, since the desired protein-content of 10% is considerably higher than that of milk-based yoghurts, there is

no need to take full advantage of intermolecular interactions and pre-aggregation as it may lead to an undesirably strong texture and consistency of the final gels.

II 3.2 Structure-formation during fermentation

This section covers the changes of pH value and complex shear modulus |G*| during and after fermentation as well as the influence of supplementation with rapeseed oil and / or oat fibre on structure formation. By combining those results with results from ζ-potential measurement and scanning electron microscopy, we deduce information on the nature of the structuring process and on the gel structure itself.

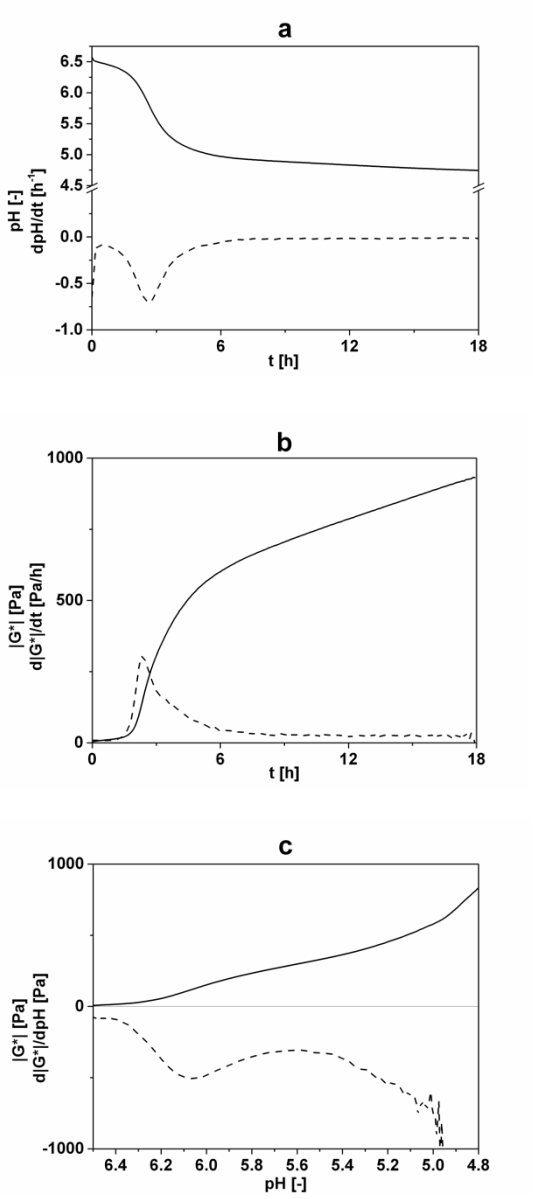

Fig II 2 development of pH (a) and complex shear modulus |G| (b) over time and |G*| over pH (c) during the fermentation process of samples containing oil and fibre. Development of the parameters (closed lines) is shown alongside their first derivations (dashed lines). Curves for all samples are provided in supplementary material (Appendix Fig A 1, Fig A 2 and Fig A 3)*

The main driving force in network formation and structuring of acid-induced protein gels is the decrease in pH-value. This in turn leads to changes in electrostatic properties and molecular interactions and therefore to an increase in the structure parameters |G*|, G', G'' and a decrease in tan δ. Upon fermentation of pea protein concentrate dispersions with and without oil and/or fibre supplementation, a major drop in pH-value from ~pH 6.6 to ~pH 4.7 (Table II 3) – caused by microbial digestion of sucrose from pea-protein to lactic acid – occurred within the first six hours of fermentation time (Fig II 2 a) and reached its maximum velocity after approx. 2.6 to 2.9 hours with no significant differences between the samples (Table II 2). This is in contrast with Fernández García & McGregor, 1997 and McCann, Fabre, & Day, 2011 who described an accelerated acidification rate for various fibres and linked this to a supply of additional nutrients and the natural acidity of the fibres respectively. However, the oat fibre used in our study contains a maximum of 5% soluble fraction and is therefore not believed to supply relevant amounts of additional nutrients. As expected, the drop in pH was accompanied by a decrease in the loss factor tan δ below one as indicated by complex shear modulus |G*| increasing rapidly (Fig II 2 b) and G' exceeding the loss modulus G'' (data not shown).

Table II 2 maximum values for d|G|/dt and dpH/dt and the corresponding values for time and pH. pH values at maximum and minimum values for* d|G*|/dpH.

Sample	$d\|G^*\|/dt_{max}$ [Pa/h]	$t_{d\|G^*\|/dt\ max}$ [h]	$pH_{d\|G^*\|/dt\ max}$ [-]	dpH/dt_{max} [h^{-1}]	$t_{dpH/dt\ max}$ [h]	$pH_{dpH/dt\ max}$ [h]	$pH_{d\|G^*\|/dpH,\ min}$ [-]	$pH_{d\|G^*\|/dpH,\ max}$ [-]
P	128^{a} ± 9	2.33^{a} ± 0.09	5.89^{a} ± 0.05	-0.944^{a} ± 0.13	2.64^{a} ± 0.05	5.65^{a} ± 0.04	5.5	6.0
PO	157^{a} ± 14	2.33^{a} ± 0.00	6.00^{a} ± 0.37	-0.970^{a} ± 0.06	2.89^{a} ± 0.53	5.55^{a} ± 0.54	5.5	6.1
PF	234^{b} ± 10	2.39^{a} ± 0.05	5.87^{a} ± 0.10	-0.886^{a} ± 0.12	2.67^{a} ± 0.09	5.52^{a} ± 0.13	5.5	5.9
POF	308^{c} ± 31	2.36^{a} ± 0.05	6.00^{a} ± 0.12	-0.741^{a} ± 0.21	2.79^{a} ± 0.21	5.75^{a} ± 0.10	5.6	6.1

(Samples: P = pea protein, PO = pea protein and rapeseed-oil, PF = pea protein and fibre, POF = pea protein, rapeseed-oil and fibre)
*Different letters within a column denote significant differences between individual samples as found by one factorial ANOVA followed by Tukey postHoc Test

Table II 3 complex shear modulus |G| at d|G*|/dtmax, at the end of the fermentation-process (18 h) and after 24-30 h storage at 6 °C. Loss factor tan δ at the end of the fermentation-process (18 h) and after 24-30 h storage at 6 °C.*

Sample	$\|G^*\|_{d\|G^*\|/dt\ max}$ [Pa]	$\|G^*\|_{ferm.\ end}$ [Pa]	$\|G^*\|_{24\text{-}30\ h}$ [Pa]	$\tan\delta_{ferm.\ start}$ [-]	$\tan\delta_{ferm.\ end}$ [-]	$\tan\delta_{24\text{-}30h}$ [-]	$pH_{ferm,start}$ [-]	$pH_{ferm,\ end}$ [-]
P	44^{a} ± 6.4	452^{a} ± 27	720^{a} ± 25	>1	0.164^{a} ± 0.005	0.266^{a} ± 0.002	6.55^{a} ± 0.03	4.69^{a} ± 0.03
PO	62^{a} ± 6.1	521^{a} ± 59	741^{a} ± 46	>1	0.146^{a} ± 0.015	0.255$^{b.c}$ ± 0.001	6.56^{a} ± 0.09	4.65^{a} ± 0.04
PF	97^{b} ± 5.8	842^{b} ± 92	1295^{b} ± 80	0.67 ± 0.09	0.159^{a} ± 0.004	0.261$^{a.b}$ ± 0.004	6.53^{a} ± 0.05	4.68^{a} ± 0.03
POF	149^{c} ± 20	932^{b} ± 111	1388^{b} ± 37	0.71 ± 0.07	0.145^{a} ± 0.004	0.248^{c} ± 0.004	6.58^{a} ± 0.02	4.75^{a} ± 0.11

(Samples: P = pea protein, PO = pea protein and rapeseed-oil, PF = pea protein and fibre, POF = pea protein, rapeseed-oil and fibre)
*Different letters within a column denote significant differences between individual samples as found by one factorial ANOVA followed by Tukey postHoc Test

Structuring velocity reached its maximum after approximately 2.35 hours in all samples and significantly increased in magnitude from 127.4 ± 8.5 Pa/h (P) to 308.0 ± 30.8 Pa/h (POF) with increasing fortification (Table II 2). |G*| began to increase between pH 6.2 and 6.5 and a first maximum in the slope was seen around pH 6 followed by a decline until approximately pH 5.5 and a steeper increase toward pH 4.8 (Fig II 2c) indicating a two-step gelation process. This behaviour was differently pronounced but similar for all samples (Table II 2).

The onset of increase in G' and the first maximum in structuring velocity at pH 6 took place distinctly above the isoelectric points (pI) of the two major pea globulins (pH 5.5 for vicilin and pH 4.8 for legumin (Danielsson, 1950)). This is in contrast with the structuring process of yoghurts based on milk protein, where the formation of a three dimensional network occurs close to the isoelectric point (W. J. Lee & Lucey, 2010). Upon acidification with glucono-δ-lactone, Ben-Harb et al., 2017 described faster structuring in pea protein samples than in those consisting of milk protein. They did however not give any pH values at which the structuring occurred. Mession et al., 2015 reported gel-points at pH 6.7 for pea protein acidified with glucono-δ-lactone but offered no reference to this value being distinctly above the isoelectric point. Some explanations can be found in Grygorczyk & Corredig, 2013, who previously reported a gel-point at pH 6.29 ± 0.05 for soy-protein acidified via fermentation. They ascribe the early onset of structuring to aggregation of 11S basic subunits with β subunits of 7S molecules caused by their individual isoelectric points of pH 6.8-8.5 and pH 5.7-6 (Thanh & Shibasaki, 1976) respectively. In brief: these subunits begin to aggregate as their individual charges decline, starting to form a network by bringing individual molecules closer together. In our experiments, this accounts for the initial first increase in gel strength at pH 6. However, at this pH value, the overall electrostatic repulsion is strong enough to prevent uncontrolled aggregation of the acidic legumin subunits and the remaining vicilin units. This can be supported by SEM micrographs at 300-fold magnification (Fig II 3a), which shows an overall percolated network. Similar structures were found by (Yang et al., 2017) for the acid-induced gelation of oat protein by glucono-δ-lactone, even though in their case the underlying mechanism was described differently. As the pH decreased further, charges on the more acidic subunits reduced as they approached their isoelectric points. This in turn led to the formation of further intermolecular bonds and the pronounced increase in G' at pH values below 5.5. Most likely, this also led to the condensation of small aggregates at the previously formed structures leading to the rough appearance of the structure-surface in SEM pictures at 3000-fold magnification (Fig II 3b).

Despite no significant differences in pH curves, samples containing oil and/or fibre showed an increased structuring velocity. This increase could be correlated (R=0.97) to the relative protein concentration in the samples and was therefore more pronounced if samples contained fibre. This is well in agreement with Azim et al., 2010 who reported similar behaviour in samples where modified starch immobilised some of the continuous phase, thus increasing the relative protein concentration. Moreover, the relative protein concentration also correlated with the values of |G*| at various times throughout the fermentation process and subsequent storage (supplementary material, Fig A 4, Appendix). We therefore propose the increase in relative protein concentration to be the main cause for the increase in structuring velocities and |G*| values.

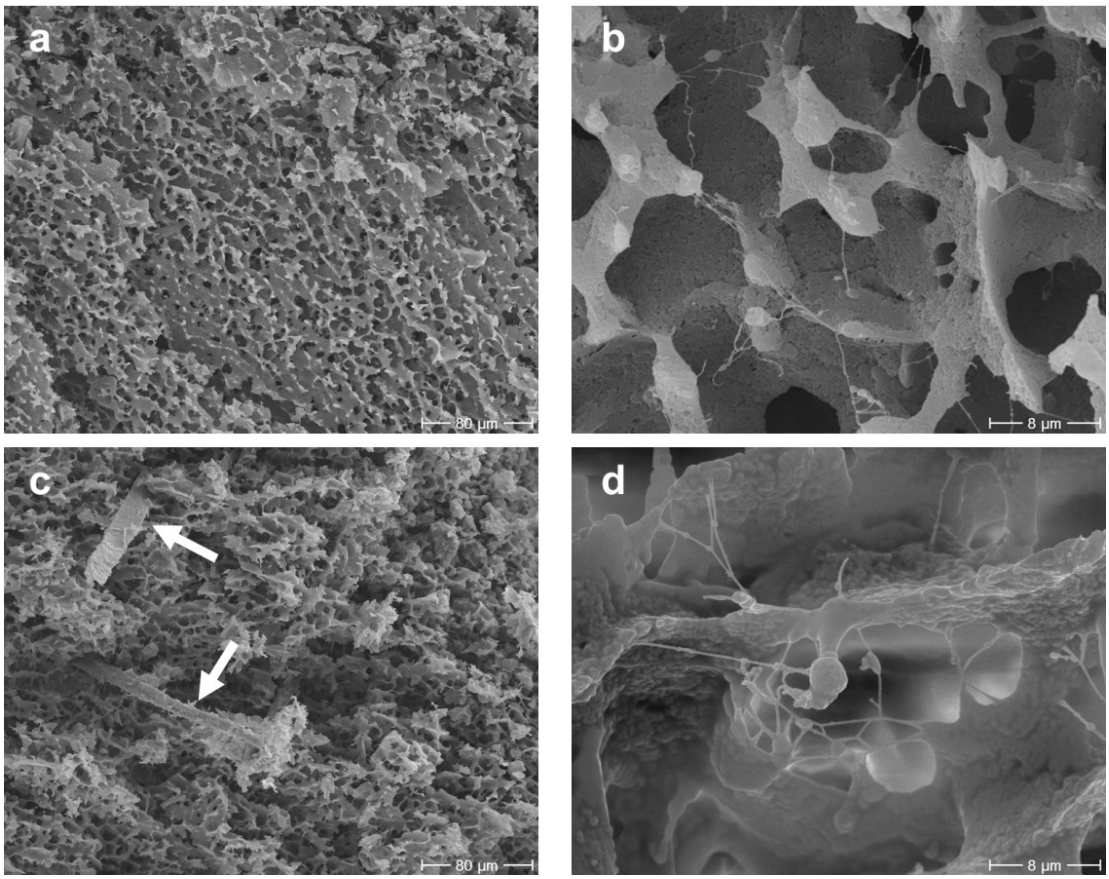

Fig II 3 SEM images of fermented pea protein gels. SEM of pea protein only at 300-fold (a) and 3000-fold (b) magnification, SEM of pea protein supplemented with fibre at 300-fold (c) and supplemented with oil at 3000-fold (d) magnification.

Additionally, in samples containing fibre tan δ values were < 1 (Table II 3) from the beginning of fermentation indicating a gel like structure throughout. On the one hand, this may have been caused by the increased relative protein content; on the other hand, fibres themselves may have been responsible for this effect. The general structuring behaviour of cellulose-rich fibre in aqueous environment was summarised by Kerekes, 2006. The author explains different models to describe restraint imposed on translational and rotational motion of individual fibres. In contrast to hydrocolloid and protein gels, the attracting effects in network-formation of fibre are mainly mechanic and are divided into hooking and friction (Derakhshandeh et al., 2011; Kerekes, 2006). In our samples, hooking and friction probably caused the formation of an initial fibre network, in turn leading to tan δ values < 1 even before the start of fermentation. As fermentation proceeded, the protein network started to form analogously to samples without added fibre, became dominant, and led to a continuous structure with embedded fibres (Fig II 3c). Within the protein network the fibre acts as nearly inactive filler due to its non-ionic and hydrophilic nature as previously described for starch by Corredig, Sharafbafi, & Kristo, 2011 and is therefore believed not to interact with the protein-network on a relevant scale. Domination of the protein network is further supported by the lack of significant differences in tan δ between supplemented and unsupplemented samples. This is in agreement with results on yoghurt enriched with functional

asparagus fibre, where the authors came to the conclusion, that the addition of fibre did not modify the structural organisation or the type of molecular interactions (Sanz et al., 2008).

When rapeseed oil was added to the samples, the oil was emulsified by the protein during the homogenisation step before fermentation. From a previous study (Klost & Drusch, 2019a) we know that a protein content of 1% is sufficient to stabilise 5% rapeseed oil. Samples in the current study contained 10% protein and 4% oil, leading to sufficient bulk protein for network formation. Consequently, these samples were expected to form filled emulsion gels where oil droplets are embedded in a continuous protein matrix as described by Dickinson, 2012. In the context of emulsion gels, literature usually considers protein-stabilised oil-droplets as active fillers due to their affinity to the gel matrix (Dickinson, 2012). In our study, during emulsification the pea protein stabilised small droplets of rapeseed oil by migrating to and unfolding and adsorbing at the interface (Damodaran, 2005). The extent of unfolding of soy protein at the interface was previously described to exceeded that of previous temperature induced unfolding (Miriani et al., 2011) and led to the exposure of buried hydrophobic areas. These areas orient towards the oil-phase (Wilde et al., 2004), while the charged areas point toward the aqueous phase (Ducel et al., 2004). At the same time the surface denaturation may also cause an increase in surface hydrophobicity of the emulsion droplets (H. J. Kim et al., 2002). Despite the change in interfacial protein conformation, due to the excess of bulk protein, the increase in relative protein concentration was still the main reason for increased structuring velocity and values for |G*| upon addition of oil. During the structuring process protein-covered oil droplets were embedded in the protein-matrix leading to the blistery appearance in SEM pictures (Fig II 3d). If both oil and fibre were added fibre was incorporated between the protein network (inactive filler) and the oil (active filler) leads to a blistery appearance of the protein network itself (pictures shown in supplementary material, Fig A 8, Appendix).

II 3.3 Rheological characterisation of the fully set gels

This section covers the values for |G*| and tan δ after storage for 24 hours at 4°C. Moreover, behaviour of the fully set gels in thixotropy tests, amplitude and penetration tests (large strain deformation) and frequency sweeps (small strain deformation testing), was investigated. As a result of some structural rearrangements upon resting and cooling |G*| and tan δ increased by approximately 1.5% and 1.7% respectively (Table II 3) during storage at 4°C for 24 h. The complex shear modulus increased due to the formation of more but probably very weak interactions leading to a more pronounced rise in the loss modulus G'' than in the storage modulus G' and therefore to larger values of tan δ. Supplementation with oil significantly reduced tan δ by approx. 4% (Table II 3), while |G*| was unaffected. The decrease in tan δ indicated a slight increase in elastic contributions to |G*| and is ascribed to the active filler properties of the oil. In a study on heat set whey protein emulsion gels active fillers decreased tan δ due to a less homogenous distribution of crosslinks in emulsified gels and in turn restricted the amount of viscous dissipation in small strain testing (Dickinson & Chen, 1999). In a different study the supplementation with varying amounts of oils to heat set soy-protein emulsions reduced tan δ with increasing oil concentrations (Gu et al., 2009). However, it is also known

that active fillers increase the storage modulus G' (Ben-Harb et al., 2018). This effect was dependent on the absolute magnitude of G' and references showed an increase in G' of approx. 20% at an oil to protein ratio of 5:6, steeply increasing at higher ratios (Dickinson & Chen, 1999). The small but significant decrease in tan δ in our study is in agreement with the described effects. The low ratio of oil to protein (2:5) is the reason for the small reduction in tan δ.

In thixotropy measurements (Fig II 4a), the gel was oscillated at parameters within the linear viscoelastic regime, consecutively sheared and again oscillated. The results (Table II 4) showed that intense shearing destroyed parts of the structure of the system irreversibly, while other parts restructured. Overall, G' and G'' regained around 60% of their former value in samples without fibre and around 50% in samples with fibre (Table II 5). All samples attained a gel state throughout the oscillation part of the experiment, as indicated by tan δ < 1. This indicated that restructuring occurred immediately after shearing and was not detectable in the experiment. Loss of structure after shearing was more pronounced in samples with fibre and may in all cases be attributed to the initial formation of smooth, linear structures at pH away from the isoelectric point during fermentation. At the pH-value of the set gels, the protein initially involved in the linear structure would re-associate in a more disordered manner after structure destruction thus lowering G' and G''. If fibres were present, these may have hindered some of the restructuring.

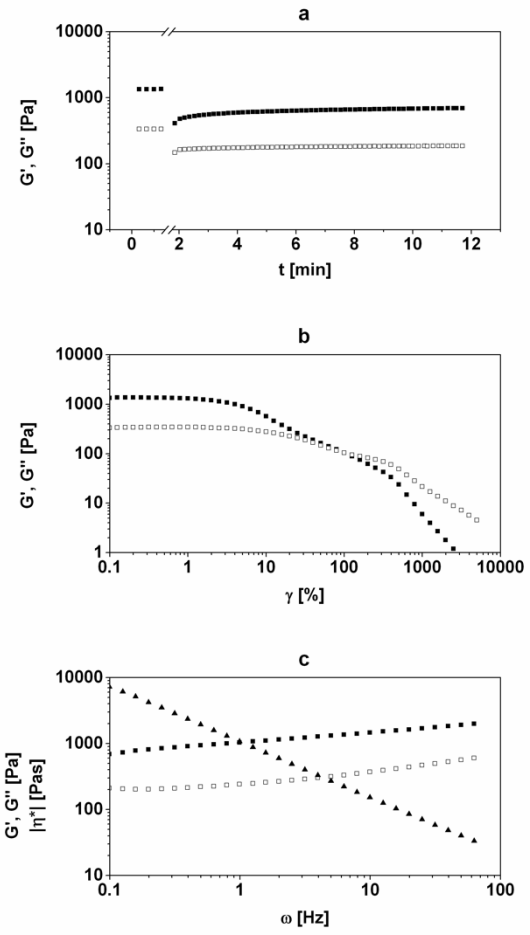

Fig II 4 rheological properties of fermented pea protein gels after 24-30 h storage (6 °C). Thixotropy test (a), amplitude sweep (b) and frequency sweep (c) of samples containing oil and fibre (■ G', □ G'', ▲ |η|). Curves for all samples are provided in supplementary material (Appendix Fig A 5, Fig A 6 and Fig A 7)*

In amplitude sweeps (Fig II 4b) the deformations at the maximum strain (Table II 4) within the linear viscoelastic regime did not differ significantly between the samples but were slightly lower in samples containing fibre which may be attributed to fibres' ability to disrupt inter-protein bonds (Espírito-Santo et al., 2013; Sendra et al., 2010). With values between 0.74% (PF) and 1.26% (PO) the maximum strains within the linear viscoelastic regime were found to be clearly below the required strain resistance for strong gels (up to at least γ_0 = 25% proposed by Ross-Murphy & Shatwell, 1993) and the curve from the amplitude sweep gradually declined

indicating a development towards flowing. This is also consistent with penetration tests where it was not possible to determine a classical breaking point (results not shown).

Table II 4 Data from amplitude sweeps (deformation γ_0 at the end of the linear viscoelastic regime and at the yield point. G'. G'' at the yield point) and thixotropy measurements (difference in G' and G'' after intense shearing). All measured after 24-30 h storage at 6 °C.

sample	$\gamma_{0,\text{ end LVE}}$ [%]			$\gamma_{0,\text{ yield point}}$ [%]			G', G''$_{\text{yield point}}$ [Pa]			ΔG' [%]			G'' [%]		
P	1.21^{a}	±	0.40	68.6^{a}	±	9	72^{a}	±	4	39.1^{a}	±	1.15	38.7^{a,c}	±	1.62
PO	1.26^{a}	±	0.00	56.5^{a}	±	21	98^{a}	±	24	35.5^{a}	±	2.15	33.9^{a}	±	2.18
PF	0.74^{a}	±	0.09	86.3^{a}	±	12	88^{a}	±	14	51.2^{b}	±	2.04	49.7^{b,c}	±	1.83
POF	1.00^{a}	±	0.00	93.2^{a}	±	12	105^{a}	±	9	48.5^{b}	±	1.73	44.3^{c}	±	2.52

(Samples: P = pea protein, PO = pea protein and rapeseed-oil, PF = pea protein and fibre, POF = pea protein, rapeseed-oil and fibre)

*Different letters within a column denote significant differences between individual samples as found by one factorial ANOVA followed by Tukey postHoc Test

Table II 5 Data from frequency sweeps (slopes of logG', logG'' and log|η| versus logω).*

Sample	dlogG'/dlogω			dlogG''/dlogω			dlog|η*|/dlogω		
P	0.192^{a}	±	0.005	0.200^{a}	±	0.004	-0.810^{a}	±	0.004
PO	0.183^{a,b}	±	0.002	0.188^{a,b}	±	0.021	-0.817^{a,b}	±	0.003
PF	0.179^{b}	±	0.004	0.168^{b}	±	0.011	-0.823^{b}	±	0.005
POF	0.163^{c}	±	0.005	0.155^{c}	±	0.008	-0.840^{c}	±	0.002

(Samples: P = pea protein, PO = pea protein and rapeseed-oil, PF = pea protein and fibre, POF = pea protein, rapeseed-oil and fibre)

*Different letters within a column denote significant differences between individual samples as found by one factorial ANOVA followed by Tukey postHoc Test

Results from frequency sweeps (Fig II 4c, Table II 5) were close to the behaviour of true gels:

- G' showed values approximately four times larger than G'' with some deviations at high frequencies. This indicates gel characteristics throughout the sweep.
- G' and G'' increased with slopes (dlogG'/dlogω and dlogG'/dlogω) of 0.15 (G'', POF) to 0.2 (G'' P), indicating a small frequency dependence of similar magnitude for all samples despite a significant decrease with increasing supplementation.
- The slopes of dlog|η*|/dlogω were between -0.81 (P) and -0.84 (POF) Pas/Hz in the double-logarithmic plot with significantly higher values in supplemented samples. These were however still of similar magnitude to each other.
- The decrease in slopes of G' and G'' as well as the increase in slope of |η*| can again be correlated to the relative protein content (R=-0.885, R=-0.983 and R=-0.877 respectively)

Even though these values are close to those described for true gels, they do not quite meet them. Despite the fairly low influence of frequency on G' and G'' they differ by less than an order of magnitude and even though dlog|η*|/dlogω shows linear behaviour, its slope distinctly differs from -1 and may be caused by the high protein content of the samples rather than by actual true gel properties. Liu & Tang, 2011 and C. H. Tang & Liu, 2013 reported similar slight but progressive increases of G' with increasing frequency in gel-like whey and soy protein emulsions and linked it to a non-covalently cross-linked gel-

structure. They also concluded, that even though tan δ was almost independent of frequency its values of around 0.3 indicated weak (and predominantly viscous) gels.

Given, that acidified protein generally tends to form gels via non-covalent bonds, we can assume, that despite the near true gel like behaviour in frequency sweeps, the gel investigated in our study can generally be considered weak in nature as confirmed by amplitude sweeps and large deformation rheology. The rheological behaviour of samples containing oil is close to an emulsion-filled protein gel as the results show a clear dominance of the protein-network (Dickinson, 2012) and the supplementation with fibre did only marginally influence parameters in frequency and amplitude sweeps. We therefore come to the conclusion, that supplementation with oil and/or fibre only had minor effects on the rheological properties of the samples which was consequently dominated by the protein network.

II 4 Conclusions

In all investigated samples pea protein was able to form gels upon fermentation after being heated to 60 °C (holding time 60 minutes). We assume a two-phase gelation process comprising the association of pea protein units with high isoelectric points into a linear and overall percolated network structure followed by condensation of aggregates at the structure-surface at the subsequent fast pH-decline leading to an increased gel strength. Supplementation with oil and/or fibre increased the maximum structuring velocity of the developing protein-network due to an increase in the relative protein concentration. During refrigerated storage some structural rearrangements occurred, mainly due to the formation of weak non-covalent links, which increased the viscous proportions of the gel. Rheological tests showed mostly weak gel properties. The protein network was the dominating structure, even though incorporated oil increased the elastic proportion of the system. Added fibre significantly increased |G*| due to increased net protein concentration and initial hooking and friction effects. Mostly, oil and fibre did not show any synergistic effects if added in combination but their effects coexisted. Therefore, pea protein was found to be a suitable alternative base for plant protein-based yoghurt alternatives. Moreover, the attained gels could be further supplemented with nutritionally valuable rapeseed oil and/or oat fibre, making them a promising approach for nutritional strategies related to improvement of health and well-being in general and healthy aging in particular. From a consumer's point of view, sensorial shortcomings of the pea protein yoghurt alternatives are the most important issue to be addressed in the future. Besides this, it is worthwhile to further investigate the material scientific properties of the system concerning clarification of the types of interactions involved in forming fermented pea protein gel systems and their respective contributions to the network.

Acknowledgments:
The Authors gratefully acknowledge the skilful lab-work of J. Nissen (SEM).

Funding:
This work was supported by NutriAct – Competence Cluster Nutrition Research Berlin-Potsdam funded by the Federal Ministry of Education and Research (BMBF) (FKZ: 01EA1408C)

CRediT authorship contribution statement:[4]
M.Klost: Conceptualization, Writing – original draft, Writing – review & editing, Formal analysis, investigation, Data curation, Visualization. S. Drusch: Supervision, Writing - review & editing, Funding acquisition, Resources

[4] This was not part of the original manuscript, but was added upon writing this thesis to clearly state the contributions of each author

Manuscript III[5,6]:

Enzymatic hydrolysis of pea protein: Interactions and protein fractions involved in fermentation induced gels and their influence on rheological properties

Food Hydrocolloids (2020), 105, 105793.
https://doi.org/10.1016/j.foodhyd.2020.105793

Authors

Martina Klost [a,b*]

Gerard Giménez-Ribes[c]

Stephan Drusch [a,b]

[a] Technische Universität Berlin, Department of Food Technology and Food Material Science, Königin-Luise-Str. 22, 14195 Berlin, Germany

[b] NutriAct – Competence Cluster Nutrition Research Berlin-Potsdam

[c] Physics and Physical Chemistry of Foods, Wageningen University, Bornse Weilanden 9, 6708WG Wageningen, The Netherlands

---

[5] intercycle strain / deformation was abbreviated as γ in the original publication but was changed to γ_0 in this thesis to ensure consistent nomenclature with regard to the other manuscripts.

[6] The research presented in this manuscript was part of Mr. Giménez-Ribes' internship work at TU Berlin. Parts of this manuscript were transferred from his internship report directly into this manuscript. These sections are clearly marked in this thesis.

Abstract

In the light of changing nutritional trends and recommendations, yoghurt style gels from plant proteins are a promising way to incorporate relevant amounts of plant derived proteins into the diet. However, in order to attain a high level of consumer acceptance, a thorough understanding of rheological behaviour, involved protein fractions and relevant interactions is mandatory in order to later be able to customise properties of fermentation induced gels. Therefore, the aim of this study was to first characterise the type of dominating interactions within the gel network and the protein fractions involved followed by determination of the rheological properties of gels made from pea protein and pea protein hydrolysates. Results showed that the protein-protein interactions were mainly hydrophobic in nature and involved mostly the legumin fraction. A smaller contribution could be ascribed to electrostatic interactions between vicilin and the basic legumin-β chain, thus incorporating some vicilin into the gel. The interaction between vicilin and the basic legumin-β chain was influenced by modification of the molecular weight distribution via enzymatic hydrolysis. Especially hydrolysis with trypsin led to an enhanced involvement of vicilin in the gel structure due to the increased availability of legumin-β. The molecular weight distribution only had a minor impact on the rheological properties of the fermentation induced pea protein gels leading to the conclusion that in rheology the type of interactions is more important, than the protein fractions involved.

Keywords: pea protein, gelation, fermentation, enzymatic hydrolysis, acid-induced

III 1 Introduction[7]

The consumption of plant proteins in northern and western Europe is steadily increasing and the accompanying market is growing (European Commission, 2018). Reasons for this vary from lifestyle choices to environmental and health issues. E.g. the substitution of animal derived proteins with those from plants was shown to prevent chronic degenerative diseases (Krajcovicova-Kudlackova et al., 2005) and pulses can be cultivated as catch crop, leading to environmental side benefits.

Some of the most popular vehicle foods associated with a high protein content are yoghurts and yoghurt-type products (Banovic et al., 2018). From a physicochemical point of view, yoghurt and yoghurt-type products are classified as protein gels. Gelation of proteins in general is achieved either by heat denaturation of proteins or by acidification for example via fermentation with lactic acid bacteria, as is the case in yoghurt and yoghurt-type products. Moreover, acid-induced gelation requires a heating step prior to acidification in order to unfold and partially denature the protein-molecules with formation of aggregates and soluble complexes due to the exposure of more hydrophobic amino acids (e.g. Ringgenberg et al., 2013). Subsequently, the gradual decrease of pH results in the neutralisation of the negatively charged amino acids, changes in the balance between electrostatic repulsion and van der Waals interactions (Mezzenga & Fischer,

[7] *Parts of the introduction were written by G. Giménez-Ribes as part of his internship report and transferred directly into this manuscript. This concerns some of the section on acid induced gelation and some of the section on the influence of enzymatic hydrolysis on gelation properties*

2013) and favours interaction through hydrophobic forces (Guo & Ono, 2006; Kohyama et al., 1995).

It becomes obvious that gelation of protein is always based on protein – protein interactions which might be non-covalent (such as hydrogen bonds, electrostatic attractive forces and hydrophobic interactions), or covalent, like disulphide bonds. One approach to determine dominating types of interactions are gel solubility experiments. These experiments are based on the cleavage of different bonds (e.g. disulphide bonds) and the interference with different interactions (e.g. hydrophobic and electrostatic interactions) via incubation of gels in different solvents (O'Kane et al., 2004c; Papalamprou et al., 2009; Utsumi & Kinsella, 1985). Rheological measurements may be used to describe the structuring process in time-sweep experiments and to indicate product behaviour during processing and transport via frequency and amplitude sweep experiments. Especially Large Amplitude Oscillatory Shear (LAOS) measurements can indicate product behaviour during processes like mastication that are well outside the linear viscoelastic regime. Additionally, haptic sensorial properties can be derived from rheology (Akhtar et al., 2005; Brückner-Gühmann, Banovic, et al., 2019).

Regarding the gelation of pea protein, most publications focus on heat induced gelation of isolated pea globular fractions (e.g. O'Kane et al., 2004c, 2004b) and/or pea protein in general (e.g. Sun & Arntfield, 2010, 2012) and most commonly only the influence of the globular fractions is discussed. Globular pea protein fractions (legumin, vicilin and convicilin) account for at least 60% of total protein (Gueguen & Barbot, 1988) and their molecular properties have been subject to extensive research in the past (Table III 1). The gelation mechanism for heat induced pea protein gels is mainly ascribed to hydrophobic interactions, hydrogen bonds and electrostatic interactions (e.g. O'Kane et al., 2004c; Sun & Arntfield, 2012). The relevant types of interactions may be influenced by enzymatic hydrolysis of the protein and in turn influence rheological gel properties, as – depending on the specificity of applied enzymes – the molecular weight decreases, the amount of ionisable groups increases and previously buried hydrophobic groups become exposed (Panyam & Kilara, 1996). Knowledge on customisation of rheological properties (e.g. via enzymatic hydrolysis) can in turn be very useful when tailoring haptic sensorial properties like texture or creaminess. So far the impact of hydrolysis on heat induced gels was studied with varying results: gel strength increased for soy proteins using Flavourzyme® or Alcalase® at a low degree of hydrolysis (Hrckova et al., 2009) and oat protein gel strength was improved using Flavourzyme® or tryptic hydrolysis (Nieto-Nieto et al., 2014). However, an impairment of gel formation for soy proteins using bromelain has also been observed (Lamsal et al., 2007). The only study investigating the effect of enzymatic hydrolysis on glucono-δ-lactone induced gelation of soy protein found that the gels have a softer texture and more syneresis with increasing degree of hydrolysis using subtilisin Carlsberg (Kuipers et al., 2005). To our knowledge, so far, the effect of hydrolysis on fermentation induced plant protein gels has not been investigated.

Table III 1 specific molecular parameters of pea globular proteins derived from literature

	parameter		reference
legumin	sedimentation coefficient	11S	
	quaternary structure	hexameric	
	molecular weight monomer	60 kDa	(Croy et al., 1979; Croy, Gatehouse, Evans, et al., 1980)
	subunits	acidic α-chain (40kDa) basic β-chain (20 kDa) linked via disulphide bond	(Croy et al., 1979; Croy, Gatehouse, Evans, et al., 1980)
vicilin	sedimentation coefficient	7S	
	quaternary structure	trimeric	
	molecular weight monomer	50 kDa	(Gatehouse et al., 1981, 1982)
	subunits	α+β, β+γ, α, β, γ peptides via post-translational autolysis	(Gatehouse et al., 1981, 1982, 1983; Lycett et al., 1983)
convicilin	quaternary structure	tetrameric	(Croy, Gatehouse, Tyler, et al., 1980)
	molecular weight monomer	71 kDa	(Crévieu et al., 1997; Croy, Gatehouse, Tyler, et al., 1980)
	N-terminus	Highly charged	(Bown et al., 1988)

Moreover, while in the area of fermentation induced plant protein gels in general considerable amounts of research exist on soy protein (e.g. Cheng et al., 1990; Donkor et al., 2007; Ferragut et al., 2009; Karleskind et al., 1991; Yazici et al., 1997), other protein sources such as oat (Brückner-Gühmann, Banovic, et al., 2019), lupine (Hickisch et al., 2016) and pea (Klost & Drusch, 2019b) have been less investigated so far but are believed to follow the general acid-induced gelation process outlined above. With regard to pea proteins we previously described its ability to form fermentation induced self-supporting gels and proposed a two-step gelation process that consists of the formation of an overall percolated network structure followed by condensation of smaller aggregates (Klost & Drusch, 2019b). However, there is no specific knowledge on the type and ratios of interactions participating in the formation and stabilisation of these gels or on the influence of hydrolysis on gel properties.

Therefore, the focus of this study is to investigate protein fractions and relevant interactions involved in fermentation induced gelation of pea protein. It was expected, that enzymatic hydrolysis with different enzymes would change electrostatic and hydrophobic properties of pea protein, in turn influencing rheological gel properties giving indications for future customisation of haptic sensorial properties.

III 2 Materials and methods

III 2.1 Materials[8]

Pea protein concentrate (LOT-Nr.: 16041801) (78% protein) was obtained from IGV (Institut für Getreideverarbeitung) GmbH, Nuthetal, Germany. Materials and chemicals used for SDS-PAGE were purchased from BioRad Laboratories GmbH (München, Germany), and all other chemicals were purchased from Carl Roth GmbH + Co.KG (Karlsruhe, Germany), Merck and Sigma Aldrich (Darmstadt, Germany). The lactic acid culture (YoFlex®) was kindly provided by Chr. Hansen, Hoersholm, Denmark and contained *S. thermophilus* and *L. bulgaricus.* The enzymes were kindly provided by Novozymes (Bagsværd, Denmark): Protamex® (Batch: PW2A1135), Alcalase® 2.4 L FG (Batch: PLN05508), trypsin (Formea RTL 1200 BG, Batch: PF130006).

III 2.2 Hydrolysis of pea protein[9]

Enzymes (trypsin, Protamex® and Alcalase®) with different specificities were chosen to generate different peptide profiles. Slurries of pea protein concentrate in distilled water were prepared considering the volume of NaOH needed for the pH stat method, so that all samples had a 10% (w/w) protein concentration at the end of the hydrolysis. The pH value of slurries was adjusted to pH 8 with 0.1 M NaOH before the start of hydrolysis. Due to the buffering capacity of the proteins, the adjustment of the pH took around 30-45 min, and was performed with constant agitation while heating the sample at 50 °C. Hydrolysis was performed to a degree of hydrolysis (DH) 1 at pH 8 and 50°C using the pH-stat method with an automated titrator (902 Titrando, Metrohm AG, Herisau, Switzerland). The required amount of NaOH to reach DH 1 was calculated from:

$$B = \frac{DH \cdot \alpha \cdot mp \cdot h_{tot}}{N_b \cdot 100\%} \qquad \text{(III 1)}$$

where B is the volume of base consumption [mL], N_b is the molarity of the base [M], α is the average degree of dissociation of the α-NH groups [-], h_{tot} is the total number of peptide bonds in the substrate [meqv/g protein], and mp is the mass of protein used [g] (Adler-Nissen, 1986). After the required volume of NaOH was added, hydrolysis was terminated by quickly transferring the sample to a water bath at 80 °C for 30 min. During this heating step, 5,3% saccharose was added to act as a supplement for the lactic acid

[8] *This paragraph was written by G. Giménez-Ribes as part of his internship report and transferred directly into this manuscript.*
[9] *Parts of this section were written by G. Giménez-Ribes as part of his internship report and transferred directly into this manuscript.*

bacteria later on. Subsequently the protein slurry was cooled down and homogenised (Panda Plus, Niro Soavi, Germany) at 800 bar and 1 pass and directly processed for fermentation without a freeze drying step. Additionally, hydrolysates without added sugar were prepared following the same protocol. Those hydrolysates were not fermented but freeze dried directly after homogenisation and stored at 4°C until further use.

III 2.3 SDS-PAGE of freeze-dried hydrolysates[10]

The molecular weight distribution of the freeze-dried hydrolysates was carried out by SDS-PAGE on 12% Criterion™ TGX™ Gel with 26 wells (BioRad Laboratories GmbH, München, Germany). Running of the gels was done according to the BioRad Bulletin #4110001. 10 µL of sample (0.1% protein in sample buffer, reducing conditions (Biorad 2xLaemmli sample buffer, Cat# 161-0737) with added dithiothreitol (DTT)) were applied to the gel alongside lanes of the molecular weight marker (PageRuler™ Prestained Protein Ladder, Cat# 26616, ThermoScientific). Running buffer was Biorad 10xTris/Glycine/SDS (Cat# 161-0732). The gels were photographed, and the bands were transformed to peaks using the inverted intensity of the green channel generated via graphics → RGB profile plot plugin (open source software ImageJ 1.52d (Schneider et al., 2012)). Bands were appointed to individual protein fractions by estimating their position in relation to the molecular weight marker and reference values from literature.

III 2.4 Fermentation

The fermentation of the samples was performed at 43 °C for 18 h using a thermophilic yoghurt culture (YoFlex®). This culture was added to the homogenised pea protein slurry and subsequently filled into disposable rheology beaker for the concentric cylinder system CC27 (Cat No 3716, Anton Paar, Graz, Austria) and 10 ml centrifuge tubes for fermentation. After the fermentation, the gels were stored for 24 h at 4 °C before performing the gel characterisation. Additionally, the fermentation process was tracked in a rheometer using a concentric cylinder system (Physica UDS 200 and MCR 502, Anton Paar, Graz, Austria, Z3DIN (measuring bob radius = 12.5 mm, measuring cup radius = 13.56 mm, gap length = 37.5 mm) and CC27 (measuring bob radius = 13.33 mm, measuring cup radius = 14.46 mm, gap length = 40 mm) respectively, f = 1 Hz, γ_0 = 0.1%) and via pH monitoring (Lab 865, blueline 14 electrode, SI Analytics, Xylem, USA). Storage modulus G' and loss factor tan δ were used to compare the obtained gels at the end of fermentation.

[10] *This paragraph was written by G. Giménez-Ribes as part of his internship report and transferred directly into this manuscript*

Syneresis of fermentation induced pea protein gels[11]

Samples of 10 g were introduced in three 12 mL centrifuge tubes and fermented under the same conditions as explained above. After resting for 24 h at 4 °C the supernatant was weight without a preceding centrifugation step. Syneresis was calculated as the weight of liquid released, in relation to the total weight of sample in the tube.

III 2.5 Gel solubility[12]

0.3 g of each gel without supernatant were weight and put into 2 mL Eppendorf caps. 1.5 mL of the following solutions were used as solvents: 0.5 M NaCl, 1.5% SDS, 0.1 M dithiothreitol (DTT), 20% propylene glycol (PG), distilled water. All the solutions were previously adjusted to pH 4.7 with 0.1 M HCl/NaCl. This method is based on gel solubility experiments by O'Kane,et al., 2004b; Utsumi & Kinsella, 1985, with modifications. The samples were left on an agitator with gentle agitation for 6h at room temperature. After agitation, samples were centrifuged at 10,000 x g for 15 min at room temperature. The protein content in the supernatant was quantified with the Dumas method and calculated as percent of the protein content of the undissolved gel. Additionally, the molecular weight distribution in the supernatants was analysed by SDS-PAGE as described above.

III 2.6 Rheological characterisation of fermentation induced pea protein gels[13]

The frequency and amplitude sweeps of the pea protein hydrolysate gels were carried out after resting the gels for 24 h at 4 °C using the Anton Paar MCR 502 with a concentric cylinder system (CC27, as described above). For both sweeps, storage modulus G' and loss modulus G'' were measured and plotted in double logarithmic plots against frequency and amplitude respectively. Additionally, the slope of G' vs. frequency (dlogG'/dlogf) was calculated from the double logarithmic plot of frequency sweeps. Frequency sweeps were performed at 10 °C and an amplitude that was found to be within the linear viscoelastic regime, γ_0 = 0.1%, for frequency values from 0.01 to 10 Hz. For the amplitude sweeps with SAOS and LAOS measurements oscillations were performed at 10 °C, ω = 1 rad·s^{-1} and γ_0 = 0.01% to 1010%. For further evaluation of the amplitude sweeps, results were plotted in Lissajous plots (Ewoldt et al., 2008). Within the linear viscoelastic regime, the shape of an elastic Lissajous plot (stress τ vs deformation γ) can vary from a straight line for purely elastic materials, over an ellipse for viscoelastic materials to a circle for purely viscous materials, while the shape of the viscous Lissajous plot (τ vs. shear rate $\dot{\gamma}$) follows the opposite behaviour. Beyond the linear viscoelastic regime, the shapes of the Lissajous plots become distorted. Numerical information can be obtained from the stiffening (S-factor)- and thickening (T-factor) ratios defined by Ewoldt et al., 2008:

$$S \equiv \frac{G'_L - G'_M}{G'_L} \qquad \text{(III 2)}$$

[11,10] Some of these paragraphs were written by G. Giménez-Ribes as part of his internship report and transferred directly into this manuscript.

[12] *Most of this paragraph was written by G. Giménez-Ribes as part of his internship report and transferred directly into this manuscript.*

where G'_L and G'_M are the large strain elastic modulus (secant line) and minimum strain elastic modulus (slope of the elastic Lissajous plot at zero strain), respectively. And

$$T \equiv \frac{\eta'_L - \eta'_M}{\eta'_L} \qquad \text{(III 3)}$$

where the η'_L and the η'_M are the large-rate dynamic viscosity (secant line) and the minimum rate dynamic viscosity (slope of the viscous Lissajous plot at zero shear rate), respectively.

III 2.7 Statistic evaluation

Statistic evaluation was performed by one way ANOVA followed by Tukey postHoc test ($\alpha = 0.05$) for G' and tan δ at the end of fermentation. A two way ANOVA followed by Tukey postHoc test was performed for statistical evaluation of gel solubility. Standard deviation is given in tables and represented as error bars in figures. All statistical evaluation was performed using OriginPro 9G software (OriginLab, Northhampton, USA).

III 3 Results and Discussion

III 3.1 Molecular weight distribution[14]

Fig III 1 shows the molecular weight distributions of the unhydrolyzed pea protein and the three different hydrolysates. The unhydrolyzed protein displays the typical molecular weight profile of pea protein as can be derived from Table III 1. Despite showing a molecular weight just above 70 kDa we associate the band marked "con" with convicilin. This is in agreement with findings from (Adal et al., 2017). The pronounced bands at ~50 kDa and ~30 kDa correspond to the monomer of vicilin and the α+β fraction of vicilin respectively. Moreover, many of the fractions between 25 and 20 kDa and below 19 kDa may also be various smaller vicilin fragments including the β+γ fraction and individual α, β and γ fractions, as vicilin is prone to post translational proteolysis (Gatehouse et al., 1982). The third main pea globulin is legumin, which in SDS-PAGE under reducing conditions appears as two peaks at 38 and

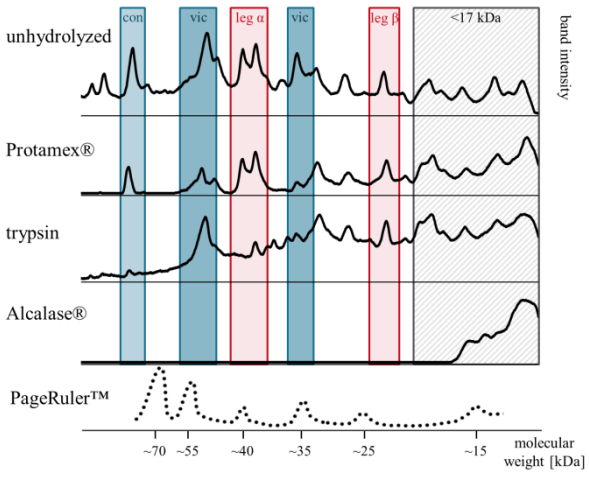

Fig III 1 pea protein hydrolysates obtained by enzymatic hydrolysis with Protamex®, trypsin and Alcalase® determined by SDS-PAGE under reducing conditions.
(con = convicilin, vic = vicilin, leg = legumin)

[14] *Some of this section was written by G. Giménez-Ribes as part of his internship report and transferred directly into this manuscript.*

40 kDa (acidic α-chain) and ~20 kDa (basic β-chain). Application of different enzymes let to different molecular weight patterns (Fig III 1). Hydrolysis with Protamex® mainly degraded the larger vicilin fractions, and some of the convicilin as can be seen by the decrease in the height of the corresponding peaks while the legumin fractions were almost unaffected. In contrast, trypsin cleaved mainly the legumin-α chain as well as the vicilin α+β and the convicilin and generally led to a wider distribution of peptides including a larger proportion of peptides < 17 kDa as can be seen from the more elevated baseline. The pronounced degradation of legumin-α and convicilin can be ascribed to the specificity of trypsin, that mainly cleaves at legumin-α and convicilin (Cheison et al., 2010). In addition to being less accessible, legumin-β contains less arginine and lysine than legumin-α (13 Arg and 9 Lys in legumin-β vs. 35 Arg and 13 Lys in legumin-α) as counted from the UniProtKB database (Bateman et al., 2017), and convicilin contains a highly charged N-terminus (Bown et al., 1988), making it also a favourable substrate for trypsin. Both, hydrolysis with Protamex® and trypsin did not affect the legumin-β. Resistance of the 12S-β fraction of oat protein was previously related to its burial at the interior of the 12S protein structure (Nieto-Nieto et al., 2014).

The third enzyme investigated in this study was Alcalase® (Fig III 1). Alcalase® cleaved nonspecifically (Doucet et al., 2003) and left only peptides smaller than 17 kDa.

III 3.2 Fermentation and syneresis

The gels made from unhydrolyzed protein can be considered as reference samples. At the end of fermentation, the elastic modulus G' was 5260 ± 203 Pa, the value for tan δ = 0.15 ± 0.01 clearly indicated a mainly elastic behaviour and syneresis after resting for 24 h was low (0.53 ± 0.19%). Table III 2 shows storage modulus G' and loss factor tan δ at the end of fermentation and syneresis after 24 h of gel storage for all samples. G' decreased in the order unhydrolyzed, Protamex®, trypsin, Alcalase®. Despite being in the same order of magnitude, G' of the gels made from tryptic hydrolysate was significantly lower than the storage moduli of gels from unhydrolyzed protein and Protamex® hydrolysates. However, all three gels showed similar tan δ indicating similar viscoelasticity and can be described as weak gels (Sun & Arntfield, 2010).

Syneresis follows an opposite trend to G' at the end of fermentation which in turn may be related to the increasing content of smaller peptides in the respective hydrolysates. When considering the protein fractions present after hydrolysis (mainly legumin in Protamex® hydrolysates and mainly vicilin in tryptic hydrolysates), our results are to some extend contradictory to those found by Mession, Chihi, Sok, & Saurel, 2015, who described higher values in G' for acid-induced vicilin gels, than for pea protein or legumin gels, with legumin reaching the lowest values. However, in our study protein concentration was much higher (10% vs. 3.5/4%), which may have led to different behaviour, as Kohyama & Nishinari, 1993 described higher storage moduli for soy 11 S proteins than soy 7 S proteins at protein concentrations above 5%. Similar results with higher G' values for 11S protein than 7S proteins were also found in heat induced soy protein gels (Renkema et al., 2001).

Table III 2 Characteristics of gels prepared from pea protein and pea protein hydrolysates obtained by enzymatic hydrolysis with Protamex®, trypsin and Alcalase®: storage modulus G',end and loss factor tanδ,end (f = 1 Hz and γ_0 = 0.1%) at the end of fermenation, syneresis of fully set of gels.

Sample	G'_{end} [Pa]	$\tan\delta_{end}$ [-]	syneresis [%]
no enzyme	5260^{a} ± 203	0.15^{a} ± 0.01	0.53 ± 0.19
Protamex®	4860^{a} ± 455	0.16^{a} ± 0.01	2.81 ± 0.27
trypsin	3650^{b} ± 711	0.15^{a} ± 0.01	5.64#
Alcalase®	*7^{c} ± 004	0.34^{b} ± 0.09	14.70 ± 1.80

Values are mean of triplicate determination and the corresponding standard deviations.
#owing to insufficient data, this is the mean of a duplicate determination
Different letters represent significant differences (α=0.05) as determined by one way ANOVA followed by Tukey postHoc test.
*despite tan δ<1, this sample was more like a thick protein dispersion than a gel and is therefore not considered in further rheology experiments.

In contrast to the first three gels, samples from Alcalase® showed very low values of G' (7 ± 4 Pa) alongside significantly higher values of tan δ (0.34 ± 0.09). Similar values were previously reported for acid-induced pea legumin gels below their least gelling concentration and were ascribed to coagulation rather than gelation (Mession et al., 2015). Nieto-Nieto et al., 2014 found similar results for heat induced gelation of oat protein hydrolysates, where Alcalase® hydrolysed protein was only able to gel at pH 9. Furthermore, in our study high syneresis (Table III 2) and visual assessment also supports the assumption of coagulation and sedimentation instead of gelation. C. Wang & Damodaran, 1990 reported a minimum molecular weight of 23 kDa for globular proteins to be able to gel at all, therefore at maximum molecular weight of 17 kDa gelation is unlikely. For these reasons, we conclude, that Alcalase® hydrolysates were unable to form self-supporting gels under the conditions of our study and therefore this hydrolysate was considered any further.

III 3.3 Interactions and gel fractions

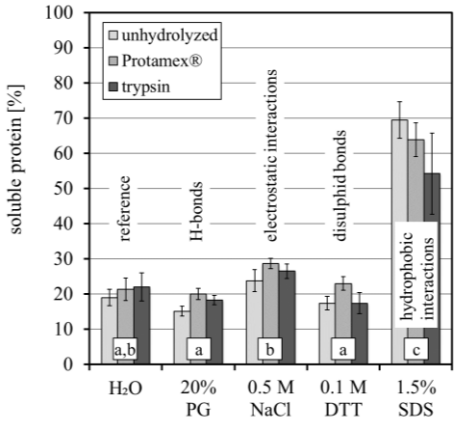

Fig III 2 Gel solubility of gels prepared from pea protein and pea protein hydrolysates obtained by enzymatic hydrolysis with Protamex® and trypsin in different solvents. (H2O=distilled water, PG=propylene glycol, NaCl=sodium chloride, DTT= dithiothreitol, SDS= sodium dodecyl sulfate). Error bars represent the standard deviations of triplicate determinations.

The following section covers the influence of different types of interactions on the formation of fermentation induced pea protein gels. Additionally, those types of interactions may be influenced by the decrease in individual protein fractions, the increase in the number of ionisable groups and the increased exposure of previously buried hydrophobic groups after hydrolysis.

In gel solubility experiments (Fig III 2), aliquots of gels made from hydrolysed and unhydrolyzed pea protein were incubated in various solvents followed by centrifugation and analysis of the supernatants. 0.5 M NaCl solution acts by screening the charges of the proteins, hence reducing the working range

of its electrostatic interactions by reducing the Debye double layer (Delahaije et al., 2015). This will result in a decrease of the attractive electrostatic interactions that might be present between proteins. SDS acts as an anionic surfactant, thus reducing the amount of hydrophobic interactions (O'Kane, 2004). DTT acts as a reducing agent, disrupting the disulphide bonds that might be present in the gels and PG acts by enhancing the hydrogen bonds, and the electrostatic interactions, but may decrease the hydrophobic contributions (Utsumi & Kinsella, 1985). There was no significant influence of the applied enzymes on gel solubility. But, all gels incubated in SDS showed a significantly increased gel solubility (α=0.05) and incubation in NaCl increased the gel solubility compared to incubation in PG and DTT, while there was no significant difference between the reference (H_2O) and the gels incubated in PG, NaCl and DTT (Fig III 2). Literature has described interaction in heat set gels to be hydrophobic, electrostatic and via hydrogen bonds (e.g. O'Kane et al., 2004c; Sun & Arntfield, 2012). In contrast, our results indicate interactions in the fermentation induced gel network to be mainly hydrophobic in nature regardless of enzymatic treatment. This is not unexpected as the final pH-value of all gels is close to the isoelectric point of the pea protein and therefore net charge is low.

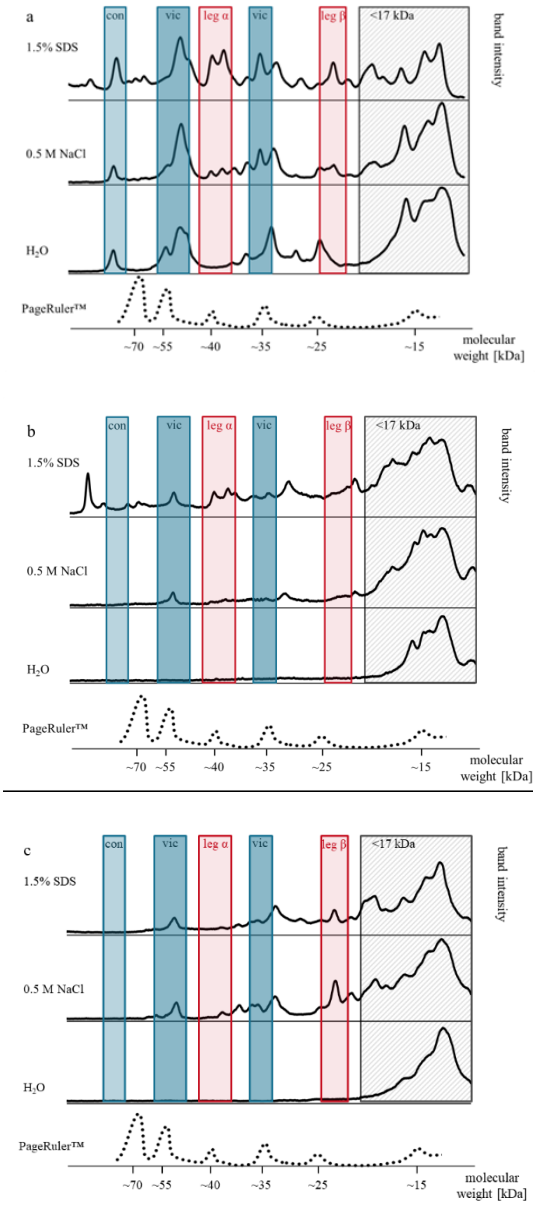

Fig III 3 Molecular weight distribution of supernatants from gel solubility experiments in H2O, NaCl and SDS of gels from pea protein (a) and pea protein hydrolysates obtained by enzymatic hydrolysis with Protamex® (b) and trypsin (c) determined by SDS-PAGE under reducing conditions. (con = convicilin, vic = vicilin, leg = legumin)

In order to further investigate the contributions of the different types of interactions, and to look into the protein fractions involved, SDS-PAGE of the supernatants was performed. From differences in molecular weight profiles, it can be deducted, which protein fractions participate in the gel structure via which type of interactions.

No differences could be found between the molecular weight profiles in H_2O, PG and DTT (results for PG and DTT are therefore not shown), thus leading to the assumption, that neither hydrogen- nor disulphide-bonds play a relevant role in the formation of the gel structure. Concerning disulphide-bonds, this was expected, as acid-induced gels are usually formed by non-covalent interactions (Grygorczyk & Corredig, 2013; Kohyama et

al., 1995). As a result, Fig III 3 only shows molecular weight profiles of supernatants from gels incubated in H_2O, NaCl and SDS.

Fig III 3a shows the molecular weight profiles of the gel from unhydrolyzed protein. In the bottom row, the soluble protein fraction in water is shown. The most apparent difference between the water-soluble fractions of the gel (Fig III 3a) and the original molecular weight profile of the pea protein (Fig III 1) is the complete lack of legumin fractions, which leads to the conclusion, that the legumin is a major contributor in building the gel network. Moreover, the height of the 50 kDa vicilin peak is decreased and the 30 kDa vicilin peak is missing, implying that some vicilin participates in the gel network as well. Similar dominance of legumin was previously described by Nieto-Nieto et al., 2014 who found a large influence of oat 12S α-subunits on the heat induced gelation of oat protein. The last apparent difference between the molecular weight profile of the soluble fraction in water and that of the protein before fermentation is a very large increase in peptides smaller than 17 kDa. Since these peptides are smaller than 23 kDa (C. H. Wang & Damodaran, 1990) we conclude, that these peptides are too small to have a relevant impact on the gelation properties. These findings are also in agreement with the findings for the Alcalase® hydrolysates that showed no relevant gelation ability (Table III 2) and only contained peptides smaller than 17 kDa (Fig III 1). Moreover, similar behaviour was also reported for pepsin hydrolysates of oat protein, where only small peptides remained after hydrolysis (Nieto-Nieto et al., 2014).

Fig III 3a shows the soluble protein fraction in NaCl solution. Here, both vicilin peaks are clearly present again, with the 50 kDa fraction being very pronounced. It has been previously described for soy, that upon heating the basic subunit of the 11S fraction and the 7S fraction form a soluble complex via electrostatic interactions (Damodaran & Kinsella, 1982; German et al., 1982). Moreover, similar results were found in the acidification of soy milk, where the basic subunit of the 11S fraction together with the β-subunits of the 7S fraction were not part of the soluble fraction at pH-values below 5.9 (Ringgenberg et al., 2013). This is in full agreement with our results, where vicilin was released upon disturbing the electrostatic interactions via charge screening upon addition of NaCl (Delahaije et al., 2015) and confirms the assumption, that electrostatic interactions have a relevant contribution in network stabilisation by incorporating some of the vicilin. Furthermore, this assumption is supported by a significantly lower solubility in PG than in NaCl, as PG may enhance electrostatic interactions while NaCl interferes with them. Finally, in SDS (Fig III 3a), all fractions seen in Fig III 1 are present, with the only difference being a larger fraction at molecular weights smaller than 17 kDa. This increase in the number of smaller peptides again confirms the assumption, that these fractions do no integrate in the gel, while some of the larger fractions remain undissolved even in SDS (gel solubility 69.5±5.2%).

A slightly different picture arises, when considering the H_2O soluble fractions of gels from Protamex® and tryptic hydrolysates (Fig III 3b and c): from these gels only fractions smaller than 17 kDa were dissolved. In case of the Protamex® hydrolysate, this may be due to the fact, that the 50 kDa vicilin fraction was already cleaved prior to fermentation. Considering the tryptic hydrolysate, the interaction between legumin-β and the vicilin would have been favoured by the increased accessibility of the legumin-β following the degradation of legumin-α by tryptic hydrolysis. These assumptions are

mirrored in the NaCl soluble fractions (Fig III 3b and c). The Protamex® hydrolysate only showed a very small increase in fractions >17 kDa, as mainly vicilin (which is already degraded during hydrolysis) would be released under these conditions. On the other hand, the NaCl soluble fraction of the trypsin hydrolysates showed a clear increase in vicilin, as well as in legumin-β fractions, again due to the disruption of the electrostatic interactions between the two. Due to the lack of legumin-α (that is usually bound to the legumin-β via a disulphide bond), the legumin-β becomes dislodged from the gel more easily.

Fig III 3b, shows the SDS soluble fractions of gel made from Protamex® hydrolysates. In general, all fractions shown in Fig 1 can be recovered. However, as already observed for the gel made from unhydrolyzed protein (Fig III 3a) the proportion of peptides smaller than 17 kDa is also increased. This increase is more pronounced in gels from Protamex® and tryptic hydrolysates (Fig III 3c) than in those from unhydrolyzed protein due to the development of small peptides during hydrolysis. In the Protamex® hydrolysates the absence of legumin-β and the small peaks for legumin-α in the molecular weight profile indicate, that due to lack of sufficient amounts of vicilin more insoluble legumin-β complexes are formed (German et al., 1982). In the molecular weight profile of the SDS soluble fraction of gels made from tryptic hydrolysates, fewer and less pronounced peaks are visible, compared to the NaCl soluble fraction. This agrees with the mechanism proposed for the interaction between legumin-β and vicilin, that is most pronounced in tryptic hydrolysates and may not be disrupted by SDS. Despite the influence of electrostatic interactions with regards to legumin-β – vicilin complexes, it needs to be kept in mind, that the hydrophobic interactions still dominate all pea protein gels regardless of hydrolysis, and should therefore have the largest impact on the functional properties.

III 3.4 Rheology of fermentation induced pea protein gels[15]

After resting the gels for 24 h at 4 °C, more extensive rheological tests were performed to characterise the gels beyond the structuring process and to account for rearrangements during cooling. To this purpose, frequency and amplitude sweeps were performed. From frequency sweeps the slopes (dlogG'/dlogf) of G' were calculated while amplitude sweeps were used to investigate small and large amplitude rheological behaviour. The slopes (dlogG'/dlogf) of G' from frequency sweeps (Fig III 4a) were 0.13 which is slightly lower, but still similar to results found in previous work (Klost & Drusch, 2019b) and can be ascribed to the high protein content of the gels. In amplitude sweeps (Fig III 4b), according to the classification made by Hyun, Kim, Ahn, & Lee, 2002, the shape of G' and G'' over strain shows an overall strain thinning behaviour of the gels with a decrease of G' and G'' from γ_0 = 1%. The elastic Lissajous plots (shear stress τ against shear strain γ) at this strain (Fig III 5a) exhibit shapes close to an ellipse which is characteristic for the linear viscoelastic regime.

[15] *Most of this section was written by G. Giménez-Ribes as part of his internship report and transferred directly into this manuscript.*

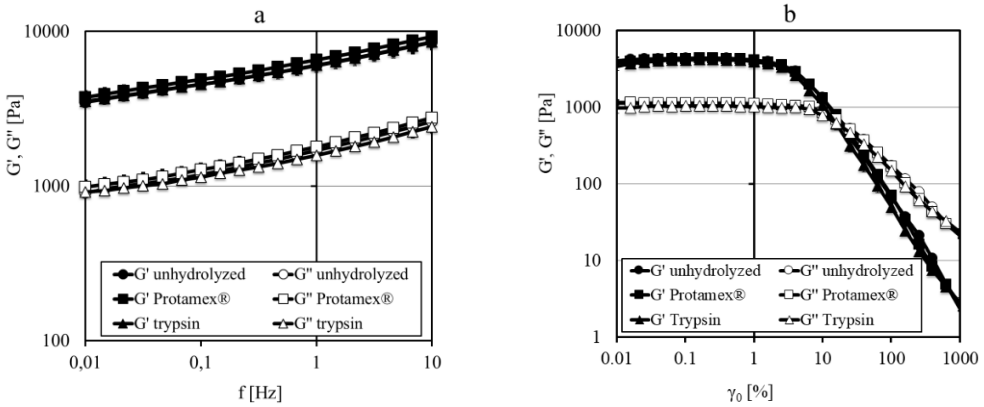

Fig III 4 Storage modulus G' and loss modulus G'' from Frequency- (a) and amplitude- (b) sweeps of fully set of gels prepared from pea protein and pea protein hydrolysates obtained by enzymatic hydrolysis with Protamex® and trypsin

As the amplitude increases, the ellipse starts to widen, as a result of G' decreasing faster than G''. Around γ_0 = 10%, a crossover occurs between G' and G'' (Fig III 4b) and the Lissajous plots clearly deviate from an ellipse, indicating that the measured storage and loss moduli are not representative of the mechanical response anymore due to the presence of higher harmonics in the oscillation spectrum. As γ_0 increases, the Lissajous curves turn into a squared box shape. This is due to an initial elastic response within each oscillation cycle, where the stress sharply increases, reaching a yield point after which the gel starts to flow (nearly horizontal part). This is a typical shape for yield stress response (Ewoldt et al., 2010). When the shear rate decreases to 0 as the maximum strain is reached, interactions recover, and the same response is observed in the opposite direction, resulting in the square shape. This box shape has been observed before in bulk rheology of food products like tuna myofibrillar protein (Q. Liu et al., 2014), debranched waxy rice starch (Precha-Atsawanan et al., 2018) or waxy maize starch pastes (B. Wang et al., 2012). The viscous Lissajous plots (Fig III 5b) obtained plotting the stress τ against the strain rate $\dot{\gamma}$ also showed non-linear behaviour when γ_0 is increased, resulting in an S-shape as seen in previous studies (Domenech & Velankar, 2015; Precha-Atsawanan et al., 2018).

This behaviour was further quantified using the shear stiffening (S-Factor) and shear thickening (T-Factor) ratios (Fig III 6). The S-Factor is close to 0 until γ_0 = 1.6%, indicating that the tangent line at minimum and the secant line at maximum strain, have the same slope. This is because in the linear viscoelastic regime, $G' = G'_M = G'_L$ (Ng et al., 2011) as only the first harmonic contributes to the signal. Above γ_0 = 1.6%, higher harmonics start to appear in the oscillation pattern, and the S-factor deviates from 0. The increase of the S-factor indicates intra cycle stiffening. This behaviour of intra cycle strain stiffening has been addressed before (Mermet-Guyennet et al., 2014), and should not be confused with the shear thinning response seen above for the overall behaviour of the gels (Fig III 4b).

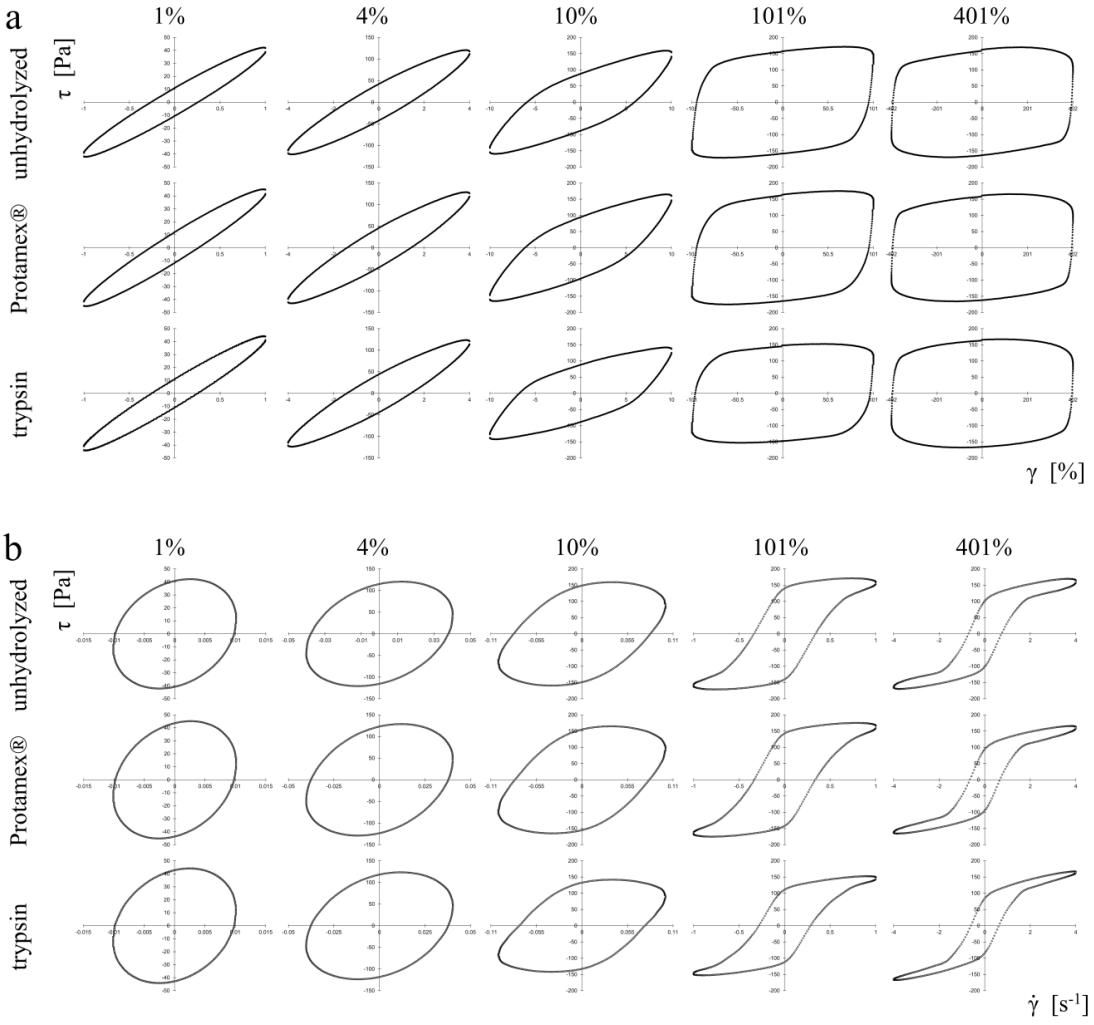

Fig III 5 Lissajous plots of fully set of gels prepared from pea protein and pea protein hydrolysates obtained by enzymatic hydrolysis with Protamex® and trypsin: (a) elastic curves of stress τ versus strain γ, (b) viscous curves of stress τ versus shear rate γ̇.

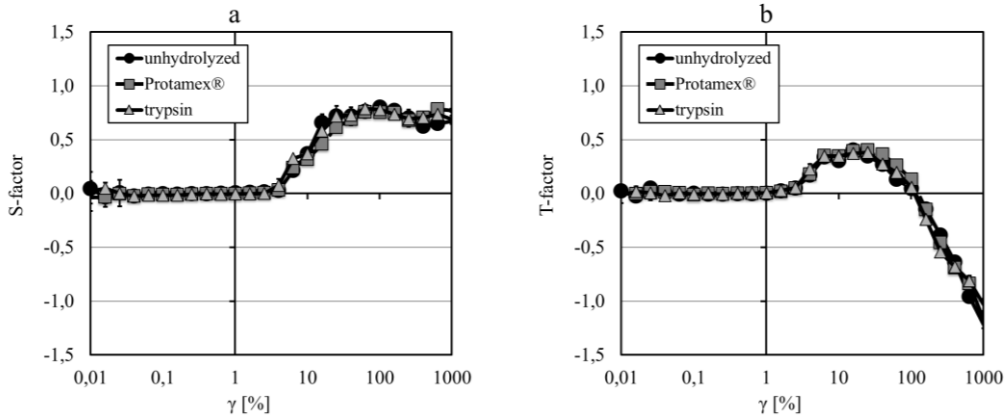

Fig III 6 Shear stiffening ratio (S-factor) (a) and shear thickening ratio (T-factor) (b) of gels prepared from pea protein and pea protein hydrolysates obtained by enzymatic hydrolysis with Protamex® and trypsin.

The strain stiffening is a result of G'_M being lower than G'_L, when the slope of the tangent line at minimum strain is lower than the slope of the secant line at maximum strain. A similar behaviour occurs for the T-Factor at γ_0 = 1.6% with initial positive values due to $\eta'_M < \eta'_L$, but decreases below 0 at γ_0 > 160%, indicating shear thinning of these gels, as observed also in Fig III 5b with the S-shape of the curves. The absolute values reached by the T-Factor are larger than the S-Factor, and therefore indicate that the gels exhibit a softening/thinning behaviour (Precha-Atsawanan et al., 2018). After resting at 4 °C for 24 hours, all three gels showed similar G' and G'' values. This may be due to different types of rearrangements in the different gels during resting, and to experimentally necessary discarding of supernatants before further rheological measurements. As decrease in G' after fermentation was complementary to the increase in syneresis (Table III 2), the discarding of the supernatants would have increased the protein concentration in the remaining gels which may in turn have contributed to the alignment of G' values. Moreover, all gels showed identical behaviour in all further rheological tests (Figs. III 4-6), indicating a prevailing influence of the type of interactions over the influence of the protein fractions involved.

III 4 Conclusions

The results from this study show, that upon fermentation pea protein forms mainly legumin-gels that are stabilised via hydrophobic interactions. However, part of the vicilin gets incorporated in the protein gels via electrostatic interactions with the legumin-β chain. This effect is promoted, if tryptic hydrolysis is applied to the protein prior to fermentation, while hydrolysis with Protamex® inhibits this effect due to degradation of vicilin. Peptides smaller than 17 kDa, were not incorporated into the gel network, thus explaining the inability of Alcalase® hydrolysates to form a gel network.

Nevertheless, the stabilisation of the gel networks is dominated by hydrophobic interactions, with no influence of the enzymatic treatment. This is reflected by the lack of differences in rheological properties between gels from differently pre-treated protein. The slopes (dlog G'/dlogf) of G' from the frequency sweeps were 0.13 for all gels and can be ascribed to the high protein content of the gels, while in amplitude sweeps, the shapes of G' and G'' show an overall strain thinning behaviour. In large amplitude oscillatory shear experiments between amplitudes of γ_0 = 1.6% and γ_0 = 160% all gels show intra cycle strain stiffening behaviour while at amplitudes above γ_0 = 160% intra cycle shear thinning prevails, indicating a softening/thinning behaviour.

This study helped to obtain a more thorough understanding of rheological behaviour, involved protein fractions and relevant interactions in fermented pea protein gels and therefore contributes to the development of strategies for the customisation of such gels for use in pea protein-based yoghurt alternatives with a high consumer acceptance.

Acknowledgements:
The authors gratefully acknowledge the skillfull lab-work of C. Härter and the proofreading by H. Kastner and M. Brückner-Gühmann.

Funding:
This work was supported by NutriAct – Competence Cluster Nutrition Research Berlin-Potsdam funded by the Federal Ministry of Education and Research (BMBF) (FKZ: 01EA1806C).

CRediT authorship contribution statement:
M. Klost: Conceptualization, Supervision, Writing - original draft, Writing - review & editing, Formal analysis, Investigation, Data curation, Visualization. G. Giménez-Ribes: Writing - original draft, Writing - review & editing, Formal analysis, Investigation, Data curation, Visualization. S. Drusch: Supervision, Writing - review & editing, Funding acquisition, Resources.

Manuscript IV:

Effect of protein aggregation on rheological properties of pea protein gels

Food Hydrocolloids (2020), 108, 106036.
https://doi.org/10.1016/j.foodhyd.2020.106036
(this thesis contains the accepted manuscript version)

Authors
Martina Klost [a,b*]
Celina Brzeski[a]
Stephan Drusch [a,b]

[a] Technische Universität Berlin, Department of Food Technology and Food Material Science, Königin-Luise-Str. 22, 14195 Berlin, Germany

[b] NutriAct – Competence Cluster Nutrition Research Berlin-Potsdam

Abstract

Yoghurt style gels are a promising way to increase the consumption of plant derived proteins. However, reaching texture properties similar to those commonly known from milk yoghurts while incorporating large amounts of plant-derived proteins, is a challenge that needs to be addressed to meet consumers expectations. Therefore, this study aims to investigate the influence of pH conditions (pH 6.0 to pH 8.0) during pre-treatment on the rheological properties of fermentation induced pea protein gels with a protein content of 10%. Results showed a strong correlation between the pH value during pre-treatment and the protein solubility after pH readjustment to pH 8. Solubility was highest if pea protein was pre-treated at pH 8.0 and lowest if it was pre-treated at pH 6.0. Since only soluble aggregates are believed to participate in network formation, networks formed by pea protein pre-treated at pH 6 were coarser, than those formed by pea protein pre-treated at pH 8 owing to a lower degree of crosslinking caused by less available protein. Coarser networks and higher proportions of insoluble particles increased loss of water and lowered the storage modulus G' as well as the ability of the networks to recover after intense shearing. In particular pre-treatment at pH values below 7.0 led to gels with storage moduli of the same magnitude as those measured in commercial milk derived yoghurts. Adjusting the pH value during pre-treatment of pea protein can therefore be considered a promising approach for the customisation of texture properties while maintaining a constantly high protein content.

Keywords: pea protein, plant protein, rheology, fermentation, aggregation, pH value

IV 1 Introduction

In the light of increasing life expectancy, it is inevitable to address the issue of age related non-communicable diseases in a preventive manner (WHO, 2013). One approach is to increase consumer awareness for a healthy lifestyle and a balanced nutrition and to provide a range of corresponding foods. In this context, plant derived proteins have been proposed to contribute to the prevention of chronic degenerative diseases (Krajcovicova-Kudlackova et al., 2005). As a consequence, an adequate intake through consumption of plant -based foods needs to be achieved. Plant protein-enriched beverages and emulsion products cannot deliver the required amounts of plant derived protein for this purpose. In contrast, gels are dispersed systems more suitable for the incorporation of relevant amounts of plant derived protein. E. g. yoghurt has a high consumer acceptance when it comes to protein-rich foods (Banovic et al., 2018), and yoghurt type products from plant derived proteins allow for the incorporation of up to at least 10% plant derived protein (Klost et al., 2020; Klost & Drusch, 2019b).

Plant-derived proteins (such as pea and soy) consist of hexameric 11S and trimeric 7S globular protein fractions. The general process of acid-induced gelation has been extensively described by a variety of authors and for proteins from various plants. It starts with a heating step during which the protein undergoes heat induced structural rearrangements that lead to the formation of aggregates. When electrostatic repulsion is lowered during acidification, soluble aggregates form network structures by hydrophobic interactions e. g. (Ringgenberg et al., 2013). However, during heat treatment – apart from

the soluble aggregates required for gelation – insoluble aggregates may form. Whether soluble or insoluble aggregates are formed depends on the sensitivity of the different protein fractions to environmental factors like ionic strength, temperature and pH conditions (Yamagishi et al., 1983). In this context, changes in pH conditions or ionic strength may decrease the electrostatic repulsion between two particles (Cano-Sarmiento et al., 2018) and consequently promote short range particle interactions (Klemmer et al., 2012). Generally, differences in sensitivity towards environmental factors can lead to a variety of aggregates that are formed between different protein fractions and/or different protein fraction subunits via disulphide or non-covalent bonds. Due to lack of detailed studies on the aggregation behaviour of pea protein and vast similarities between pea and soy proteins we refer to literature on soy protein as an indicator for pea protein's aggregation behaviour. Generally speaking, various 7S and 11S fractions can form aggregates with other 7S or 11S fractions via various types of interactions. A summary of soy protein fractions and types of interactions involved in those soluble and insoluble aggregates is given in Table IV 1.

Table IV 1 types of aggregates formed upon heating of mixtures of soy 11S and 7S: types of interactions involved in aggregate formation and composition of aggregates (corresponding pea proteins are: 11S → Legumin, 7Sαα' → Convicilin, 7Sβ → Vicilin)

	subunits involved	interactions	reference
soluble	7S αα'	disulphide bond	(Yamagishi et al., 1983)
	7S αα' and 11S acidic	disulphide bond	(Yamagishi et al., 1983)
	7S β and 11S basic	disulphide bond	(Damodaran & Kinsella, 1982; German et al., 1982)
	7S αα' and 7S β	no disulphide bond	(Yamagishi et al., 1983)
	7S β	no disulphide bond	(Yamagishi et al., 1983)
	7S β and 11S basic	no disulphide bond	(Petruccelli & Añón, 1995)
insoluble	11S acidic and basic	disulphide bond	(Yamagishi et al., 1983)
	7S αα' and 11S acidic+basic	disulphide bond	(Yamagishi et al., 1983)
	7S β	no disulphide bond	(Yamagishi et al., 1983)
	11S basic	no disulphide bond	(e.g. German et al., 1982)

Different ratios of soluble to insoluble aggregates may influence a protein's ability to form fermentation induced gels. While soluble aggregates are a prerequisite for the formation of fermentation induced gels (e.g. Ringgenberg et al., 2013) insoluble aggregates may act as inactive fillers and weaken an emerging gel matrix (Britten & Giroux, 2001). Weakened gel matrices should in turn be reflected in rheological and texture parameters. In two previous studies (Klost et al., 2020; Klost & Drusch, 2019b) with different objectives – and therefore different environmental parameters such as pH, homogenisation pressure, heating temperature and heating time during protein pre-treatment prior to fermentation – we found relevant inter-study differences in rheological moduli G' and G''. While for the first study no specific pre-treatment – apart from heating – was performed (Klost & Drusch, 2019b), we additionally applied enzymatic hydrolysis as a pre-treatment before fermentation in the second study (Klost et al., 2020). In preliminary experiments from this study we tested different pH values (pH 7.0, 7.5 and 8.0) during

hydrolysis for one of the applied enzymes (Protamex®) to determine its pH optimum (unpublished data). Interestingly, we found significant differences between the storage moduli G' at the end of fermentation but no differences in the molecular weight distribution of the corresponding hydrolysates (Appendix, Fig A 9). G' decreased from 5052 ± 172 Pa (hydrolysis at pH 8.0) to 1487 ± 180 Pa (hydrolysis at pH 7.0). Putting these values in line with the results from the first study (complex shear modulus |G*| = 452 ± 27 Pa (corresponding to storage modulus G' = 446 ± 26 Pa)) where heating was conducted at pH ~6.5 we suspect the influence of pH value during heat pre-treatment to be the most important parameter for these inter-study differences. However, this presumption needs to be confirmed in a systematic investigation.

Therefore, the focus of this study is to investigate the application of pH variation during pre-treatment of pea protein to specifically customise the rheological properties of subsequently produced yoghurt alternatives. To this regard, we propose the following mechanism by which the pH value during pre-treatment (heating and homogenising) influences the aggregation behaviour of pea protein: at a pH that leads to reduced electrostatic repulsion close-range interactions lead to an increase in insoluble aggregates. A higher proportion of insoluble aggregates will weaken the gel structure and will result in less stable gels. With this in mind it should be possible to customise the rheological properties of fermentation induced pea protein gels by targeted manipulation of environmental parameters during a pre-treatment step prior to fermentation while maintaining the protein content constant at 10%. Moreover, beyond the development of yoghurt alternatives, customising the texture of fermentation induced pea-protein gels may lead to a variety of new products such as spreads, cream fillings for bakery and confectionary products, etc. in the future.

IV 2 Materials and methods

Fig IV 1 gives a general overview over the experimental setup. In a first set of experiments the difference in intrinsic fluorescence before and after heating, the ζ-potential and the protein solubility, of the untreated protein were analysed in dependence of the pH value to gain a deeper understanding of the unfolding behaviour during heating, the electrostatic properties and the formation of insoluble aggregates respectively. Slurries with a protein content of 10% were prepared from this raw material. In subsequent steps the pH of the slurries was adjusted according to the experimental setup, the slurries were heated and homogenised followed by pH readjustment to pH 8. Afterwards these pre-treated slurries were either lyophilised for molecular weight analysis and further protein solubility tests, or fermented for subsequent rheological, microscopic and loss of water characterisation.

IV 2.1 Materials

Pea protein concentrate (LOT-Nr.: 16041801) with a protein content of 78% was obtained from IGV (Institut für Getreideverarbeitung) GmbH, Nuthetal, Germany. The lactic acid culture (YoFlex®; *S. thermophilus* and *L. bulgaricus*) was kindly provided by Chr.

Hansen, Hoersholm, Denmark. Gels and buffer-solutions for SDS-PAGE analysis were purchased from BioRad Laboratories GmbH (München, Germany). All other chemicals were of analytical grade and purchased from Merck and Sigma Aldrich (Darmstadt, Germany) and Carl Roth GmbH + Co.KG (Karlsruhe, Germany).

IV 2.2 ζ-potential measurement of untreated pea protein

ζ-potential measurements were conducted to estimate the electrostatic repulsive properties of the untreated protein in dependence of the pH-value. Measurements were carried out in triplicate in protein solutions containing 0.3% (w/w) of the untreated protein prepared in 0.01 M phosphate buffer at pH 6.0, 6.5, 7.0, 7.5, 8.0 (Zetasizer Nano-ZS, Malvern Instruments GmbH, Herrenberg, Germany).

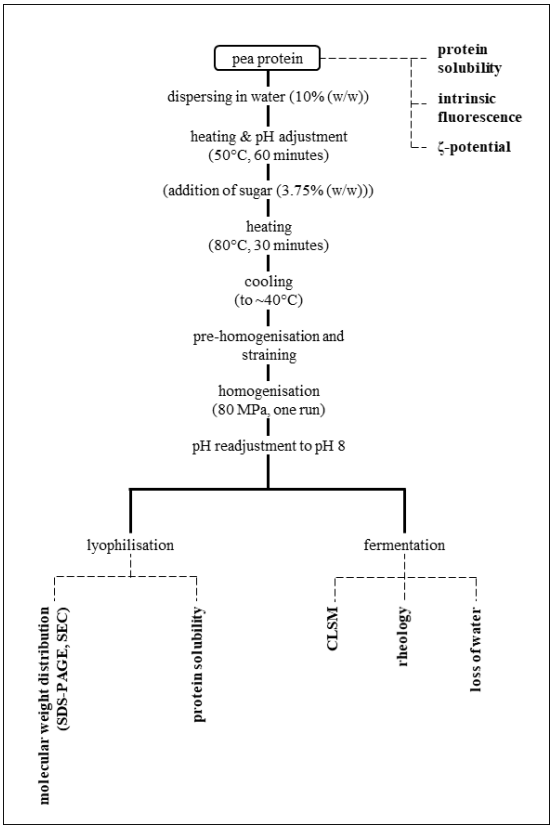

Fig IV 1 flow chart of experimental setup

IV 2.3 Determination of intrinsic fluorescence of untreated pea protein

Intrinsic fluorescence measurements were carried out in order to determine differences in the unfolding behaviour of pea protein, when heated at different pH values. Protein solutions of 0.05% (w/w) protein in 0.01 M phosphate buffer were prepared at pH 6.0, 6.5, 7.0, 7.5 and 8.0. Samples were measured in a Cary Eclipse Fluorescence Spectrophotometer (Agilent Technologies, Victoria, Australia) at an excitation wavelength of 290 nm and the emission wavelength was scanned between 300 and 400 nm. Emission wavelengths were scanned before heating, followed by subsequent heating to 50 °C, holding for 60 minutes, further heating to 80 °C, holding for 30 minutes and another scan of the emission wavelength. All samples were prepared in triplicate. For evaluation the wavelengths at maximum emission before and after heating were determined and the red shift during heating was calculated as the difference between the two values.

IV 2.4 Solubility of pea protein

Protein solubility was measured before and after the pre-treatment process and before fermentation. More specific, the solubility of the raw material was measured at pH 6 to 8 with steps of 0.5, the solubility of pre-treated and freeze-dried samples was measured at the pH value during pre-treatment as well as at pH 8 representing the pH at the start of fermentation. To this purpose, suspensions with a protein content of 5% were prepared and the pH values were readjusted to the required value with 0.1 M/1 M NaOH or 0.1 M/1 M HCl if necessary. Suspensions were then left to stir for 60 minutes. An aliquot of the suspensions was used to determine the total protein content and another

aliquot was centrifuged at 10000xg for 15 minutes for the determination of the soluble protein fraction. Protein contents were determined with a Dumatherm® (C. Gerhardt GmbH&Co. KG, Königswinter, Germany) at an oxygen flow rate of 100 mL/min and 0.8 mg oxygen/mg sample. Protein solubility was then calculated as

$$\text{protein solubility} = \frac{c_{\text{soluble protein}}}{c_{\text{total protein}}} \cdot 100\% \qquad \text{(IV 1)}$$

IV 2.5 Pea protein pre-treatment, lyophilisation and fermentation

A protein slurry (10% protein (w/w)) was heated to 50 °C under constant stirring and the pH value was adjusted to 6.0, 6.5, 7.0, 7.5 or 8.0 respectively with 1 M NaOH and/or 1 M HCl. After a holding time of 60 minutes 3.75% (w/w) sugar was added to slurries for fermentation, the temperature was increased to 80 °C and the sample was held for further 30 minutes followed by cooling to approximately 40 °C in an ice bath. Samples for lyophilisation were prepared without the addition of sugar. The cooled slurries were pre-homogenised (Ultraturrax T25 basic, IKA, Germany, 30 s, 17500 rpm), strained through a sieve and high pressure homogenised (Panda Plus, Niro Soavi, Germany, 80 MPa, one run). To samples for fermentation, starter culture (YC-X11 Yo-Flex®, Chr. Hansen, Hoersholm, Denmark) was added subsequently and the samples were filled into centrifuge tubes for loss of water experiments, beaker for confocal laser scan microscopy (CLSM) and disposable rheology cups (Cat No 3716, Anton Paar, Graz, Austria) for rheological tests. Samples were then fermented in a water-bath at 43 °C for 18 h. After fermentation, the samples were stored at 4 °C for 24 hours before further investigation. Samples for lyophilisation were frozen in an ethanol bath after homogenisation followed by lyophilisation. All samples were prepared in triplicate for fermentation and lyophilisation. Additionally, one repetition of each sample was prepared for CLSM experiments.

IV 2.6 Molecular weight distribution of pre-treated and lyophilised pea protein via SDS-PAGE and size exclusion chromatography

SDS-PAGE on 12% Criterion™ TGX™ Gels (26 wells) (BioRad Laboratories GmbH, München, Germany) was used to characterise the molecular weight profiles of pre-treated and lyophilised samples. Experiments were conducted according to the BioRad Bulletin #4110001 under reducing and non-reducing conditions with Biorad 10xTris/Glycine/SDS (Cat# 161-0732) as running buffer. Sample concentration was 0.1% in sample buffer (Biorad 2xLaemmli sample buffer, Cat# 161-0737 with or without addition of dithiothreitol) and 10 µL of the samples were applied to the gels alongside a molecular weight marker (PageRuler™ Prestained Protein Ladder, Cat# 26616, ThermoScientific). Evaluation of the gels was carried out via photography of the gels followed by band identification via estimation of their position in relation to the marker in combination with reference values from literature and transformation to peaks for presentation (open source software ImageJ 1.52d (Schneider et al., 2012)). Transformation to peaks was done as mean of three gel lanes.

Size exclusion chromatography (SEC) of lyophilised samples (0.1% (w/w) in 0.1 M phosphate buffer, pH 8) was performed in triplicate on a Superdex 200 Increase 10/300 GL (GE healthcare GmbH, Solingen, Germany) column with 0.1 M phosphate buffer as eluent (HPLC ÄKTAbasicTM 10 system, Amersham Biosciences, Uppsala, Sweden). Detection took place via an UV detector at 280 nm. Qualification of peaks was not possible, but determination of the calibration area was performed by using the highest and lowest calibration points from previous experiments.

IV 2.7 Confocal laser scan microscopy (CLSM) of fermentation induced pea protein gels

For CLSM, 20 µl rhodamine B solution (0.2% (w/w) in distilled water) per gram sample were added to the protein suspension before fermentation. CLSM was performed on one set of fermented samples. The microscope was a Leica SP8 (Leica Microsystems GmbH, Wetzlar, Germany) with a HC PL APO CS2 63x/1.20 water objective (pinhole at airy unit 1 AU (111.5 µm)). Image resolution was 512x512 pixels. For GFP detection a 3% laser (552 nm) intensity was coupled with emission detection of 580 nm at a gain of 357. The number of required z-stacks was determined using the system optimised calculation of z-stacks.

IV 2.8 Loss of water

The fermented samples in the centrifuge tubes were centrifuged (500 g, 20 °C, 10 minutes, Avanti J-E, Beckman Coulter GmbH, Krefeld, Germany) in a method adapted from (Guzmán-González et al., 1999). Subsequently the supernatant was discarded and the remaining sample was weight. Loss of water was calculated as:

$$\text{loss of water} = \frac{\text{mass, total-mass, pellet}}{\text{mass, total}} \cdot 100\% \qquad \text{(IV 2)}$$

IV 2.9 Rheology

Determination of all rheological properties was carried out in triplicate on an MCR 502 (Anton Paar, Austria, concentric cylinder system CC 27 (measuring bob radius = 13.33 mm, measuring cup radius = 14.46 mm, gap length = 40 mm)). For time-sweeps additional rheometers were used (Physica UDS and MCR 301, Anton Paar, Austria, concentric cylinder system Z 3 DIN (measuring bob radius = 12.5 mm, measuring cup radius = 13.56 mm, gap length = 37.5 mm) and CC 27 (measuring bob radius = 13.33 mm, measuring cup radius = 14.46 mm, gap length = 40 mm) respectively). Special care was taken, that replications of each sample were performed on at least two different rheometers. Time sweeps were carried out during fermentation at 43 °C for 18 hours (f = 1 Hz, γ = 0.1%) in order to track the structuring process. G' and tan δ were chosen as parameters for evaluation. Thixotropy tests were performed according to DIN SPEC 91143-2, 2012: samples were oscillated (f = 1 Hz, γ = 0.1%) for 120 s followed by shearing for 120 s at $\dot{\gamma}$ = 200 s^{-1} and oscillation for another 300 seconds. From these experiments recovery of structure was calculated as:

$$\text{recovery} = \frac{G'_{End}}{G'_{Start}} \cdot 100\%. \qquad \text{(IV 3)}$$

Frequency sweeps were conducted at $\gamma = 0.1\%$ and frequencies ranging from 10 Hz to 0,01 Hz. For evaluation the slopes dlogG' / dlogω from the double logarithmic plots were determined and compared.

For the characterisation of non-linear deformation behaviour, amplitude-sweeps were performed at f = 1 Hz and strain amplitude γ_0 between 0.01% and 1000%. First of all, the end of the linear viscoelastic regime was determined as the point, where G' varies more than 5% from the original value. Evaluation of the non-linear deformation was carried out via Lissajous plots, stress decomposition and calculation of the stiffening ratio (S-factor) and dissipation ratio φ. In this context, information about both inter- and intracycle behaviour can be derived from Lissajous plots and the interpretation of the elastic stress curves can contribute to understanding changes within the network structure by application of a model that links rupture of colloidal gels to the bond number between individual particles in the gel network (e.g. Hsiao et al., 2012; Park et al., 2015; Park & Ahn, 2013) or the description of microcracks that occur prior to the complete rupture of gels (Faber et al., 2017). Consequently, perfectly elastic behaviour – represented by a straight line in the intracycle strain γ-elastic stress τ' diagram – is related to a rigid cluster structure with high bond numbers (i.e. 4 to 6) in the gels (Park et al., 2015). At intercycle strain amplitude γ_0 above the linear viscoelastic regime, shear and strain amplitude begin to interfere with the network structures. Depending on the applied model, this may be reflected in the decrease of bonding numbers (e.g. Hsiao et al., 2012; Park et al., 2015; Park & Ahn, 2013) or the occurrence of microcracks (Faber et al., 2017). Both would reduce the size and volume fraction of rigid clusters which in turn leads to a reduction in the load bearing network that would be capable of supporting elastic stress (Hsiao et al., 2012). If such behaviour occurs, it is reflected in the onset of deviation of the curves from a straight line. This deviation often leads to an inversed sigmoidal shape. This shape can be interpreted as follows: the decline of the slope at small intracycle strain γ indicates a decrease in the ability to support elastic stress owing to the reduced size and volume fraction of rigid clusters (Park et al., 2015) and therefore relates to overall intercycle strain softening with increasing intercycle strain amplitude γ_0. The increase of the slope at higher intracycle strain γ can be related to the stretching of remaining rigid clusters which in turn causes strong intracycle elasticity (Park et al., 2015) and indicates intracycle stiffening. The calculation of S-factors reflects this intracycle behaviour onto the entire range of intercycle strain amplitudes γ_0. S-factors were calculated according to (Ewoldt et al., 2008):

$$S \equiv \frac{G'_L - G'_M}{G'_L} \qquad \text{(IV 4)}$$

where G'_L is the large strain modulus (secant line of elastic Lissajous plot) and G'_M is the minimum strain modulus (slope of elastic Lissajous plots at zero). In this context an S-factor $S > 0$ indicates intracycle strain stiffening, whereas $S < 0$ refers to intracycle strain softening (Ewoldt et al., 2008). However, when evaluating S-factors the special case of pseudoplastic and elastoviscoplastic materials needs to be considered. While in

truly strain stiffening systems the overall stress will increase towards higher intracycle strains γ (elastic Lissajous plot) as shown by Park et al in their Fig 11 (Park et al., 2015) and by Ewoldt et al in their Fig 10 (Ewoldt et al., 2010) and the S-factor may become S > 1, in pseudoplastic and elastoviscoplastic materials the overall stress may approach a perfectly rectangular shape in elastic Lissajous plots (Ewoldt et al., 2010) and the S-factor will trend towards a maximum value of one. Especially in the latter case the elastic stress curve will be horizontal at low intracycle strain γ and its slope may increase towards higher intracycle strain γ. This leads to the S-factors trending towards one – and therefore S > 0 – despite a strain softening overall rheology (Mermet-Guyennet et al., 2015). This effect is owing to the mathematical definitions of the S-factor (Ewoldt et al., 2010). More specifically, in this case the tangent modulus at minimum intracycle strain γ (G_M) approaches zero and therefore equation 2 reduces to

$$\text{S-factor} = \frac{G_L}{G_L} = 1 \text{ (Ewoldt et al., 2010)} \quad . \qquad \text{(IV 4a)}$$

In order to distinguish between true intracycle strain stiffening and a shift from predominantly elastic to mainly plastic behaviour it is therefore important, to consider the S-factor in combination with the dissipation ratio φ (Ewoldt et al., 2010)

$$\varphi = \frac{E_D}{E_{D,pp}} = \frac{\pi \gamma_0 G''}{4\tau_{max}} \qquad \text{(IV 5)}$$

where E_D is the dissipated energy per cycle and corresponds to the area enclosed by the elastic Lissaous plot, $E_{D,pp}$ is the dissipated energy in the corresponding perfect plastic system, γ_0 is the intercycle strain amplitude, G'' is the loss modulus at that strain amplitude and τ_{max} is the maximum shear stress in the considered oscillatory cycle. In this context the dissipation ratio φ relates the dissipated energy in the sample to the dissipated energy in a corresponding perfectly plastic material and consequently allows to categorise rheological behaviour into elastic ($\varphi \rightarrow 0$) or plastic ($\varphi \rightarrow 1$) behaviour with a known critical value ($\varphi = \pi/4$) for Newtonian behaviour (Ewoldt et al., 2010).

All data was obtained and – except for the dissipation ratio φ – automatically calculated by RheoCompass™ Software (Anton Paar, Austria).

IV 3 Results and discussion

IV 3.1 Protein characterisation

IV 3.1.1. Electrostatic interactions and unfolding properties of untreated pea protein

The ζ-potential reflects electrostatic interactions between individual protein molecules and depends on the pH value of the surrounding medium. Results show, that the absolute value of the ζ-potential significantly decreased from |20.4| ± 0.5 mV to |11.7| ± 1.0 mV with decreasing pH values during pre-treatment (Table IV 2) indicating lower electrostatic repulsion at lower pH values.

Table IV 2 ζ-potential and protein solubility before heating, protein solubility of heated, homogenised and lyophilised protein at the original pH value and at pH 8 simulating the beginning of fermentation and red shift during heating of the protein.

sample	ζ-potential before heating [mV]	Protein solubility unheated samples [%]	Protein solubility heated samples [%]	Protein solubility heated samples at pH 8 [%]	red shift during heating [nm]
pH 6.0	$-11.7^{a}\pm 1.0$	$20.8^{a,1}\pm 0.4$	$17.5^{a,2}\pm 0.9$	$37.6^{a,3}\pm 1.1$	$10.0^{(\blacklozenge)}$
pH 6.5	$-14.2^{b}\pm 0.6$	$26.0^{b,1}\pm 1.5$	$21.1^{a,b,2}\pm 0.3$	$40.0^{a,b,3}\pm 2.1$	$7.7^{a}\pm 4.0$
pH 7.0	$-17.1^{c}\pm 0.8$	$35.2^{c,1}\pm 1.9$	$27.4^{b,2}\pm 1.4$	$44.7^{a,b,3}\pm 3.1$	$8.3^{a}\pm 1.2$
pH 7.5	$-19.9^{d}\pm 0.8$	$63.9^{d,1}\pm 0.1$	$40.3^{c,2}\pm 3.4$	$47.1^{b,2}\pm 3.2$	$11.0^{a}\pm 2.0$
pH 8.0	$-20.4^{d}\pm 0.5$	$68.8^{e,1}\pm 1.2$	$57.2^{d,2}\pm 4.0$	$57.2^{c,2}\pm 4.0$	$7.0^{a}\pm 3.6$

Different letters represent significant differences (α=0.05) within columns, different superscript numbers represent significant differences (α=0.05) within rows as derived from ANOVA followed by Tukey post-Hoc test.
(♦) value calculated from double determination due to equipment failure. Data point was excluded from ANOVA and post-Hoc test.

However, it is generally accepted, that ζ-potentials above |30| mV are a prerequisite for full electrostatic stabilisation. As a general rule, stability of hydrocolloid stabilised oil-droplets with ζ-potentials below |15| mV cannot exclusively be explained by double-layer repulsion (Dickinson, 2009) and (Piorkowski & McClements, 2014) recommend ζ-potentials above |20| mV for long-term stability of electrostatically stabilised beverage emulsions. We therefore need to assume, that electrostatic stabilisation is insufficient to prevent flocculation at pH 6.0 and 6.5 and is inadequate to fully stabilise a protein dispersion at pH 7.0 and 7.5. In turn we can assume, that the chosen pH-range is suitable to produce samples with differently pronounced electrostatic repulsion, which may in turn lead to differences in aggregation. While the degree of electrostatic repulsion determines how close individual particles may get to each other, the aggregation itself may take place via further non-covalent interactions and via disulphide-bonds. The ability to form these types of interactions and bonds in turn strongly depends on the accessibility of relevant protein side chains and therefore on the protein unfolding. Protein unfolding can be determined via intrinsic fluorescence measurements. Generally, a red shift i.e. an increase in the wavelength at emission maximum represents the unfolding of a protein as indicated by the decrease in the interactions of tryptophan residues with quenching groups and thus an increase in its exposure to the solvent (Cairoli et al., 1994). In our study the red shift by 7 to 11 nm upon heating of protein solutions from 20 °C to 80 °C (Table IV 2) was not significantly dependent on the pH value during pre-treatment. We therefore propose similar unfolding kinetics during heating in all samples. Consequently, the electrostatic repulsion – or lack thereof – must be the main influence factor on aggregation behaviour.

IV 3.1.2. Protein solubility of untreated, pre-treated and pH readjusted pea protein

Solubility experiments were carried out at three conditions. First of all, solubility of the untreated samples was measured after pH adjustment to pH 6.0, 6.5, 7.0, 7.5 and 8.0 to characterise the individual influence of pH. In a subsequent step the pre-treated, lyophilised samples were re-dispersed at the pH value of their respective pre-treatment to characterise the additional impact of heating and homogenisation under those pH conditions. Last but not least solubility of the lyophilised samples re-dispersed at pH 8.0 was measured to differentiate irreversible loss of solubility from reversible loss and to simulate conditions at the beginning of fermentation.

Table IV 3 correlation matrix for results that showed significant differences in Tables IV 2 & IV 4

	pH at heating [-]	Solubility (unheated) [%]	Solubility (heated,pH 8) [%]	G'$_{end}$ [Pa]	G'$_{24h}$ [Pa]	recovery [%]	loss of water [%]	ζ-potential [mV]	
pH at heating [-]	1.000								
solubility$_{unheated}$ [%]	0.959***	1.000							
solubility$_{pH\ 8}$ [%]	0.885***	0.842***	1.000						
G'end [Pa]	0.962***	0.971***	0.892***	1.000					
G'24h [Pa]	0.932***	0.942***	0.910***	0.981***	1.000				
recovery [%]	0.911***	0.873***	0.771***	0.871***	0.860***	1.000			
loss of water [%]	-0.718***	-0.602**	-0.576**	-0.581**	-0.564**	-0.704***	1.000		
ζ-potential [mV]	-0.966***	-0.939***	-0.834***	-0,913***	-0,891***	-0,925***	0,746***	1.000	
1^{rst} Peak area (SDS)	0.891***	0.851***	0.703***	0.797***	0.730***	0.852***	-0.582**	-0.884	***

*α = 0.1 **α = 0.05 ***α = 0.01

Solubility of the untreated protein showed a significant pH dependency (Table IV 2). Solubility decreased with decreasing pH and correlated with the ζ-potential (R=-0,939, Table IV 3). Similar behaviour has been extensively described for various plant derived proteins (e.g. Barac et al., 2010) and can be ascribed to the formation of insoluble protein aggregates due to decrease in electrostatic repulsion with decreasing pH value. In a second step, the solubility of pre-treated, lyophilised samples at the pH-value of their respective pre-treatment was measured. Compared to the untreated protein at respective pH values, a further significant decrease of protein solubility (Table IV 2) was found, indicating an additional influence of the pre-treatment process on protein solubility. Similar behaviour was previously reported for heating of soybeans (Nishinari et al., 2014).

Finally, from solubility experiments with lyophilised samples readjusted to simulate the starting pH of fermentation (pH 8) we obtained the following information. First of all, increasing the pH value increased the solubility compared to the values measured at the pH of pre-treatment and secondly, we found a decrease of solubility compared to the untreated sample at pH 8. The former can be ascribed to the presence of some pH reversible aggregates, that dissolve owing to the increased electrostatic repulsion upon increasing the pH. At the same time, the latter indicates an increase of insoluble aggregates caused by irreversible protein denaturation during the pre-treatment. This increase of insoluble aggregates was most pronounced in samples pre-treated at pH 6.0 and led to overall solubilities between 37.6 ±1.1% (pre-treatment at pH 6.0) and 57.2 ± 4.0% (pre-treatment at pH 8.0, Table IV 2) with a correlation coefficient of R=0.885 (Table IV 3). This indicates a shift in the proportions of soluble and insoluble fractions caused by the pH-value during pre-treatment. Higher protein solubility can be ascribed to a higher number of soluble aggregates and vice versa. More specific this means, that samples pre-treated at lower pH values contain fewer soluble and more insoluble aggregates than samples pre-treated at higher pH values. Since soluble aggregates are a prerequisite for gelation while insoluble aggregates may act as inactive fillers (Britten & Giroux, 2001), the differently pre-treated samples are expected to exhibit differences in gelation behaviour.

IV 3.1.3. Molecular weight distribution

SDS-PAGE is most suitable to investigate individual protein sub-fractions involved in aggregation since samples lose their quaternary structure and any non-covalent protein-

protein interactions during sample preparation. Moreover, if SDS-PAGE is performed under reducing and non-reducing conditions, insights in the presence and constitution of disulphide bound aggregates can be gained. However, SDS-PAGE does not distinguish between soluble and insoluble aggregates. To this purpose SEC can be used to investigate the undenatured protein molecules and the formation of soluble aggregates. Consequently, applying both methods leads to a more detailed understanding of the aggregation behaviour of pea protein upon pre-treatment under different pH conditions and the protein fractions involved. For both types of investigation, the lyophilised samples were re-dispersed at the starting pH of fermentation (pH 8.0).

SDS-PAGE under reducing and non-reducing conditions (Fig IV 2a) shows all bands typically expected in pea protein. In more detail, the major pea protein fractions are convicilin at ~70 kDa (Crévieu et al., 1997; Croy, Gatehouse, Tyler, et al., 1980; Swanson, 1990), legumin at ~60 kDa (Croy, Gatehouse, Evans, et al., 1980) and vicilin at ~50 kDa (Gatehouse et al., 1981, 1982, 1983). Moreover, legumin consists of an acidic α-chain (MW~38-40 kDa) and a basic β-chain (MW~20 kDa) (Croy et al., 1979; Croy, Gatehouse, Evans, et al., 1980), that are connected via a disulphide-bond and appear as separate bands on SDS-PAGE under reducing conditions. Vicilin on the other hand is prone to post-translational autolysis which leads to various subunits of lower molecular weights (Dziuba et al., 2014; Gatehouse et al., 1982).

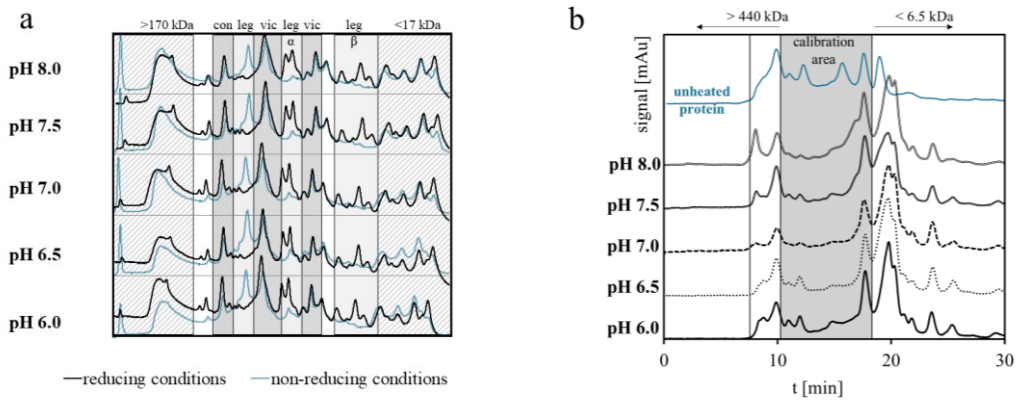

Fig IV 2 SDS-PAGE under reducing and non-reducing conditions (a) and SEC (b) of pea protein heated at pH 6 to 8.

Generally, Fig IV 2a shows similar molecular weight profiles for all samples, independent of pH value during pre-treatment. Besides the bands regularly associated with pea protein, all samples contain two fractions of protein > 170 kDa. Out of these, the fraction with lower molecular weight appears to remain unaffected by the pH value during pre-treatment and shows no relevant differences between reducing and non-reducing conditions. However, upon repetition of the experiment for a random sample with increased SDS-content in the sample buffer (results not shown) this fraction was decreased under reducing conditions, indicating aggregates held together by a mixture of disulphide bonds and strong, non-covalent interactions. The fraction with higher molecular weight only occurs as a prominent peak under non-reducing conditions and corresponds to fractions of the sample that did not migrate into the gel at these conditions. Since this

peak is not present under reducing conditions, the previously retained aggregates must have been formed via disulphide bonds. Disulphide bonds can stabilise both, soluble and insoluble aggregates (Table IV 1). Taking the results from solubility experiments (higher solubility at higher pH during pre-treatment) into account, the larger amount of retained fraction at higher pH during pre-treatment indicates an increased contribution of soluble disulphide bound aggregates.

Considering the aggregation behaviour known for soy where the 7S αα' (corresponding to pea convicilin) fraction forms soluble, disulphide bound aggregates with itself or the acidic 11S (corresponding to the legumin-α subunit) fractions (Yamagishi et al., 1983) (Table IV 1) these soluble aggregates may be constituted from the corresponding pea protein fractions convicilin and legumin α. However, if legumin α subunits were involved, leftover legumin-β subunits (~20 kDa) should appear under non-reducing conditions. As this is not the case, we propose soluble disulphide bound aggregates to only consist of the convicilin fraction. Moreover, given the small differences in convicilin peak heights under reducing and non-reducing conditions, this type of aggregates is unlikely to be exclusively responsible for the retained, disulphide bound fractions. We therefore propose a mixture of soluble disulphide bound convicilin aggregates and various insoluble disulphide bound aggregates consisting of legumin and convicilin (Yamagishi et al., 1983) (Table IV 1).

In SEC (Fig IV 2b, blue line), the untreated pea protein included various fractions within the calibration area while results from pre-treated samples only showed very small fractions and fractions larger than 440 kDa. This indicates heat induced aggregation of legumin (~360 kDa (Croy et al., 1979)) vicilin (~150 kDa (Gatehouse et al., 1981)) and convicilin (280 kDa (Croy, Gatehouse, Tyler, et al., 1980)). Owing to the preliminary filtration step in the method, aggregates detected in SEC can be considered soluble and are therefore likely to consist of various combinations of vicilin, convicilin and convicilin plus legumin β (Table IV 1). Fig IV 2b shows a decrease in these soluble aggregates with decreasing pH value during pre-treatment as indicated by the decrease in peak size of the peak at ~8 minutes, again supporting the conclusions drawn from protein solubility experiments and SDS-PAGE.

In summary, the combined results from protein solubility experiments, SDS-PAGE and SEC show a decrease in the number of disulphide-stabilised and soluble aggregates with decreasing pH during pre-treatment. Insoluble aggregates that may be stabilised via other types of interactions (especially hydrophobic ones) cannot be determined with either method due to sample preparation.

IV 3.2 Gel characterisation

IV 3.2.1. Kinetics of rheological parameters and pH value during fermentation

During fermentation, the pH value dropped from pH 8 to pH values around 4.8. Pre-treatment at different pH values did not significantly influence the kinetics or final pH value (Table IV 4, Fig A 10a Appendix). In contrast, storage moduli (G') at the end of fermentation increased significantly with increasing pH values during pre-treatment (Table IV 4 and Fig A 10b, Appendix) and show a strong correlation (R = 0.842, Table IV 3)

to the protein solubility at the start of fermentation. Higher pH values during pre-treatment led to an increased number of soluble aggregates which are a prerequisite for network formation, while lower pH values led to an increased number of insoluble aggregates that may act as inactive fillers (Britten & Giroux, 2001). Larger numbers of soluble aggregates will lead to a higher degree of crosslinking and therefore to the formation of denser network structures with higher storage and loss moduli. In contrast, a larger proportion of insoluble aggregates reduces the number of soluble aggregates, which leads to a lower degree of crosslinking. Insoluble aggregates may additionally disturb the network formation by acting as inactive fillers. In combination, this leads to coarser network structures with lower moduli.

Table IV 4 pH, storage modulus G' and loss factor tan δ at the end of fermentation, G', recovery from thixotropy test, slope dlogG'/dlogω from frequency sweeps and loss of water after 24 hours of gel storage.

sample	pH_{end} [-]	G'_{end} [Pa]	tan δ_{end}	G'_{24h} [Pa]
pH 6.0	$4.75^{a}\pm0.10$	$164^{a}\pm 84$	$0.167^{a}\pm0.006$	$517^{a}\pm 164$
pH 6.5	$4.77^{a}\pm0.03$	$281^{a}\pm 80$	$0.158^{a}\pm0.015$	$459^{a}\pm 63$
pH 7.0	$4.79^{a}\pm0.08$	$1623^{b}\pm 97$	$0.164^{a}\pm0.005$	$2275^{a}\pm 238$
pH 7.5	$4.82^{a}\pm0.05$	$3665^{c}\pm320$	$0.147^{a}\pm0.006$	$4712^{b}\pm 678$
pH 8.0	$4.77^{a}\pm0.02$	$5488^{d}\pm325$	$0.153^{a}\pm0.003$	$7285^{c}\pm1565$

sample	recovery [%]	dlogG'/dlogω	loss of water [%]
pH 6.0	$14.1^{a}\pm 2.0$	$0.11^{a}\pm0.01$	$4.8^{a}\pm2.0$
pH 6.5	$21.3^{(\blacklozenge)}$	$0.14^{a}\pm0.03$	$2.1^{(\blacklozenge)}$
pH 7.0	$28.7^{b}\pm 3.7$	$0.11^{a}\pm0.02$	$0.9^{b}\pm0.3$
pH 7.5	$32.0^{b}\pm 0.7$	$0.12^{a}\pm0.00$	$1.0^{b}\pm0.3$
pH 8.0	$33.0^{b}\pm 2.6$	$0.11^{a}\pm0.01$	$0.9^{b}\pm0.8$

Different letters represent significant differences (α=0.05) as derived from ANOVA followed by Tukey post-Hoc test.
(♦) value calculated from double determination due to equipment failure. Data point was excluded from ANOVA and post-Hoc test.

The differences in absolute values of G' and G'' caused by different pre-treatments did not affect the ratio between elastic and viscous proportions. Loss factor tan δ was similar for all samples (Table 4), indicating similar viscoelastic network-properties under linear viscoelastic conditions at all pre-treatment conditions. If the viscoelastic network properties of gels produced from the same raw material under the same gelation conditions are similar while the absolute value of storage and loss modulus G' and G'' varies, it is reasonable to assume a similar general gelation mechanism based on similar types of interactions, where the main difference between samples is the number of available soluble aggregates and resulting degrees of crosslinking.

IV 3.2.2. Characterisation of pea protein gels after resting at 4 °C for 24 hours

This proposed gel structure with different degrees of crosslinking was further investigated by small and large amplitude rheology, loss of water and CLSM experiments.

Frequency sweeps are generally used as an indicator for time dependent deformation of samples. In this context, short time behaviour is reflected by higher frequencies, and long-term behaviour by lower frequencies. In our study – independent of pre-treatment conditions – all samples showed a similar, low slope of log G' over log ω

(Table IV 4 and Fig A 11) for the investigated frequency range. This is typical for gels and dispersions (Mezger, 2006). Furthermore, the values of ~0.12 were of the same magnitude as in our previous work (Klost & Drusch, 2019b) and are in line with values reported for milk yoghurts (Hassan et al., 2003). At lower frequencies, the storage modulus additionally indicates the degree of crosslinking. The higher the modulus, the higher the degree of crosslinking and vice versa (Mezger, 2006). For our samples this implies an increase in the degree of crosslinking and network density with increasing pH value during pre-treatment. Moreover, differences in network density were also found in CLSM experiments (Fig IV 3). In gels made from protein pre-treated at pH 6.0 mainly large protein fragments are apparent with only a coarse network-structure visible. With increasing pH values during protein pre-treatment, the corresponding gels become denser and the number of large particles decreases.

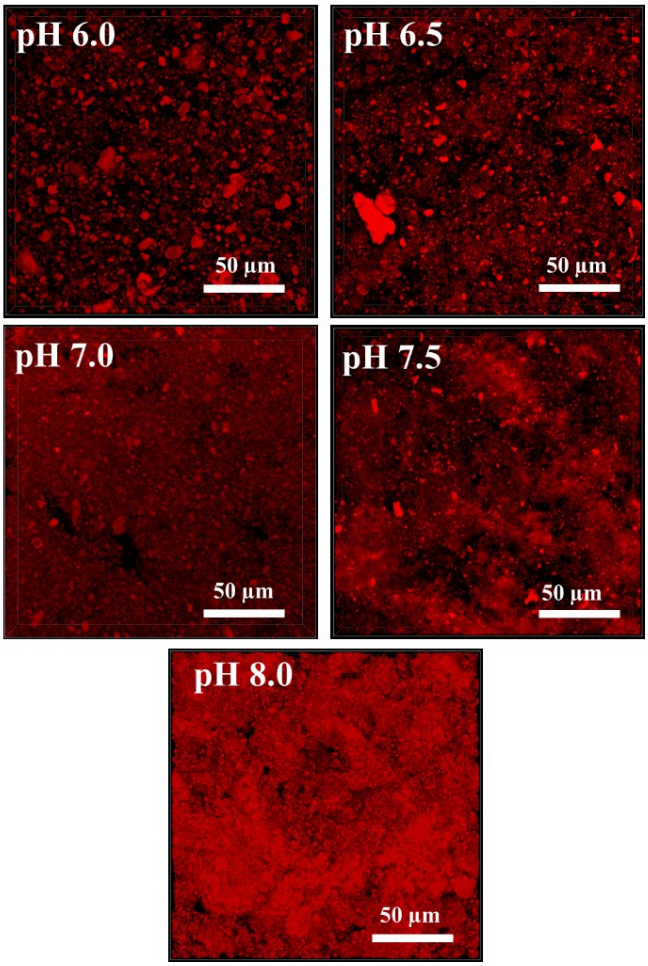

Fig IV 3 CLSM micrographs of fermentation induced pea protein gels made from pea protein slurry pre-treated at pH 6.0 to 8.0. pH values during heating are noted in the upper left-hand corner of the micrographs.

From thixotropy experiments we derive differences in the restructuring ability of the gels (Table IV 4). The higher the pH during pre-treatment, the more pronounced was the structure recovery. Values ranged from 14.1 ± 2.0% at pH 6.0 to 33.0 ± 2.6% at pH 8.0 with pH 7.0 to pH 8.0 showing significantly higher recovery than samples pre-treated at pH 6.0. We ascribe these differences in structure recovery to the lower degree of crosslinking in samples pre-treated at lower pH values. In gels with lower degrees of crosslinking, the remaining network fragments are less likely to find a suitable counterpart for restructuring after intense shearing. Owing to their inactive filler properties, insoluble aggregates may additionally enhance this effect. In combination this leads to a decreased structure recovery. The results from thixotropy experiments correlate (R = -0.704, Table IV 3) with the results from loss of water experiments. Moreover, in loss of water experiments, samples made from protein pre-treated at pH 6.0 significantly differed from samples pre-treated at pH values ≥7.0. This increased loss of water after protein pre-treatment at low pH values is caused by larger pores in the coarser network structure of the corresponding gels.

Amplitude sweeps (Fig IV 4) were performed to characterise the non-viscoelastic behaviour of the gels. Outside the linear viscoelastic regime, the rheological behaviour cannot exclusively be described by G' and G'' (Fig IV 4a, top row) as higher harmonics become more relevant (Hyun et al., 2011). Appropriate additional means to interpret the transition from linear viscoelastic to non-linear viscoelastic behaviour as well as the non-linear viscoelastic behaviour itself are Lissajous plots (Fig IV 4b), stress decomposition (Fig IV 4c), dissipation ratio φ (Fig IV 4a, middle row) and the calculation of the stiffening ratio (S-factor) (Fig IV 4a, bottom row). Especially with regard to dissipation ratio φ and S-factor it needs to be kept in mind, that they describe the intracycle behaviour at a fixed intercycle strain amplitude γ_0, rather than the overall intercycle behaviour. Lissajous plots can be used to interpret the overall intercycle behaviour of gels as well as the intracycle deviation from linear viscoelastic behaviour by analysing their rotational behaviour and overall shapes. From stress decomposition a closer insight into the changes to elastic stress and more detailed knowledge on the intracycle stiffening/softening behaviour can be obtained. The calculation of S-factors reflects this intracycle behaviour onto the entire range of intercycle strain amplitudes γ_0 and the dissipation ratio φ can be applied to distinguish intracycle strain stiffening behaviour from effects caused by the transition from predominantly elastic to mainly plastic behaviour. Results for all investigated samples in our study are shown in Fig IV 4. Fig IV 4a shows the intercycle development of storage modulus G' and loss modulus G'' (top row), alongside the projection of intracycle parameters dissipation ratio φ and stiffening ratio (S-factor) on the entire range of investigated intercycle strain amplitudes γ_0 (middle and bottom row respectively). Fig IV 4b uses Lissajous plots to show the total stress τ over the intracycle strain γ for all samples at various intercycle strain amplitudes γ_0 and Fig IV 4c shows the corresponding elastic stress τ' over the intracycle strain γ for all samples at various intercycle strain amplitudes γ_0.

Analogous to observations in all other rheological tests, results from amplitude sweeps showed similar curves of storage modulus G' and loss modulus G'' for all samples (Fig IV 4a, top row). Between samples, these curves mainly differed in the absolute values of G' and G''. Linear viscoelastic regimes – calculated as intercycle strain amplitude γ_0 up to which G' deviated no more than 5% from the value at the lowest intercycle strain amplitude γ_0 – extended to $\gamma_0 \approx 1\%$ with no relevant influence of pH during pre-treatment. The extend of the linear viscoelastic regime is further supported by results from the dissipation ratio φ and S-factor, where constant values are remained up to intercycle strain amplitudes γ_0 between 1% and 2.5% (Fig IV 4a, second and third row). Beyond the viscoelastic regime the overall intercycle rheological behaviour is strain softening. However, in order to take higher harmonics into account and to determine potential differences between samples it is worthwhile to also investigate the intracycle rheological behaviour by means of the parameters illustrated above.

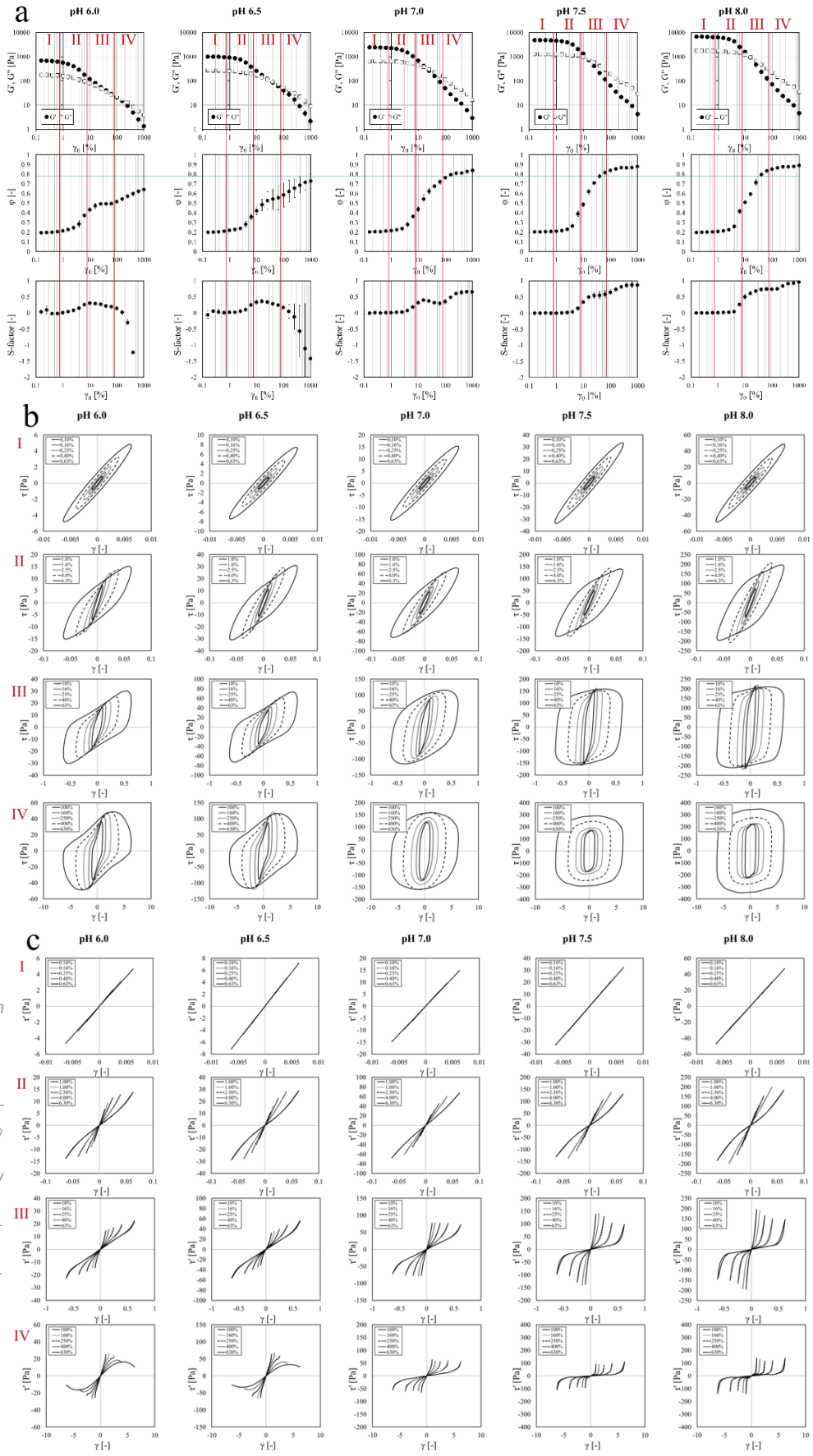

Fig IV 4 amplitude sweeps of fermentation induced pea protein gels made from pea protein pre-treated at pH 6.0 to 8.0 at intercycle strain amplitudes γ_0 between 0.1% and 1010% and a frequency of 1 s^{-1}. (a) top row: storage and loss modulus G' and G'' over, γ_0, (a) middle row: dissipation ratio φ over γ_0, (a) bottom row: stiffening ratio (S-factor) over γ_0, (b): elastic Lissajous plots, (c) elastic stress.

At intercycle strain amplitudes γ_0 within the linear-viscoelastic regime ($\gamma_0 \leq 1\%$, marked "I" in Fig IV 4a to c) elastic Lissajous plots (Fig IV 4b I) have distinct elliptical shapes and the elastic stress τ' assumes the shape of a straight line (Fig IV 4c I) as expected for linear viscoelastic behaviour. Moreover, no differences were observed between samples and the narrow shape of the Lissajous plots indicates predominantly elastic properties. This corresponds to the tan δ values, which are closer to zero than to one (Table IV 4) and to dissipation ratios φ of approximately 0.2 (Fig IV 4a I, middle row) that indicate predominantly elastic behaviour.

Lissajous plots and elastic stress τ' at intercycle strain amplitudes $1\% \leq \gamma_0 \leq 6.3\%$ (Fig IV 4b and c II), begin to rotate clockwise with increasing intercycle strain amplitude γ_0, which indicates a gradual overall intercycle softening of the material (Ng et al., 2011) and reflects the overall behaviour seen in Fig IV 4a, top row. This behaviour is likely to be caused by alignment of network segments within the flow field or loss of network junctions that – similar to the effects observed in thixotropy tests – may lead to network segments which are unable to rejoin the network (Hyun et al., 2011). Moreover, in this range of intercycle strain amplitude γ_0 the shape of the Lissajous plots begins to get distorted from the elliptical shape, and elastic stress τ' starts to deviate from a straight line showing a clear impact of higher harmonics. However, depending on the pH value during pre-treatment, the distortion to the Lissajous plots is of different character and magnitude. If samples were pre-treated at pH 6.0 or pH 6.5, the corresponding elastic plots (Fig IV 4d, II) begin to rotate and distort from an elliptical shape sooner, but the distortion appears to be gradual and fairly uniform. With increasing pH value during pre-treatment, rotation starts at higher amplitudes, and – especially for samples pre-treated at pH 7.5 and pH 8.0 – the distortion from elliptical shape starts more sudden ($\gamma_0 = 6.3\%$) and leads to more pronounced changes in shape. Lissajous plots from samples pre-treated at pH 7.0 show intermediate rotation and deformation behaviour. In addition, the shapes of the Lissajous plots are widening thus increasing the enclosed area indicating an increasingly dissipative response (Ng et al., 2011).

This effect is further quantified in the dissipation ratio φ (Fig IV 4a II second row) which starts to become dependent of the intercycle strain amplitude γ_0 and begins to increase, thus indicating a beginning shift from predominantly elastic behaviour towards an increasing contribution of plastic properties (Ewoldt et al., 2010). The deviation in the shape of Lissajous plots and the increase in dissipation ratio φ are accompanied by the transition of elastic stress τ' curves from a straight line towards an inversed sigmoidal shape. The decreased slope at low intracycle strain γ indicates a beginning reduction of size and volume fraction of rigid clusters (Park et al., 2015) and supports the beginning shift from elastic to plastic properties, while the increasing slope at higher intracycle strain γ reflects the stretching of remaining clusters that cause intracycle stiffening (Park et al., 2015). This is reflected in the increase of the S-factor (Fig IV 4a II, third row) which – in this range of intercycle strain amplitudes γ_0 is likely to be related to intracycle strain stiffening since the dissipation ratio φ is still well within the elastic range and the network structures only just began to be disrupted.

At intercycle strain γ_0 yet another order of magnitude higher ($10\% \leq \gamma_0 \leq 63\%$, Fig IV 4b and c III) all shapes are distorted and show clear differences between samples.

While Lissajous plots of samples pre-treated at pH 6.0 or pH 6.5 assume slightly bone shaped profiles, pre-treatment at pH 8.0 leads to Lissajous plots that are nearly rectangular shaped which implies an approximation towards perfect plastic behaviour (Fig IV 4b and c III) (Ewoldt et al., 2010). Samples pre-treated at pH-values in between, show in-between distortions. In this range of intercycle strain amplitude γ_0 the clockwise rotation also proceeds, as visible in Lissajous plots, and – more distinctly – in the elastic stress (Fig IV 4b III). Consequently, the slopes at small intracycle strain γ decrease further, indicating a continued intercycle strain softening behaviour owing to further reduction of rigid clusters. Nevertheless, at large intracycle strain the slope of the elastic stress still increases apparently indicating some remaining intracycle strain stiffening properties and therefore some residual elastic properties resulting in continuously positive S-factors in Fig IV 4a III (third row). Despite overall similarities of the elastic stress curves, differences between samples become apparent in the considered range of intercycle strain γ_0. While samples pre-treated at pH 6.0 and pH 6.5 showed more moderate rotation and a less pronounced inversed sigmoidal shape, increased pH values during pre-treatment led to an almost horizontal slope at low intracycle strain γ which indicates an almost complete loss of rigid structures. These observations are reflected in the development of the dissipation ratio φ (Fig IV 4a III, second row). While samples pre-treated at pH 6.0 and pH 6.5 only reach values in the range of $\varphi \approx 0.5$ in the discussed range of intracycle strain amplitudes γ_0 ($10\% \leq \gamma_0 \leq 63$) pre-treatment at pH 7.5 or pH 8.0 leads to $\varphi > \pi/4$ and therefore – in agreement with the vast loss of rigid structures deduced from elastic stress τ' and the shape of the Lissajous plots – the intracycle behaviour becomes predominantly plastic for these samples.

At the highest intercycle strain amplitudes γ_0 distortion of the Lissajous plots proceeds even further (Fig IV 4b IV). In case of samples pre-treated at pH 6.0 and pH 6.5, the increase in dissipated energy as indicated by the increase of the enclosed area in Lissajous plots (Fig IV 4b IV) is accompanied by a transition from intracycle strain stiffening to intracycle strain softening behaviour as derived from the shift of elastic stress τ' curves from inversed sigmoidal to sigmoidal shape at the highest intercycle strains γ_0. This shift is accompanied by a decrease of the S-factor below 0 and a second increase in the curves of the dissipation ratio φ. Despite the increase in dissipation ratio φ to final values of 0.64 ± 0.01 (pre-treatment at pH 6.0) and 0.73 ± 0.07 (pre-treatment at pH 6.5), these samples maintain a relevant proportion of elastic behaviour within the investigated deformation range, since final values of the dissipation ratio φ remain below $\pi/4$ and the S-factors become negative. In contrast, for samples pre-treated at pH 7.0 to pH 8.0 the shapes approach rectangles with slightly rounded tops and bottoms which are similar to those described by (Ewoldt et al., 2010) for predominantly plastic systems. The shift to predominantly plastic behaviour is further reflected in the dissipation ratio φ that reaches final values of 0.84 ± 0.01, 0.88 ± 0.00 and 0.89 ± 0.00 for samples pre-treated at pH 7.0, pH 7.5 and pH 8.0 respectively and S-factors that increase further and approach final values of 0.66 ± 0.06, 0.87 ± 0.09 and 0.96 ± 0.03 respectively. Since positive S-factors generally indicate strain stiffening behaviour but may also indicate a transition from elastic to plastic behaviour as explained in the materials and methods section above, a closer investigation of the obtained S-factors is necessary. The curves of the S-factor (Fig IV 4a, bottom row) show an indentation at the beginning of the considered

amplitude range (100% ≤ γ_0 ≤ 630%, section IV) followed by a second increase. This indentation is most pronounced upon pre-treatment at pH 7.0 and decreases with increasing pH during pre-treatment. While it is reasonable to assume that in analogy to the curves of samples pre-treated at pH 6.0 and pH 6.5 the initial increase in these curves can be related to intracycle strain stiffening effects, this second increase must not necessarily be an indicator of continuing intracycle strain stiffening behaviour at the highest intercycle strain amplitudes γ_0. In fact, this would be very unlikely based on the presented results for elastic stress at the corresponding intercycle strain amplitudes γ_0 but can rather be explained by the fact, that in this case the tangent modulus at minimum intracycle strain γ (G_M) becomes negligible and the S-factor consequently diverges towards one as explained in the materials and methods section above for plastic behaviour (Ewoldt et al., 2010). Overall, these samples lost the majority of elastic properties while samples pre-treated at pH 6.0 and pH 6.5 retained a higher proportion of elastic properties. This leads to the conclusion, that coarser network structures are less prone to a complete transition towards plastic properties under the applied oscillatory strain conditions owing to an increased structural flexibility.

The underlying effects and differences between rheological behaviour of the samples outside the linear viscoelastic regime can best be related to their differences in network densities. In summary, all samples show intercycle strain softening, as derived from the clockwise rotation of the Lissajous plots (Ng et al., 2011) and elastic stress curves. For samples pre-treated at pH 6.0 and pH 6.5, the rotation starts sooner, indicating a higher flexibility of coarser networks to follow deformation, as a more flexible network is more likely to orient in the flow field. Additionally, the higher flexibility leads to a more gradual decrease in bond numbers and is reflected in transition from intracycle strain stiffening towards intracycle strain softening at higher intercycle strain γ_0. Denser gels (i.e. samples pre-treated at pH 7.0 to 8.0) are able to resist intercycle strain softening slightly longer, but – owing to their denser structures – have a higher degree of crosslinking and are therefore more prone to small microcracks (Faber et al., 2017) and decreasing bond numbers (Hsiao et al., 2012; Park et al., 2015; Park & Ahn, 2013) in the gel network. This in turn leads to the gradual disintegration of the gel and the transition from predominantly elastic properties to mainly plastic behaviour.

IV 4 Conclusions

In summary our results show, that different pH values during pre-treatment of pea protein lead to different ratios between soluble and insoluble protein aggregates in the protein slurry before fermentation. These different ratios in turn are the determining factor, when it comes to the degree of crosslinking during gelation and the content of inactive fillers, that may disrupt the gel network structure and thus directly influence the rheological properties. It was found, that all gels showed frequency dependencies similar to milk yoghurts. However, storage and loss moduli were at significantly different magnitudes if pre-treatment was carried out between pH 6.5 and pH 8.0, confirming different degrees of crosslinking. Furthermore, the ability to recover network structures after intense shearing decreased with decreasing pH values during pre-treatment. Large amplitude oscillatory shear rheology indicated an overall intercycle strain softening behaviour

and further confirmed differences in network densities. While denser networks started to decompose into smaller clusters sooner and eventually changed from predominantly elastic to mainly plastic behaviour, coarser networks displayed a higher flexibility towards deformation. Adjusting the pH value during pre-treatment of pea protein prior to fermentation induced gelation is therefore a valid tool for the customisation of the texture properties of pea protein-based yoghurt alternatives. With this knowledge in mind – besides catering to consumers preferences concerning yoghurt alternatives – further opportunities for the development of a wide range of fermented pea protein products with different texture requirements such as bread spreads, confectionary fillings etc. open up.

Acknowledgements:

The authors gratefully acknowledge the assistance and expertise of L. Barthel for CLSM measurements and the skilful lab-work of C. Härter as well as the proofreading by M. Brückner-Gühmann.

Funding:

This work was supported by NutriAct – Competence Cluster Nutrition Research Berlin-Potsdam funded by the Federal Ministry of Education and Research (BMBF) (FKZ: 01EA1806C).

CRediT authorship contribution statement

M. Klost: Conceptualization, Supervision, Writing - original draft, Writing - review & editing, Formal analysis, Data curation, Visualization. C. Brzeski: Formal analysis, Investigation, Data curation, Visualization. S. Drusch: Supervision, Writing - review & editing, Funding acquisition, Resource

General discussion

Characterisation of molecular and physico-chemical properties of pea protein and pea protein hydrolysates

This section will discuss results from Manuscripts I, II, III, and IV with focus on the influence of enzymatic hydrolysis, pH value and temperature on molecular and physico-chemical properties like molecular weight distribution, hydrophobicity, surface electrical properties (measured as ζ-potential) and protein solubility.

Generally, the molecular weight distribution followed a typical pea protein pattern (convicilin at ~70-80 kDa (Adal et al., 2017; Croy, Gatehouse, Tyler, et al., 1980), legumin at 60 KDa (Croy, Gatehouse, Evans, et al., 1980) (with legumin-α at 38 to 40 kDa and legumin-β at 20 KDa under reducing conditions), Vicilin at 50 kDa and various smaller vicilin fractions at 33 kDa, 19 kDa and <17 kDa (Gatehouse et al., 1982)) in SDS-PAGE under reducing and non-reducing conditions, respectively (Manuscripts I, III and IV (Fig I 1a, Fig III 1 and Fig IV 2a)). Upon enzymatic hydrolysis, molecular weight profiles deviated from the original profile (Manuscripts I and III (Fig I 1a and Fig III 1)). In Manuscript III hydrolysis with Protamex® only slightly decreased the major protein fractions as described in literature for lentil protein (Garcia-Mora et al., 2015), while Alcalase® cleaved all fractions and only left peptides smaller than 17 kDa (Fig III 1). More specifically, it could be shown that Protamex® mainly cleaved the larger vicilin fractions and some of the convicilin, but had little effect on the legumin fractions (Fig III 1). Out of the three enzymes used in this thesis, trypsin is best described in literature with regard to specificity and cleavage kinetics in the individual pea protein fractions (Krause & Schwenke, 1995; Plumb et al., 1989; Plumb & Lambert, 1990). Tryptic hydrolysis in Manuscripts I and III generally followed the cleavage behaviour described in this literature: it mainly cleaved legumin-α, convicilin and the vicilin α+β fragment (Manuscript III, Fig III 1) or generated legumin-T while degrading almost all other fractions (Manuscript I, Fig I 1a). While at first sight, the results from Manuscripts I and III appear inconsistent, a second look shows they match quite well: in Manuscript I, SDS-PAGE was performed under non-reducing conditions, and one main peak appeared at ~50 kDa after hydrolysis (Fig I 1a). In combination with results from SEC (Fig I 1b), this peak was solely assigned to legumin-T because of the observed molecular weight distribution in the chromatogram. However, results from Manuscript IV (Fig IV 2b) show clearly that in unhydrolysed but heated samples, all native pea protein fractions disappear. This was ascribed to the formation of aggregates during heating which, in turn, could not pass the filtration step prior to SEC experiments. Therefore, retrospectively the absence of vicilin in the SEC profile in Manuscript I does not necessarily indicate its complete cleavage, and the 50 kDa peak in the SDS-PAGE may contain both legumin-T and vicilin. Smaller differences in molecular weight profiles between Manuscripts I and III may be ascribed to different degrees of hydrolysis (DH 2 and DH 4 in Manuscript I vs. DH 1 in Manuscript III),

different pea protein (lab scale in Manuscript I vs. pilot scale in Manuscript III) and different sources of enzyme (trypsin from bovine pancreas in Manuscript I vs. microbial trypsin in Manuscript III).

As expected, enzymatic hydrolysis of pea protein led to increased solubility (Manuscript I, Fig I 2 and unpublished material from Manuscript III, Fig A 12 Appendix) especially at pH values close to pI = 4.8. In Manuscript I, the increase at pH 5 was 18% (DH 2) and 29% (DH 4) respectively upon hydrolysis of lab scale produced pea protein concentrate with trypsin from bovine pancreas. The increase in Manuscript III was 17% (Protamex®, DH 1), 16% (microbial trypsin, DH 1) and 36% (Alcalase®, DH 1) respectively upon hydrolysis of a pilot scale produced pea protein isolate. Even though the type of pea protein, degree of hydrolysis and choice of enzyme or – in the case of trypsin – enzyme origin varied between studies, a tendency towards a higher solubility increase upon generation of smaller peptides can be observed. More specifically, hydrolysis with Alcalase® that only generated small peptides of molecular weight below 17 kDa (Manuscript III, Fig III 1) yielded the highest increase in solubility (Fig A 12, Appendix), whereas both trypsin at DH 1 and DH 2 and Protamex® at DH 1 which were found to only slightly decrease some of the major protein fractions (Manuscripts I and III, Fig I 1 and Fig III 1), only increased the solubility by 16 to 18% (Fig I 2, Manuscript I and Fig A 12, Appendix). If pea protein was hydrolysed to DH 4 by trypsin, a higher proportion of smaller peptides was generated, which led to an increase in solubility by 29% (Manuscript I, Fig I 2), thus confirming the proposed increase in solubility with decreasing molecular weight. The increase in solubility can be explained with an increase in exposed charged (or chargeable) groups, i.e. terminal carboxyl groups and amino groups of the emerging peptides (Panyam & Kilara, 1996), as well as previously buried charged or polar side chains. These peptides can be hydrated more easily and are therefore less likely to aggregate and precipitate. However, if very small peptides are generated e.g. owing to cleavage specificities where peptide sizes are distributed very inhomogenously, as for example in tryptic hydrolysis, small hydrophobic peptides may also emerge especially from the hydrophobic and predominantly basic β-chain of legumin. These peptides will subsequently begin to aggregate especially at neutral and basic pH values, where their respective net charges are low and consequently cause a decrease in solubility at those pH values (Manuscript I, Fig I 2) (Barac et al., 2011; Tsoukala et al., 2006; Tsumura et al., 2005).

Another factor that was found to influence the solubility of pea protein was the pH value of the aqueous phase (Manuscript I, Fig I 2, Manuscript III, Fig A 12 (Appendix) and Manuscript IV, Table IV 2). pH dependency of protein solubility is a well-known phenomenon that occurs for many proteins and is very pronounced in most plant-derived storage proteins. It can be related to the shift in the ratio of protonated to dissociated carboxyl groups ($COOH/COO^-$) and amino groups (NH_3^+/NH_2) which will be influenced by the changing concentration of H^+ and OH^- ions in the solvent upon adjustment of pH value. This shift in the ratio of protonated to dissociated groups can, in turn, be measured e.g. as ζ-potential. ζ-potentials in Manuscript I (Fig I 3), Manuscript III (data not shown, but presented in Fig A 13, Appendix) and Manuscript IV (Table IV 2) follow this general concept. As extensively discussed in Manuscript IV, the heating of protein slurries at various pH values and therefore at various ratios of protonated to dissociated groups led to different ratios between soluble and insoluble aggregates and therefore different

solubilities (Table IV 2). In this context, the solubility could be correlated with the ζ-potential at the respective pH values (R=-0.834, Table IV 3) and increased with increasing |ζ-potential| owing to a decrease in interactions between protein molecules upon increase of electrostatic repulsion.

Additionally, from Manuscript I (Fig I 3) and Manuscript III (Fig A 13, Appendix), the pI can be derived as the pH value, where the ζ-potential becomes zero. For the pea protein this value is ~4.8. However, similar to effects previously described for hydrolysis of soy protein (Ochiai et al., 1982), both heating and hydrolysis led to a shift of the pI towards lower pH values. This shift was lowest in unhydrolysed but heated protein and increased with an increasing degree of hydrolysis (Manuscript I) and decreasing enzyme specificity (Manuscript III). In both cases, it is likely that this is caused by aggregation and the resulting development of insoluble aggregates. More specifically, upon heating the protein began to unfold, and consequently exposed previously buried hydrophobic patches which were measured as red shifts of 6 to 10 nm in intrinsic fluorescence measurements in Manuscripts II and IV respectively (Fig II 1a and Table IV 2). This increase in exposed hydrophobic patches may in turn have promoted the interaction between areas of the protein that are less charged at the pH value of heating (pH 8 in Manuscripts I and III). It is therefore very likely that predominantly areas of newly exposed legumin-β interacted, since the pI of legumin-β is between pH 8.4 and pH 8.8 (Krishna et al., 1979) and therefore this region of the protein will carry only a weak net charge under the applied conditions. Enzymatic hydrolysis additionally enhanced this effect owing to promotion of protein flexibility and therefore easier unfolding and the release of individual peptides, some of which will also carry low net charges at the environmental condition. Consequently, if more basic fractions are involved in the formation of aggregates, fewer amino groups are available for protonation and the pI shifts towards lower pH values.

Elucidation and understanding of gelation kinetics and gel network properties of pea protein and pea protein hydrolysates based on molecular interactions in bulk and at the oil-water interface.

This section will discuss results from Manuscripts I, II, III and VI with focus on gelation kinetics and network properties in bulk and at the oil-water interface. For this purpose, gelation behaviour, involved interactions and protein fractions were investigated intensively for fermentation-induced bulk gels, and will be transferred to the interfacial gelation behaviour further down.

As expected, pea protein was able to form viscoelastic network structures both in bulk and at the interface (Manuscripts I, II, III and IV). The general acidification mechanism in fermentation-induced gelation is based on the gradual release of lactic acid upon microbial digestion of sucrose. Upon decrease of pH, the formation of a space-spanning network is initiated and can be tracked with rheological time sweeps as extensively described in Manuscript II. In brief, the loss factor tan δ began to decrease and the complex shear modulus |G*| increased (Fig II 2, Manuscript II) shortly after the onset of pH decline. The increase of |G*| began between pH 6.5 and 6.2 and therefore distinctly above the isoelectric points of legumin (pH 4.8) and vicilin (pH 5.5) (Danielsson, 1950). A first

maximum in structuring velocity d|G*|/dpH was found at pH 6.0 followed by a decline and another steep increase between pH 5.5 and 4.8 where fermentation ended (Fig II 2c, Manuscript II). First of all, from the two maxima found in the maximum structuring velocity d|G*|/dpH a two-step gelation process was deduced comprising the formation of an overall percolating (i.e. porous, mesh-like) network followed by condensation of small aggregates that further stabilise the primary network structure. This proposed gelation behaviour was further supported by SEM where an overall percolating network was seen at 300x magnification (Fig II 3a, Manuscript II) and the rough appearance of the structure surface at 3000x magnification (Fig II 3b, Manuscript II) indicates the condensation of smaller aggregates. The onset of gelation distinctly above the pI can be ascribed to the heterogeneity of pea protein. More specifically, owing to their pI above pH 8 (Krishna et al., 1979), at pH values below pH 8, the basic legumin-β chains carry a positive charge, while most other fractions will be negatively charged, thus first interactions will begin to occur between the legumin-β sections of legumin and other fractions even above the pI. Literature on soy protein specifies these interactions to occur between the 11S basic chain (corresponding to legumin-β in pea protein) and the β-subunits of the 7S protein (corresponding to vicilin in pea protein) (Grygorczyk & Corredig, 2013).

Results from Manuscript III revealed these interactions to be mainly electrostatic in nature as indicated by gel solubility experiments, where mainly legumin-β and vicilin were released upon incubation of a gel sample in a 0.5 M NaCl solution (Fig III 3, Manuscript III). Moreover, the smaller maximum in structuring velocity at this pH range (~pH 6.0) compared to the larger effect at pH values between pH 5.5 and pH 4.8 (Fig II 2, Manuscript II) is in agreement with the overall results from gel solubility experiments (Fig III 2, Manuscript III) where the overall influence of electrostatic interactions as derived from the combination of effects seen by incubation in propylene glycol (PG) and NaCl is small compared to that of hydrophobic effects. By inference, it can be additionally deduced that the second, larger maximum in structuring velocity at pH values between pH 5.5 and pH 4.8 described in Manuscript II (Fig II 2) should be related to the formation of hydrophobic interactions that were found to be the predominant types of interactions in Manuscript III (Fig III 2). Owing to the close proximity of the discussed pH range to the isoelectric points of legumin and vicilin (pH 4.8 and pH 5.5, respectively (Danielsson, 1950)), these hydrophobic interactions were most likely promoted by the low overall net charge (as indicated by low ζ-potentials in Fig I 3 and Fig A 13) and the resulting lack of electrostatic repulsion.

Results from Manuscript III further indicate that despite some incorporation of vicilin via electrostatic interactions, the gel network is mainly constituted from legumin. Considering the isoelectric points of legumin and vicilin in relation to the pH value at the end of fermentation (pH 4.8 (pI legumin) and pH 5.5 (pI vicilin) (Danielsson, 1950) vs. pH 4.7 to pH 4.8 (end of fermentation), Manuscripts II and IV, Table II 3 and Table IV 4), a possible explanation for the lower integration of vicilin via hydrophobic interactions may be a remaining net charge on this fraction which allows for some electrostatic repulsion. In summary, combining the results from Manuscripts II and III, fermentation-induced bulk gelation is likely to follow a mechanism of initial formation of a percolating network structure via electrostatic interactions between legumin-β and vicilin. Upon further decrease of pH, electrostatic repulsion decreases, thus promoting hydrophobic

interactions that lead to the condensation of aggregates at the previously formed structures. These may initially involve the vicilin fraction, as the pronounced increase of structuring velocity starts at the pI of this fraction. When the pH shifts further towards the pI of legumin, more legumin fractions will be incorporated into the network, while some of the vicilin may disconnect again.

The effects shown for fermentation-induced bulk gelation can be transferred to interfacial network formation behaviour in emulsions despite differences in the pre-gelation unfolding mechanism and the adjustment to selected pH values (pH 4, pH 5 and pH 7) instead of a gradual pH decrease. The effect of changes in electrostatic repulsion caused by pH-decrease during fermentation can be directly reflected on the pH dependency of pea protein stabilised interfacial films made from unhydrolysed pea protein at selected pH values (Manuscript I). In this context, in fermentation-induced bulk gelation (Manuscripts II, II and IV) and interfacial gelation (Manuscript I) of unhydrolysed pea protein, the rheological parameters complex shear modulus |G*| (Manuscript II, Fig II 2), storage modulus G' (fermentation in Manuscripts III and IV, data not shown), complex interfacial shear modulus $|G_i^*|$ and interfacial dilatational modulus |E*| (Manuscript I, Fig I 6) respectively increase at pH values closer to pI. This suggests a gelation mechanism based on similar types of interactions and involved protein fractions in bulk and at the interface, i.e. some electrostatic interactions between legumin-β and vicilin at pH 7 and additional hydrophobic interactions involving legumin fractions at pH 4 and pH 5 around the pI of legumin (pH 4.8 (Danielsson, 1950)).

Upon tryptic hydrolysis the interfacial shear $|G_i^*|$ and dilatational |E*| moduli increased, while the loss factor tan δ decreased especially at pH 7, indicating overall stronger, more elastic network structures. Additionally, the slopes from interfacial dilatational frequency sweeps decreased below 0.1, indicating mainly in-plane structural rearrangement upon dilatation and compression of the interface (Wan et al., 2016). When considering results from Manuscript III that extensively investigated the protein fractions and types of interactions involved in fermentation-induced bulk networks alongside the influence of enzymatic hydrolysis on the integration of individual protein fractions into the gel network, the effects observed at the interface can be explained.

Results from Manuscript III show electrostatic interactions between legumin-β and vicilin, in particular, to be enhanced by tryptic hydrolysis owing to more exposed legumin-β. This effect may, in turn, be responsible for the increase in interfacial shear modulus $|G_i^*|$ and dilatational modulus |E*| observed at the interface after enzymatic hydrolysis. Moreover, from Manuscript III, it is known that the increased interaction between legumin-β and vicilin leads to a complete incorporation of all protein fractions into the network structure, whereas vicilin was readily released from bulk gels formed from unhydrolysed pea protein (Fig III 3a and c). Since the slopes of interfacial dilatational frequency sweeps of tryptic pea protein hydrolysates decreased below 0.1, indicating mainly in-plane structural rearrangements rather than desorption (Wan et al., 2016), an effect similar to the incorporation of all major protein fractions into fermentation-induced bulk gels in Manuscript III can also be assumed in interfacial gelation. More specifically, unhydrolysed protein forms an interfacial network that is mainly based on hydrophobic interactions within the legumin fraction and a smaller contribution of

electrostatic interactions between legumin-β and vicilin where at least parts of the vicilin fractions (50 kDa and 30 kDa) remain unattached. This, in turn, leads to the observed interchange with the bulk. Upon tryptic hydrolysis – owing to more accessible legumin-β – this effect is vastly reduced by incorporation of vicilin into the network via electrostatic interactions with the legumin β.

In summary, similar gelation behaviour can be ascribed to pea protein at the oil-water interface and in fermentation-induced bulk gels. However, while the increased incorporation of vicilin via electrostatic interactions after tryptic hydrolysis had no relevant effect on overall bulk network properties, it distinctly improved the interfacial gel properties by increasing the elastic proportion and the overall gel strength and inhibiting desorption of protein from the interface into the bulk phase.

Application of the obtained knowledge on molecular, physico-chemical and gelation properties of pea protein and pea protein hydrolysates towards the modification of texture and nutritional characteristics of fermentation-induced pea protein gels

The following section discusses the rheological behaviour of fully set, fermentation-induced bulk gels with focus on their network structure in relation to protein concentration and enzymatic modification, and aims to utilise this knowledge towards strategies for the customisation of texture properties and the fortification of gels with additional nutritionally valuable supplements, such as rapeseed oil and oat fibre.

All fully set gels were subjected to a thorough rheological characterisation. Generally, in all studies, the protein network was found to be the dominating structure in the fermentation-induced bulk gels irrespective of fortification. Furthermore, a similar loss factor tan δ was determined for all investigated samples in Manuscripts II to IV (Table II 3, Table III 2 and Table IV 4) independent of raw material, hydrolysis, differences in the ratio of soluble and insoluble aggregates or fortification, thus indicating similar basic network constitutions with regard to involved interactions and protein fractions. In rheological experiments, all studies yielded similar tendencies for the intercycle rheological behaviour of fermentation-induced pea protein gels in amplitude and frequency sweeps. Linear viscoelastic behaviour was found to occur up to deformations of approximately $\gamma_0 = 1\%$ (Manuscripts II to IV, Fig II 4c, Fig III 4b and Fig IV 4a) followed by overall strain softening behaviour (Hyun et al., 2002). Double logarithmic slopes $d\log G'/d\omega$ from frequency sweeps were in the same range as values previously reported for milk yoghurts (Hassan et al., 2003) and ranged from 0.2 to 0.1 (Manuscripts II to IV, Table II 5 and Table IV 4). In combination with approximately parallel curves for G' and G'', this indicates only a slight dependency of storage and loss moduli G' and G'' on frequency. Generally, frequency independence of storage and loss moduli G' and G'' indicates true gel properties. However, this was unlikely to be the case for the investigated gels, as true gels are normally constituted from covalently bound components, but only hydrophobic and electrostatic interactions were found in Manuscript III. Moreover, similar rheological behaviour was previously described and categorised as weak gel behaviour for xanthan gel by Ross-Murphy and Shatwell. More precisely, they distinguished the weak gel properties of their

xanthan gels from strong gel behaviour via the extent of the linear viscoelastic regime. In this context, linear visco-elastic regimes up to intercycle deformations of at least 25% confirm strong gels, while weak gels usually begin to flow at intercycle strains below 5% (Ross-Murphy & Shatwell, 1993) which is still an order of magnitude higher than the results in this thesis and therefore confirms the weak gel nature of the investigated pea protein gels.

While the overall rheological behaviour including the loss factor tan δ was similar for all samples, absolute values of complex shear modulus |G*| and storage and loss moduli G' and G'' varied between the different Manuscripts as well as between individual samples in Manuscripts II and IV. In the introduction to Manuscript IV, the differences between the complex shear modulus |G*| of unfortified samples from Manuscript II (Table II 3) and storage modulus G' of unhydrolysed samples from Manuscript III (Table III 2), both at 10% protein content were initially ascribed to variations in the pH value during the pre-treatment step before fermentation. Results from Manuscript IV subsequently related this effect to pH dependent shifts in the ratios between newly generated soluble and insoluble aggregates upon heating of pea protein slurries during the pre-treatment step. Since only soluble aggregates are believed to contribute to network formation (Ringgenberg et al., 2013), the differences in storage modulus G' between individual samples in Manuscript IV could be correlated to the protein solubility after pre-treatment prior to fermentation (R = 0.892) and are related to the concentration of available protein. Additionally, insoluble aggregates may act as inactive fillers (Britten & Giroux, 2001) which do not interact with a protein network on a relevant scale, but may interfere with it to a certain extent, thus further enhancing the formation of weaker network structures in samples with a higher ratio of insoluble to soluble aggregates. The differences in storage moduli G' between samples as influenced by the concentration of available protein were reflected in different degrees of network crosslinking as derived from G' values at low frequencies (Mezger, 2006) and led to different intracycle rheological behaviour in large amplitude oscillatory shear experiments as extensively described in Manuscript IV. Moreover, pre-treatment at pH below pH 7.0 generated rheological properties similar to those of conventional milk yoghurts while maintaining an overall protein content of 10%. Thus, actively influencing the availability of protein for network formation can be considered a suitable approach for texture customisation.

Manuscript II investigated the impact of additional fortification with dietary fibre and oil rich in unsaturated fatty acids. In particular, the addition of dietary fibre significantly increased the complex shear modulus |G*| (Table II 3). Similar to the effect described regarding the concentration of available protein in Manuscript IV, this was mainly ascribed to the immobilisation of water by fibre and to the resulting increase in relative protein concentration in the remaining aqueous phase. Additionally, mechanical hooking and friction effects between individual fibres were found to have an impact at the beginning of fermentation but were negligible in the final gels, where pea protein provides the dominating network structure. Analogous with to the insoluble aggregates in Manuscript IV, fibres also act as inactive fillers. In both studies, a decrease in recovery properties after intense shearing indicates some structural impairments (Table II 4 and Table IV 4) despite overall dominating similar network properties as derived from tan δ values. However, while in Manuscript IV the effect of decreased protein concentration

and inactive fillers both weakened the network structures, the addition of dietary fibre in Manuscript II may not only enhance the complex shear modulus |G*| via immobilisation of water and subsequent increase in relative protein concentration, but may also decrease network properties by mechanical interference. However, even if this were the case, the overall effect of inactive filler properties was small compared to the effect of increased relative protein concentration and the protein network was found to be the overall dominating structure.

In contrast, fortification with rapeseed oil led to the incorporation of oil droplets into the protein network matrix as derived from Fig II 3d and the subsequent formation of filled emulsion gels. As described in Manuscript I and discussed above, the individual oil droplets in these gels were stabilised by an interfacial pea protein network structure that was of similar nature to the bulk network. Consequently, the emulsified oil droplets could easily be integrated into the gel network by a combination of electrostatic interactions between legumin-β and vicilin as well as by hydrophobic interactions that mainly involve the legumin fraction as described above for the formation of individual interfacial and bulk networks. Therefore, pea protein-based fermentation-induced bulk gels can easily be fortified with oil rich in unsaturated fatty acids without requiring additional emulsifiers or stabilisers.

Concluding remarks and outlook

Results from this thesis confirmed a general potential for the utilisation of pea protein as a raw material for the development of nutritionally valuable plant-derived yoghurt alternatives with a high protein content. Based on molecular and physico-chemical properties of pea protein, structuring mechanisms in fermentation-induced gels – including the types of interactions involved and the contribution of individual protein fractions – were thoroughly investigated, understood and extensively described for the first time. However, with every investigated research objective, further questions worth addressing arise. In this context, from a scientific point of view, further investigations into bulk gelation properties of fermentation-induced pea protein gels should focus on the determination of the fractal dimensions of those gels. Determination of fractal dimensions allows for the distinction between the contribution of intrafloc versus interfloc interactions in gel networks and therefore contributes to further advancing the general understanding of fermentation-induced pea protein gels. Furthermore, determination of fractal dimensions would be an interesting approach to gain even deeper insights into the impact of protein pre-treatment under different conditions (as described in manuscript IV) on the gel properties. More specifically, in gels made from pea protein pre-treated at lower pH values, a prevalence of interfloc interactions would be expected as indicated by the lower loss of elastic properties in these samples, while in gels prepared from protein pre-treated at higher pH values, dominating intrafloc interactions may be the cause of the almost complete loss of structure and the transition from predominantly elastic to predominantly plastic behaviour.

Results from the examination of interfacial properties revealed similarities to fermentation-induced bulk gels and therefore indicated the possibility to incorporate oil rich in unsaturated fatty acids for nutritional fortification without the addition of further emulsifiers or stabilisers. The similarities between interfacial and bulk gelation in this thesis were derived from different experimental setups, albeit under similar conditions. Therefore, future research should focus on the direct comparison of interfacial and bulk gelation properties for proof of concept purposes. Experiments for this purpose should focus on rheological behaviour including LAOS measurements and need to be carried out under identical conditions for both systems. Obtaining such conditions for both systems would require a very elaborate experimental design, as fermentation-induced bulk gelation is based on the pH shift during the structuring process, which would need to be simulated at the oil-water interface. In this context, implementation of a glucono-δ-lactone-based model system could be an option despite the deviations in the acidification rate, or alternatively, fermentation in the aqueous phase of the interfacial rheology can be considered. However, in this case, interference of the microorganisms with the interface need to be considered, or methods preventing such interference need to be developed. Regardless of these obstacles, such investigations would be a necessary step to more

elaborately determine similarities (and potential differences) in gelation behaviour of pea protein in bulk and at the interface.

The third objective in this thesis was achieved by applying the obtained fundamental knowledge on structuring behaviour to modify texture and nutritional properties towards an increase in prospective consumer acceptance. In this context, it was possible to incorporate dietary fibre and oil into the protein network structure and to determine processing conditions under which texture properties close to those of conventional milk yoghurts could be obtained. Variation of these conditions led to textures that can be utilised as a basis suitable for the future development of alternative products such as spreads or confectionary fillings. However, further investigations into the development of such products will be needed if additional ingredients like e.g. fruit preparations, chocolate, nuts, spices, dried or fresh vegetables, salt or sugar are to be added. More specifically, depending on their physico-chemical properties, these ingredients are expected to interact or interfere with the protein network, e.g. by formation of co-networks or incompatible structures, or by influencing environmental conditions like the pH value owing to buffering capacities or acidity of the ingredient itself. In this context, the formation of incompatible structures may lead to phase separation, while changes in pH value can influence the electrostatic properties of the protein and therefore impair the network formation.

Beyond the important contribution of the results from this thesis to the prospective development of pea protein-based yoghurt alternatives, further aspects well outside the scope of his thesis need to be considered on the way to market maturity. In this context, one of the key issues is the improvement of sensorial properties. More specifically, pea protein has a distinct beany off-flavour that leads to products with low sensorial acceptance. Literature connects this off-flavour to different chemical compounds such as bitterness-causing saponins, and volatiles such as alcohols, aldehydes and ketones (Heng, 2005) that develop during lipidoxidation. Therefore, various approaches for the improvement of the off-flavour – ranging from the interference with off-flavour-causing mechanisms and the removal of off-flavour substances to masking of the flavour – are described. However, so far none of these approaches has reached market maturity. Moreover, in most cases processes suitable to remove fat, lipoxygenases, saponins and volatile compounds from the pea protein impair the techno-functionality of the protein as a side effect. However, techno-functionality of commercially available pea protein is already limited in most cases, owing to the industrial scale extraction process. Since the limited techno-functionality of commercially available proteins must be considered as an additional major drawback on the way to market maturity of pea protein-based yoghurt alternatives, a further decrease of techno-functionality owing to the removal of the off-flavour must be avoided. Therefore, the acquisition of fundamental and detailed knowledge on interactions between sensorially undesirable components and pea protein is a topic that should be thoroughly approached in order to subsequently deduce customised processing parameters for a gentle removal of these components. At the same time, processing conditions at an industrial scale should be reconsidered with the preservation or improvement of techno-functionality in mind, in order to provide a flavour neutral, highly functional raw material as the basis for pea protein-based yoghurt alternatives and other pea protein-based products.

Acknowledgements

Sometimes it's good when people push you out of your comfort zone. So, I would like to thank my supervisor Prof. Drusch for persuading me to write this thesis. It ended up being an enjoyable endeavour that allowed me to look at my research in its entirety and to bring it all together in one extensive manuscript.

Since research is never just the work of an individual, I would like to thank all the people who contributed to the work in this thesis: Lina and Gerard for working with me during their bachelor thesis and internship respectively, Sarah, Karla, Christina, Marina, Lars and Mr. Nissen for their assistance during lab work, and Hanna, Monika and Prof. Drusch for all their advice, input and support – I have learned a lot in the past five years!

Every research needs funding. So, I thank the "Competence Cluster Nutrition Research" funded by the Federal Ministry of Education and Research, Germany (FKZ: 01EA1408C/ FKZ: 01EA1806C) for the financial support.

Further thanks goes to my family and friends for always being supportive, no matter what I do! Special thanks to my friends Julie and Jonathan for volunteering to proof-read this thesis.

Every thesis needs scientists that are willing to evaluate it. Therefore, I would like to thank Prof. Dr. Leonard Sagis, Prof. Dr. Anja Wagemans and my supervisor Prof. Dr. Stephan Drusch for their willingness to evaluate this thesis and Prof. Dr. Claudia Fleck for chairing the evaluation committee.

Last but not least, it is time to thank all my colleagues at the Department of Food Technology and Food Material Science at Technische Universität Berlin for making work such a pleasant and fun place to be.

References

Adal, E., Sadeghpour, A., Connell, S., Rappolt, M., Ibanoglu, E., & Sarkar, A. (2017). Heteroprotein Complex Formation of Bovine Lactoferrin and Pea Protein Isolate: A Multiscale Structural Analysis. *Biomacromolecules*, *18*(2), 625–635. https://doi.org/10.1021/acs.biomac.6b01857

Adler-Nissen, J. (1986). *Enzymatic hydrolysis of food proteins*. Elsevier Applied Science Publishers.

Akhtar, M., Stenzel, J., Murray, B. S., & Dickinson, E. (2005). Factors affecting the perception of creaminess of oil-in-water emulsions. *Food Hydrocolloids*, *19*(3), 521–526. https://doi.org/10.1016/j.foodhyd.2004.10.017

Aluko, R. E., Mofolasayo, O. A., & Watts, B. M. (2009). Emulsifying and foaming properties of commercial yellow pea (Pisum sativum L.) seed flours. *Journal of Agricultural and Food Chemistry*, *57*(20), 9793–9800. https://doi.org/10.1021/jf902199x

Amine, C., Dreher, J., Helgason, T., & Tadros, T. (2014). Investigation of emulsifying properties and emulsion stability of plant and milk proteins using interfacial tension and interfacial elasticity. *Food Hydrocolloids*, *39*, 180–186. https://doi.org/10.1016/j.foodhyd.2014.01.001

Aportela-Palacios, A., Sosa-Morales, M. E., & Vélez-Ruiz, J. F. (2005). Rheological and physicochemical behavior of fortified yogurt, with fiber and calcium. *Journal of Texture Studies*, *36*(3), 333–349. https://doi.org/10.1111/j.1745-4603.2005.00020.x

Avramenko, N. A., Low, N. H., & Nickerson, M. T. (2013). The effects of limited enzymatic hydrolysis on the physicochemical and emulsifying properties of a lentil protein isolate. *Food Research International*, *51*(1), 162–169. https://doi.org/10.1016/j.foodres.2012.11.020

Azim, Z., Alexander, M., Koxholt, M., & Corredig, M. (2010). Influence of cross-linked waxy maize starch on the aggregation behavior of casein micelles during acid-induced gelation. *Food Biophysics*, *5*(3), 227–237. https://doi.org/10.1007/s11483-010-9164-1

Banovic, M., Lähteenmäki, L., Arvola, A., Pennanen, K., Duta, D. E., Brückner-Gühmann, M., & Grunert, K. G. (2018). Foods with increased protein content: A qualitative study on European consumer preferences and perceptions. *Appetite*, *125*, 233–243. https://doi.org/10.1016/j.appet.2018.01.034

Barac, M., Cabrilo, S., Pesic, M., Stanojevic, S., Pavlicevic, M., Macej, O., & Ristic, N. (2011). Functional properties of pea (Pisum sativum, L.) protein isolates modified with chymosin. *International Journal of Molecular Sciences*, *12*(12), 8372–8387. https://doi.org/10.3390/ijms12128372

Barac, M., Cabrilo, S., Pesic, M., Stanojevic, S., Zilic, S., Macej, O., & Ristic, N. (2010). Profile and functional properties of seed proteins from six pea (Pisum sativum) genotypes. *International Journal of Molecular Sciences*, *11*(12), 4973–4990. https://doi.org/10.3390/ijms11124973

Barac, M., Cabrilo, S., Stanojevic, S., Pesic, M., Pavlicevic, M., Zlatkovic, B., & Jankovic, M. (2012). Functional properties of protein hydrolysates from pea (Pisum sativum, L) seeds. *International Journal of Food Science and Technology*, *47*(7), 1457–1467. https://doi.org/10.1111/j.1365-2621.2012.02993.x

Barac, M., Pesic, M., Stanojevic, S., Kostic, A., & Cabrilo, S. (2015). Techno-functional properties of pea (Pisum sativum) protein isolates-a review. *Acta Periodica Technologica*, *46*, 1–18. https://doi.org/10.2298/APT1546001B

Bateman, A., Martin, M. J., O'Donovan, C., Magrane, M., Alpi, E., Antunes, R., Bely, B., Bingley, M., Bonilla, C., Britto, R., Bursteinas, B., Bye-AJee, H., Cowley, A., Da Silva, A., De Giorgi, M., Dogan, T., Fazzini, F., Castro, L. G., Figueira, L., … Zhang, J. (2017). UniProt: The universal protein knowledgebase. *Nucleic Acids Research*, *45*(D1), D158–D169. https://doi.org/10.1093/nar/gkw1099

Ben-Harb, S., Panouillé, M., Huc-Mathis, D., Moulin, G., Saint-Eve, A., Irlinger, F., Bonnarme, P., Michon, C., & Souchon, I. (2018). The rheological and microstructural properties of pea, milk, mixed pea/milk gels and gelled emulsions designed by thermal, acid, and enzyme treatments. *Food Hydrocolloids*, *77*, 75–84. https://doi.org/10.1016/j.foodhyd.2017.09.022

Berghout, J. A. M., Boom, R. M., & van der Goot, A. J. (2015). Understanding the differences in gelling properties between lupin protein isolate and soy protein isolate. *Food Hydrocolloids*, *43*, 465–472. https://doi.org/10.1016/j.foodhyd.2014.07.003

Bhattacharjee, S. (2016). DLS and zeta potential - What they are and what they are not? *Journal of Controlled Release*, *235*, 337–351. https://doi.org/10.1016/j.jconrel.2016.06.017

Bhatty, R. S., & Christison, G. I. (1984). Composition and nutritional quality of pea (Pisum sativum L.) faba bean (Vicia faba L. spp. minor) and lentil (Lens culinaris Medik.) meals, protein concentrates and isolates. *Plant Foods for Human Nutrition*, *34*, 41–51.

BMEL. (2020). *https://www.bmel.de/DE/Landwirtschaft/Pflanzenbau/Ackerbau/_Texte/Eiweisspflanzenstrategie.html*. https://www.bmel.de/DE/Landwirtschaft/Pflanzenbau/Ackerbau/_Texte/Eiweisspflanzenstrategie.html

Bora, P. S., Brekke, C. J., & Powers, J. R. (1994). Heat Induced Gelation of Pea (Pisum sativum) Mixed Globulins, Vicilin and Legumin. *Journal of Food Science*, *59*(3), 594–596. https://doi.org/10.1111/j.1365-2621.1994.tb05570.x

Boulter, D. (1983). Protein composition of grains of the leguminosae. *Qualitas Plantarum Plant Foods for Human Nutrition*, *32*(3–4), 247–252. https://doi.org/10.1007/BF01091189

Bowen, W. R., Hall, N. J., Pan, L.-C., Sharif, A. O., & Williams, P. M. (1998). The relevance of particle size and zeta-potential in protein processing. *Nature Biotechnology*, *16*, 785–787.

Bown, D., Ellis, T., & Gatehouse, J. (1988). The sequence of a gene encoding convicilin from pea (Pisum sativum L.) shows that convicilin differs from vicilin by an insertion near the N -terminus. *Biochemical Journal*, *251*(3), 717–726. https://doi.org/10.1042/bj2510717

Boye, J. I., Aksay, S., Roufik, S., Ribéreau, S., Mondor, M., Farnworth, E., & Rajamohamed, S. H. (2010). Comparison of the functional properties of pea, chickpea and lentil protein concentrates processed using ultrafiltration and isoelectric precipitation techniques. *Food Research International*, *43*(2), 537–546. https://doi.org/10.1016/j.foodres.2009.07.021

Braudo, E. E., Danilenko, A. N., Guslyannikov, P. V., Kozhevnikov, G. O., Artykova, G. P., Lapteva, N. A., Vaintraub, I. A., Sironi, E., & Duranti, M. (2006). Comparative effects of limited tryptic hydrolysis on physicochemical and structural features of seed 11S globulins. *International Journal of Biological Macromolecules*, *39*(4–5), 174–178. https://doi.org/10.1016/j.ijbiomac.2005.12.006

Britten, M., & Giroux, H. J. (2001). Acid-induced gelation of whey protein polymers: Effects of pH and calcium concentration during polymerization. *Food Hydrocolloids*, *15*(4–6), 609–617. https://doi.org/10.1016/S0268-005X(01)00049-2

Brückner-Gühmann, M., Banovic, M., & Drusch, S. (2019). Towards an increased plant protein intake: Rheological properties, sensory perception and consumer acceptability of lactic acid fermented, oat-based gels. *Food Hydrocolloids*, *96*(May), 201–208. https://doi.org/10.1016/j.foodhyd.2019.05.016

Brückner-Gühmann, M., Benthin, A., & Drusch, S. (2019). Enrichment of yoghurt with oat protein fractions: Structure formation, textural properties and sensory evaluation. *Food Hydrocolloids*, *86*, 146–153. https://doi.org/10.1016/j.foodhyd.2018.03.019

Brückner-Gühmann, M., Heiden-Hecht, T., Sözer, N., & Drusch, S. (2018). Foaming characteristics of oat protein and modification by partial hydrolysis. *European Food Research and Technology*, *244*(12), 2095–2106. https://doi.org/10.1007/s00217-018-3118-0

Brückner-Gühmann, M., Vasil'eva, E., Culetu, A., Duta, D., Sozer, N., & Drusch, S. (2019). Oat protein concentrate as alternative ingredient for non-dairy yoghurt-type product. *Journal of the Science of Food and Agriculture*, *February*. https://doi.org/10.1002/jsfa.9858

Bučko, S., Katona, J., Popović, L., Vaštag, Ž., Petrović, L., & Vučiniće-Vasić, M. (2015). Investigation on solubility, interfacial and emulsifying properties of pumpkin (Cucurbita pepo) seed protein isolate. *LWT - Food Science and Technology*, *64*(2), 609–615. https://doi.org/10.1016/j.lwt.2015.06.054

Cairoli, S., Iametti, S., & Bonomi, F. (1994). Reversible and irreversible modifications of β-lactoglobulin upon exposure to heat. *Journal of Protein Chemistry*, *13*(3), 347–354. https://doi.org/10.1007/BF01901568

Cano-Sarmiento, C., Téllez-Medina, D. I., Viveros-Contreras, R., Cornejo-Mazón, M., Figueroa-Hernández, C. Y., García-Armenta, E., Alamilla-Beltrán, L., García, H. S., & Gutiérrez-López, G. F. (2018). Zeta Potential of Food Matrices. *Food Engineering Reviews*, *10*(3), 113–138. https://doi.org/10.1007/s12393-018-9176-z

Chang, C., Tu, S., Ghosh, S., & Nickerson, M. T. (2015). Effect of pH on the inter-relationships between the physicochemical, interfacial and emulsifying properties for pea, soy, lentil and canola protein isolates. *Food Research International*, *77*, 360–367. https://doi.org/10.1016/j.foodres.2015.08.012

Cheison, S. C., Schmitt, M., Leeb, E., Letzel, T., & Kulozik, U. (2010). Influence of temperature and degree of hydrolysis on the peptide composition of trypsin hydrolysates of β-lactoglobulin: Analysis by LC-ESI-TOF/MS. *Food Chemistry*, *121*(2), 457–467. https://doi.org/10.1016/j.foodchem.2009.12.065

Chen, J., & Dickinson, E. (1998). Viscoelastic properties of heat-set whey protein emulsion gels. *Journal of Texture Studies*, *29*(3), 285–304. https://doi.org/https://doi.org/10.1111/j.1745-4603.1998.tb00171.x

Chen, N., Zhao, M., Chassenieux, C., & Nicolai, T. (2016a). Structure of self-assembled native soy globulin in aqueous solution as a function of the concentration and the pH. *Food Hydrocolloids*, *56*, 417–424. https://doi.org/10.1016/j.foodhyd.2015.12.028

Chen, N., Zhao, M., Chassenieux, C., & Nicolai, T. (2016b). Thermal aggregation and gelation of soy globulin at neutral pH. *Food Hydrocolloids*, *61*, 740–746. https://doi.org/10.1016/j.foodhyd.2016.06.028

Cheng, Y. J., Thompson, L. D., & Brittin, H. C. (1990). Sogurt, a Yogurt-like Soybean Product: Development and Properties. *Journal of Food Science*, *55*(4), 1178–1179. https://doi.org/10.1111/j.1365-2621.1990.tb01631.x

Chumchuere, S., & Robinson, R. K. (1999). Selection of starter cultures for the fermentation of soya milk. *Food Microbiology*, *16*(2), 129–137. https://doi.org/10.1006/fmic.1998.0225

Clemente, A., Vioque, J., Sánchez-Vioque, R., Pedroche, J., Bautista, J., & Millán, F. (1999). Protein quality of chickpea (Cicer arietinum L.) protein hydrolysates. *Food Chemistry*, *67*(3), 269–274. https://doi.org/10.1016/S0308-8146(99)00130-2

Conde, J. M., Patino, J. M. R., Miñones J., C., & Rodríguez Patino, J. M. (2005). Rheological properties of hydrolysates of proteins from extracted sunflower flour adsorbed at the air-water interface. *Industrial and Engineering Chemistry Research*, *44*(20), 7761–7769. https://doi.org/10.1021/ie0506163

Corredig, M., Sharafbafi, N., & Kristo, E. (2011). Polysaccharide-protein interactions in dairy matrices, control and design of structures. *Food Hydrocolloids*, *25*(8), 1833–1841. https://doi.org/10.1016/j.foodhyd.2011.05.014

Crévieu, I., Carré, B., Chagneau, A.-M. M., Quillien, L., Guéguen, J., Bérot, S., Carré, B., Chagneau, A.-M. M., Quillien, L., Guéguen, J., & Bérot, S. (1997). Identification of Resistant Pea (Pisum sativum L.) Proteins in the Digestive Tract of Chickens. *Journal of Agricultural and Food Chemistry*, *45*(4), 1295–1300. https://doi.org/10.1021/jf960806b

Croy, R., Derbyshire, E., Krishna, T., & Boulter, D. (1979). Legumin of pisum sativum and vicia faba. *The New Phytologist*, 29–35.

Croy, R., Gatehouse, J., Evans, I., & Boulter, D. (1980). Characterisation of the storage protein subunits synthesised in vitro by polyribosomes and RNA from developing pea (Pisum sativum L.) - I. Legumin. *Planta*, *148*(1), 49–56. https://doi.org/10.1007/BF00385441

Croy, R., Gatehouse, J., Tyler, M., & Boulter, D. (1980). The purification and characterization of a third storage protein (convicilin) from the seeds of pea (Pisum sativum L.). *Biochemical Journal*, *191*(2), 509–516. https://doi.org/10.1042/bj1910509

Damian, C., & Olteanu, A. (2014). Influence of dietary fiber from pea on some quality characteristics of yoghurts. *Journal of Agroalimentary Processes and Technologies*, *20*(2), 156–160.

Damodaran, S. (2005). Protein Stabilization of Emulsions and Foams. *Journal of Food Science*, *70*(3), 54–66. https://doi.org/10.1111/j.1365-2621.2005.tb07111.x

Damodaran, S., & Kinsella, J. E. (1982). Effect of Conglycinin on the Thermal Aggregation of Glycinin. *Journal of Agricultural and Food Chemistry*, *30*(5), 812–817. https://doi.org/10.1021/jf00113a003

Damodaran, S., & Rao, C. S. (2001). Molecular Basis of Protein Adsorption at Fluid-Fluid Interfaces. In E. Dickinson & R. Miller (Eds.), *Food Colloids - Fundamentals of Formulation* (1st ed., pp. 165–180). The Royal Society of Chemistry.

Danielsson, C.-E. (1948). Seed globulins of the Gramineae and Leguminosae. *Biochemical Journal*, *44*(4), 387–400. https://doi.org/10.1042/bj0440387

Danielsson, C.-E. (1950). An Electrophoretic Investigation of Vicilin and legumin from Seeds of Peas. *Acta Chemica Scandinavica*, *4*, 762–771.

Day, L. (2013). Proteins from land plants - Potential resources for human nutrition and food security. *Trends in Food Science and Technology*, *32*(1), 25–42. https://doi.org/10.1016/j.tifs.2013.05.005

Delahaije, R. J. B. M., Gruppen, H., Giuseppin, M. L. F., & Wierenga, P. A. (2015). Towards predicting the stability of protein-stabilized emulsions. *Advances in Colloid and Interface Science*, *219*, 1–9. https://doi.org/10.1016/j.cis.2015.01.008

Denkova, Z., Yanakieva, V., Denkova, R., & Dobrev, I. (2015). *Examining the possibilities for application of pea milk in obtaining fermented probiotic foods*. *June*, 31–35.

Derakhshandeh, B., Kerekes, R. J., Hatzikiriakos, S. G., & Bennington, C. P. J. (2011). Rheology of pulp fibre suspensions: A critical review. *Chemical Engineering Science*, *66*(15), 3460–3470. https://doi.org/10.1016/j.ces.2011.04.017

Destatis. (2020). *Land- und Forstwirtschaft, Fischerei, Wachstum und Ernte - Feldfrüchte-*.

Dickinson, E. (2009). Hydrocolloids as emulsifiers and emulsion stabilizers. *Food Hydrocolloids*, *23*(6), 1473–1482. https://doi.org/10.1016/j.foodhyd.2008.08.005

Dickinson, E. (2011). Mixed biopolymers at interfaces: Competitive adsorption and multilayer structures. *Food Hydrocolloids*, *25*(8), 1966–1983. https://doi.org/10.1016/j.foodhyd.2010.12.001

Dickinson, E. (2012). Emulsion gels: The structuring of soft solids with protein-stabilized oil droplets. *Food Hydrocolloids*, *28*(1), 224–241. https://doi.org/10.1016/j.foodhyd.2011.12.017

Dickinson, E., & Chen, J. (1999). Heat-set whey protein emulsion gels: Role of active and inactive filler particles. *Journal of Dispersion Science and Technology*, *20*(1–2), 197–213. https://doi.org/10.1080/01932699908943787

DIN SPEC 91143-2. (2012).

DIN Technical Report No. 143. (2005).

Domenech, T., & Velankar, S. S. (2015). On the rheology of pendular gels and morphological developments in paste-like ternary systems based on capillary attraction. *Soft Matter*, *11*(8), 1500–1516. https://doi.org/10.1039/c4sm02053g

Donkor, O. N., Henriksson, A., Vasiljevic, T., & Shah, N. P. (2007). Rheological properties and sensory characteristics of set-type soy yogurt. *Journal of Agricultural and Food Chemistry*, *55*(24), 9868–9876. https://doi.org/10.1021/jf071050r

Doucet, D., Gauthier, S. F., Otter, D. E., & Foegeding, E. A. (2003). Enzyme-induced gelation of extensively hydrolyzed whey proteins by alcalase: peptide identification and determination of enzyme specificity. *Journal of Agricultural and Food Chemistry*, *51*(20), 6036–6042. c:%5CUsers%5Crgarcia.ERRC%5CDocuments%5CLiterature Review%5CDocuments%5C#604 plastein.pdf

Ducel, V., Richard, J., Popineau, Y., & Boury, F. (2004). Adsorption kinetics and rheological interfacial properties of plant proteins at the oil-water interface. *Biomacromolecules*, *5*(6), 2088–2093. https://doi.org/10.1021/bm049739h

Dziuba, J., Szerszunowicz, I., Nalecz, D., & Dziuba, M. (2014). Proteomic Analysis of Albumin and Globulin Fractions of Pea (Pisum Sativum L .) Seeds *. *Acta Scientarium Polonorum*, *13*(2), 181–190.

Espírito-Santo, A. P., Lagazzo, A., Sousa, A. L. O. P., Perego, P., Converti, A., & Oliveira, M. N. (2013). Rheology, spontaneous whey separation, microstructure and sensorial characteristics of probiotic yoghurts enriched with passion fruit fiber. *Food Research International*, *50*(1), 224–231. https://doi.org/10.1016/j.foodres.2012.09.012

European Commission. (2018). Report from the Commision to the Council and the European Parliament on the development of plant proteins in the European Union EN. In *European Commission* (Vol. 757). https://doi.org/10.1017/CBO9781107415324.004

European Food Safety Authority, & EFSA. (2010a). Scientific Opinion on Dietary Reference Values for carbohydrates and dietary fibe. *EFSA Journal*, *8*(3), 1–77. https://doi.org/10.2903/j.efsa.2010.1462.Available

European Food Safety Authority, & EFSA. (2010b). Scientific Opinion on Dietary Reference Values for fats, including saturated fatty acids, polyunsaturated fatty acids, monounsaturated fatty acids, trans fatty acids, and cholesterol. *EFSA Journal*, *8*(3), 1–107. https://doi.org/10.2903/j.efsa.2010.1461

Ewoldt, R. H., Hosoi, A. E., & McKinley, G. H. (2008). New measures for characterizing nonlinear viscoelasticity in large amplitude oscillatory shear. *Journal of Rheology*, *52*(6), 1427–1458. https://doi.org/10.1122/1.2970095

Ewoldt, R. H., Winter, P., Maxey, J., & McKinley, G. H. (2010). Large amplitude oscillatory shear of pseudoplastic and elastoviscoplastic materials. *Rheologica Acta*, *49*(2), 191–212. https://doi.org/10.1007/s00397-009-0403-7

Faber, T. J., Van Breemen, L. C. A., & McKinley, G. H. (2017). From firm to fluid – Structure-texture relations of filled gels probed under Large Amplitude Oscillatory Shear. *Journal of Food Engineering*, *210*, 1–18. https://doi.org/10.1016/j.jfoodeng.2017.03.028

Fennema, R. O. (2017). *Fennema's food Chemistry* (5th ed.).

Fernández García, E., & McGregor, J. U. (1997). Fortification of sweetened plain yogurt with insoluble dietary fiber. *Zeitschrift Für Lebensmittel-Untersuchung Und - Forschung*, *204*(6), 433–437. https://doi.org/10.1007/s002170050108

Ferragut, V., Cruz, N. S., Trujillo, A., Guamis, B., & Capellas, M. (2009). Physical characteristics during storage of soy yogurt made from ultra-high pressure homogenized soymilk. *Journal of Food Engineering*, *92*(1), 63–69. https://doi.org/10.1016/j.jfoodeng.2008.10.026

Foegeding, E. A. (2006). Food biophysics of protein gels: A challenge of nano and macroscopic proportions. *Food Biophysics*, *1*(1), 41–50. https://doi.org/10.1007/s11483-005-9003-y

Garcia-Mora, P., Peñas, E., Frias, J., Gomez, R., & Martinez-Villaluenga, C. (2015). High-pressure improves enzymatic proteolysis and the release of peptides with angiotensin i converting enzyme inhibitory and antioxidant activities from lentil proteins. *Food Chemistry*, *171*, 224–232. https://doi.org/10.1016/j.foodchem.2014.08.116

García Arteaga, V., Apéstegui Guardia, M., Muranyi, I., Eisner, P., & Schweiggert-Weisz, U. (2020). Effect of enzymatic hydrolysis on molecular weight distribution, techno-functional properties and sensory perception of pea protein isolates. *Innovative Food Science and Emerging Technologies*, *65*(February), 102449. https://doi.org/10.1016/j.ifset.2020.102449

Gatehouse, J., Croy, R., Morton, H., Tyler, M., & Boulter, D. (1981). Characterisation and Subunit Structures of the Vicilin Storage Proteins of Pea (Pisum sativum L.). *European Journal of Biochemistry*, *118*(3), 627–633. https://doi.org/10.1111/j.1432-1033.1981.tb05565.x

Gatehouse, J., Lycett, G., Croy, R., & Boulter, D. (1982). The post-translational proteolysis of the subunits of vicilin from pea (Pisum sativum L.). *Biochemical Journal*, *207*(3), 629–632. https://doi.org/10.1042/bj2070629

Gatehouse, J., Lycett, G., Delauney, A., Croy, R., & Boulter, D. (1983). Sequence specificity of the post- translational proteolytic cleavage of vicilin, a seed storage protein of pea (Pisum sativum L.). *Biochemical Journal*, *212*, 427–432.

Genovese, D. B., & Lozano, J. E. (2001). The effect of hydrocolloids on the stability and viscosity of cloudy apple juices. *Food Hydrocolloids*, *15*(1), 1–7. https://doi.org/10.1016/S0268-005X(00)00053-9

German, B., Damodaran, S., & Kinsella, J. E. (1982). Thermal Dissociation and Association Behavior of Soy Proteins. *Journal of Agricultural and Food Chemistry*, *30*(5), 807–811. https://doi.org/10.1021/jf00113a002

Gharsallaoui, A., Cases, E., Chambin, O., & Saurel, R. (2009). Interfacial and emulsifying characteristics of acid-treated pea protein. *Food Biophysics*, *4*(4), 273–280. https://doi.org/10.1007/s11483-009-9125-8

Grosso, C. R. ., & Rao, M. . (2002). Dynamic rheology of structure development in low-methoxyl pectin+Ca2++sugar gels1. *Food Hydrocolloids*, *12*(3), 357–363. https://doi.org/10.1016/s0268-005x(98)00034-4

Gruen, L. C., Guthrie, R. E., & Blagrove, R. J. (1987). Structure of a major pea seed albumin: Implication of a free sulphydryl group. *Journal of the Science of Food and Agriculture*, *41*(2), 167–178. https://doi.org/10.1002/jsfa.2740410210

Grygorczyk, A., & Corredig, M. (2013). Acid induced gelation of soymilk, comparison between gels prepared with lactic acid bacteria and glucono-δ-lactone. *Food Chemistry*, *141*(3), 1716–1721. https://doi.org/10.1016/j.foodchem.2013.03.096

Gu, X., Campbell, L. J., & Euston, S. R. (2009). Effects of different oils on the properties of soy protein isolate emulsions and gels. *Food Research International*, *42*(8), 925–932. https://doi.org/10.1016/j.foodres.2009.04.015

Gueguen, J., & Barbot, J. (1988). Quantitative and qualitative variability of pea (Pisum sativum L.) protein composition. *Journal of the Science of Food and Agriculture*, *42*(3), 209–224. https://doi.org/10.1002/jsfa.2740420304

Gueguen, J., Chevalier, M., Barbot, J., Schaeffer, F., And, J. B., & Schaeffer, F. (1988). Dissociation and aggregation of pea legumin induced by pH and ionic strength. *Journal of the Science of Food and Agriculture*, *44*(2), 167–182. https://doi.org/10.1002/jsfa.2740440208

Guo, S.-T., & Ono, T. (2006). The Role of Composition and Content of Protein Particles in Soymilk on Tofu Curding by Glucono-δ-lactone or Calcium Sulfate. *Journal of Food Science*, *70*(4), C258–C262. https://doi.org/10.1111/j.1365-2621.2005.tb07170.x

Guzmán-González, M., Morais, F., Ramos, M., & Amigo, L. (1999). Influence of skimmed milk concentrate replacement by dry dairy products in a low fat set-type yoghurt model system. I: Use of whey protein concentrates, milk protein concentrates and skimmed milk powder. *Journal of the Science of Food and Agriculture*, *79*(8), 1117–1122. https://doi.org/10.1002/(SICI)1097-0010(199906)79:8<1117::AID-JSFA335>3.3.CO;2-6

Hassan, A. N., Ipsen, R., Janzen, T., & Qvist, K. B. (2003). Microstructure and rheology of yogurt made with cultures differing only in their ability to produce exopolysaccharides. *Journal of Dairy Science*, *86*(5), 1632–1638. https://doi.org/10.3168/jds.S0022-0302(03)73748-5

Heng, L. (2005). Flavour Aspects of Pea and its Protein Preparations in Relation to Novel Protein Foods. In *PhD Thesis Wageningen University*.

Henning, T., Mothes, R., Dudek, S., & Schwenke, K. D. (1997). Structural and functional changes of faba bean legumin during super- limited tryptic hydrolysis. *Nahrung - Food*, *41*(2), 81–86.

Herbst, S. (2015). *Funktionalisierung von Erbsenprotein zum Einsatz in sprühgetrockneten Emulsionen*. Technische Universität Berlin.

Hickisch, A., Bindl, K., Vogel, R. F., & Toelstede, S. (2016). Thermal treatment of lupin-based milk alternatives – Impact on lupin proteins and the network of respective lupin-based yogurt alternatives. *Food Research International*, *89*, 850–859. https://doi.org/10.1016/j.foodres.2016.10.013

Higgins, T. J. V., Chandler, P. M., Randall, P. J., Spencer, D., Beach, L. R., Blagrove, R. J., Kortt, A. A., & Inglis, A. S. (1986). Gene structure, protein structure, and regulation of the synthesis of a sulfur-rich protein in pea seeds. *Journal of Biological Chemistry*, *261*(24), 11124–11130.

Hirose, M. (1993). Molten globule state of food proteins. *Trends in Food Science & Technology*, *4*, 48–51.

Hrckova, M., Rusnakova, M., & Zemanovic, J. (2009). Enzymatic Hydrolysis of Defatted Soy Flour by Three Different Proteases and their Effect on the Functional Properties of Resulting Protein Hydrolysates. *Czech Journal of Food Science*, *20*(1), 7–14. https://doi.org/10.3923/ajft.2009.226.240

Hsiao, L. C., Newman, R. S., Glotzer, S. C., & Solomon, M. J. (2012). Role of isostaticity and load-bearing microstructure in the elasticity of yielded colloidal gels. *Proceedings of the National Academy of Sciences of the United States of America*, *109*(40), 16029–16034. https://doi.org/10.1073/pnas.1206742109

https://www.uniprot.org/uniprot/P02857. (n.d.).

https://www.uniprot.org/uniprot/P13915. (n.d.).

https://www.uniprot.org/uniprot/P13918. (n.d.).

Hu, H., Fan, X., Zhou, Z., Xu, X., Fan, G., Wang, L., Huang, X., Pan, S., & Zhu, L. (2013). Acid-induced gelation behavior of soybean protein isolate with high intensity ultrasonic pre-treatments. *Ultrasonics Sonochemistry*, *20*(1), 187–195. https://doi.org/10.1016/j.ultsonch.2012.07.011

Humiski, L. M., & Aluko, R. E. (2007). Physicochemical and bitterness properties of enzymatic pea protein hydrolysates. *Journal of Food Science*, *72*(8). https://doi.org/10.1111/j.1750-3841.2007.00475.x

Hyun, K., Kim, S., Ahn, K., & Lee, S. (2002). Large amplitude oscillatory shear as a way to classify the complex fluids. *Journal of Non-Newtonian Fluid Mechanics*, *107*(1–3), 51–65. https://doi.org/10.4103/2319-4170.165000

Hyun, K., Wilhelm, M., Klein, C., Cho, K., Nam, J., Ahn, K., Lee, S., Ewoldt, R., & McKinley, G. (2011). A review of nonlinear oscillatory shear tests: Analysis and application of large amplitude oscillatory shear (LAOS). *Progress in Polymer Science (Oxford)*, *36*(12), 1697–1753. https://doi.org/10.1016/j.progpolymsci.2011.02.002

Karaca, A. C., Low, N., & Nickerson, M. (2011). Emulsifying properties of chickpea, faba bean, lentil and pea proteins produced by isoelectric precipitation and salt extraction. *Food Research International*, *44*(9), 2742–2750. https://doi.org/10.1016/j.foodres.2011.06.012

Karaca, A. C., Nickerson, M. T., & Low, N. H. (2011). Lentil and chickpea protein-stabilized emulsions: Optimization of emulsion formulation. *Journal of Agricultural and Food Chemistry*, *59*(24), 13203–13211. https://doi.org/10.1021/jf203028n

Karamac, M., Amarowicz, R., & Kostyra, H. (2018). Effect of temperature and enzyme/substrate ratio on the hydrolysis of pea protein isolates by trypsin. *Czech Journal of Food Sciences*, *20*(No. 1), 1–6. https://doi.org/10.17221/3502-cjfs

Karamac, M., Amarowicz, R., Kostyra, H., & Sijtsma, L. (1998). *Hydrolysis of pea protein isolate ' Pisane ' by trypsin (Short communication)*. *7*(September 1997), 69451.

Karleskind, D., Laye, I., Halpin, E., & Morr, C. V. (1991). Improving Acid Production in Soy-Based Yogurt by Adding Cheese Whey Proteins and Mineral Salts. *Journal of Food Science*, *56*(4), 999–1001. https://doi.org/10.1111/j.1365-2621.1991.tb14626.x

Kaspchak, E., Oliveira, M. A. S. de, Simas, F. F., Franco, C. R. C., Silveira, J. L. M., Mafra, M. R., & Igarashi-Mafra, L. (2017). Determination of heat-set gelation capacity of a quinoa protein isolate (Chenopodium quinoa) by dynamic oscillatory rheological analysis. *Food Chemistry*, *232*, 263–271. https://doi.org/10.1016/j.foodchem.2017.04.014

Keogh, M. K., & O'Kennedy, B. T. (1998). Rheology of Stirred Yogurt as Affected by Added Milk Fat, Protein and Hydrocolloids. *Journal of Food Science*, *63*(1), 108–112. https://doi.org/10.1111/j.1365-2621.1998.tb15687.x

Kerekes. (2006). Rheology of fibre suspensions in papermaking: An overview of recent research. *Nordic Pulp and Paper Research Journal*, *21*(05), 598–612. https://doi.org/10.3183/NPPRJ-2006-21-05-p598-612

Khechinashvili, N. N., Janin, J., & Rodier, F. (1995). Thermodynamics of the temperature-induced unfolding of globular proteins. *Protein Science*, *4*(7), 1315–1324. https://doi.org/10.1002/pro.5560040707

Kieserling, K., Vu, T. M., Drusch, S., & Schalow, S. (2019). Impact of pectin-rich orange fibre on gel characteristics and sensory properties in lactic acid fermented yoghurt. *Food Hydrocolloids*, *94*(February), 152–163. https://doi.org/10.1016/j.foodhyd.2019.02.051

Kim, H. J., Decker, E. A., & McClements, D. J. (2002). Impact of protein surface denaturation on droplet flocculation in hexadecane oil-in-water emulsions stabilized by β-lactoglobulin. *Journal of Agricultural and Food Chemistry*, *50*(24), 7131–7137. https://doi.org/10.1021/jf020366q

Kim, J. H. J., Varankovich, N. V., & Nickerson, M. T. (2016). The effect of pH on the gelling behaviour of canola and soy protein isolates. *Food Research International*, *81*, 31–38. https://doi.org/10.1016/j.foodres.2015.12.029

Klemmer, K. J., Waldner, L., Stone, A., Low, N. H., & Nickerson, M. T. (2012). Complex coacervation of pea protein isolate and alginate polysaccharides. *Food Chemistry*, *130*(3), 710–715. https://doi.org/10.1016/j.foodchem.2011.07.114

Klost, M., & Drusch, S. (2019a). Functionalisation of pea protein by tryptic hydrolysis – Characterisation of interfacial and functional properties. *Food Hydrocolloids*, *86*, 134–140. https://doi.org/10.1016/j.foodhyd.2018.03.013

Klost, M., & Drusch, S. (2019b). Structure formation and rheological properties of pea protein-based gels. *Food Hydrocolloids*, *94*(November 2018), 622–630. https://doi.org/10.1016/j.foodhyd.2019.03.030

Klost, M., Giménez-Ribes, G., & Drusch, S. (2020). Enzymatic hydrolysis of pea protein: Interactions and protein fractions involved in fermentation induced gels and their influence on rheological properties. *Food Hydrocolloids*, *105*, 105793. https://doi.org/10.1016/j.foodhyd.2020.105793

Kohyama, K., & Nishinari, K. (1993). Rheological Studies on the Gelation Process of Soybean 7S and 11S Proteins in the Presence of Glucono-δ-lactone. *Journal of Agricultural and Food Chemistry*, *41*(1), 8–14. https://doi.org/10.1021/jf00025a003

Kohyama, K., Sano, Y., & Doi, E. (1995). Rheological Characteristics and Gelation Mechanism of Tofu (Soybean Curd). *Journal of Agricultural and Food Chemistry*, *43*(7), 1808–1812. https://doi.org/10.1021/jf00055a011

Krajcovicova-Kudlackova, M., Babinska, K., & Valachovicova, M. (2005). Health benefits and risks of plant proteins. *Bratislavské Lekárske Listy*, *106*(6–7), 231–234.

Krämer, J. (1997). *Lebensmittel-Mikrobiologie* (3. Edition). Ulmer.

Krause, J. -P, & Schwenke, K. D. (1995). Changes in interfacial properties of legumin from faba beans (Vicia faba I.) by tryptic hydrolysis. *Food / Nahrung*, *39*(5–6), 396–405. https://doi.org/10.1002/food.19950390505

Krishna, T. G., Croy, R. R. D. D., Boulter, D., Krishina, T. G., Croy, R. R. D. D., & Boulter, D. (1979). Heterogeneity in subunit composition of the legumin of Pisum sativum. *Phytochemistry*, *18*(11), 1879–1880. https://doi.org/10.1016/0031-9422(79)83077-0

Kuipers, B. J. H., Van Koningsveld, G. A., Alting, A. C., Driehuis, F., Gruppen, H., & Voragen, A. G. J. (2005). Enzymatic hydrolysis as a means of expanding the cold gelation conditions of soy proteins. *Journal of Agricultural and Food Chemistry*, *53*(4), 1031–1038. https://doi.org/10.1021/jf048622h

Ladjal-Ettoumi, Y., Boudries, H., Chibane, M., & Romero, A. (2016). Pea, Chickpea and Lentil Protein Isolates: Physicochemical Characterization and Emulsifying Properties. *Food Biophysics*, *11*(1), 43–51. https://doi.org/10.1007/s11483-015-9411-6

Lamsal, B. P., Jung, S., & Johnson, L. A. (2007). Rheological properties of soy protein hydrolysates obtained from limited enzymatic hydrolysis. *LWT - Food Science and Technology*, *40*(7), 1215–1223. https://doi.org/10.1016/j.lwt.2006.08.021

Lee, S.-Y., Morr, C. V, & Seo, A. (1990). Comparison of Milk-Based and Soymilk-Based Yogurt. *Journal of Food Science*, *55*(2), 532–536.

Lee, W. J., & Lucey, J. A. (2010). Formation and physical properties of yoghurt. *Asian-Australasian Journal of Animal Science*, *23*(9), 1127–1136. https://doi.org/10.5713/ajas.2010.r.05

Li, F., Kong, X., Zhang, C., & Hua, Y. (2012). Gelation behaviour and rheological properties of acid-induced soy protein-stabilized emulsion gels. *Food Hydrocolloids*, *29*(2), 347–355. https://doi.org/10.1016/j.foodhyd.2012.03.011

Liang, H. N., & Tang, C. H. (2013). PH-dependent emulsifying properties of pea [Pisum sativum (L.)] proteins. *Food Hydrocolloids*, *33*(2), 309–319. https://doi.org/10.1016/j.foodhyd.2013.04.005

Lin, D. Q., Brixius, P. J., Hubbuch, J. J., Thömmes, J., & Kula, M. R. (2003). Biomass/adsorbent electrostatic interactions in expanded bed adsorption: A zeta potential study. *Biotechnology and Bioengineering*, *83*(2), 149–157. https://doi.org/10.1002/bit.10654

Liu, F., & Tang, C. H. (2011). Cold, gel-like whey protein emulsions by microfluidisation emulsification: Rheological properties and microstructures. *Food Chemistry*, *127*(4), 1641–1647. https://doi.org/10.1016/j.foodchem.2011.02.031

Liu, Q., Bao, H., Xi, C., & Miao, H. (2014). Rheological characterization of tuna myofibrillar protein in linear and nonlinear viscoelastic regions. *Journal of Food Engineering*, *121*(1), 58–63. https://doi.org/10.1016/j.jfoodeng.2013.08.016

Lucey, J. A., & Singh, H. (1997). Formation and physical properties of acid milk gels: A review. *Food Research International*, *30*(7), 529–542. https://doi.org/10.1016/S0963-9969(98)00015-5

Lycett, G., Delauney, A., Gatehouse, J., Gilroy, J., & Croy, R. (1983). The vicilin gene family of pea (Pisum sativum L.): a complete cDNA coding sequence fo preprovicilin. *Nucleic Acids Research*, *11*(8), 2367–2380.

Ma, Z., Boye, J. I., & Hu, X. (2017). In vitro digestibility, protein composition and techno-functional properties of Saskatchewan grown yellow field peas (Pisum sativum L.) as affected by processing. *Food Research International*, *92*, 64–78. https://doi.org/10.1016/j.foodres.2016.12.012

Ma, Z., Boye, J. I., Simpson, B. K., Prasher, S. O., Monpetit, D., & Malcolmson, L. (2011). Thermal processing effects on the functional properties and microstructure of lentil, chickpea, and pea flours. *Food Research International*, *44*(8), 2534–2544. https://doi.org/10.1016/j.foodres.2010.12.017

Mäkinen, O. E., Zannini, E., & Arendt, E. K. (2015). Modifying the Cold Gelation Properties of Quinoa Protein Isolate: Influence of Heat-Denaturation pH in the Alkaline Range. *Plant Foods for Human Nutrition*, *70*(3), 250–256. https://doi.org/10.1007/s11130-015-0487-4

Mäkinen, O. E., Zannini, E., Koehler, P., & Arendt, E. K. (2016). Heat-denaturation and aggregation of quinoa (Chenopodium quinoa) globulins as affected by the pH value. *Food Chemistry*, *196*, 17–24. https://doi.org/10.1016/j.foodchem.2015.08.069

Makri, E., Papalamprou, E., & Doxastakis, G. (2005). Study of functional properties of seed storage proteins from indigenous European legume crops (lupin, pea, broad bean) in admixture with polysaccharides. *Food Hydrocolloids*, *19*(3), 583–594. https://doi.org/10.1016/j.foodhyd.2004.10.028

McCann, T. H., Fabre, F., & Day, L. (2011). Microstructure, rheology and storage stability of low-fat yoghurt structured by carrot cell wall particles. *Food Research International*, *44*(4), 884–892. https://doi.org/10.1016/j.foodres.2011.01.045

McClements, D. J. (2004). Protein-stabilized emulsions. *Current Opinion in Colloid and Interface Science*, *9*(5), 305–313. https://doi.org/10.1016/j.cocis.2004.09.003

McClements, D. J. (2007). Critical review of techniques and methodologies for characterization of emulsion stability. *Critical Reviews in Food Science and Nutrition*, *47*(7), 611–649. https://doi.org/10.1080/10408390701289292

McClements, D. J. (2016). *Food Emulsions Principles, Practices and Techniques* (3rd ed.). CRC Press Taylor&Francis Group.

Meinlschmidt, P., Schweiggert-Weisz, U., & Eisner, P. (2016). Soy protein hydrolysates fermentation: Effect of debittering and degradation of major soy allergens. *LWT - Food Science and Technology*, *71*, 202–212. https://doi.org/10.1016/j.lwt.2016.03.026

Mermet-Guyennet, M. R. B., Gianfelice de Castro, J., & Habibi, M. (2014). LAOS: The strain softening/strain hardening paradox. *Journal of Rheology*, *59*(21). https://doi.org/https://doi.org/10.1122/1.4902000

Mermet-Guyennet, M. R. B., Gianfelice de Castro, J., Habibi, M., Martzel, N., Denn, M. M., & Bonn, D. (2015). LAOS: The strain softening/strain hardening paradox. *Journal of Rheology*, *59*(1), 21–32. https://doi.org/10.1122/1.4902000

Mession, J. L., Chihi, M. L., Sok, N., & Saurel, R. (2015). Effect of globular pea proteins fractionation on their heat-induced aggregation and acid cold-set gelation. *Food Hydrocolloids*, *46*, 233–243. https://doi.org/10.1016/j.foodhyd.2014.11.025

Mezger, T. (2006). *Das Rheologie Handbuch* (2nd ed.). Vincentz Network GmbH & Co. KG.

Mezzenga, R., & Fischer, P. (2013). The self-assembly, aggregation and phase transitions of food protein systems in one, two and three dimensions. *Reports on Progress in Physics*, *76*(4). https://doi.org/10.1088/0034-4885/76/4/046601

Miriani, M., Keerati-u-rai, M., Corredig, M., Iametti, S., & Bonomi, F. (2011). Denaturation of soy proteins in solution and at the oil-water interface: A fluorescence study. *Food Hydrocolloids*, *25*(4), 620–626. https://doi.org/10.1016/j.foodhyd.2010.07.020

Morris, E. R., Nishinari, K., & Rinaudo, M. (2012). Gelation of gellan - A review. *Food Hydrocolloids*, *28*(2), 373–411. https://doi.org/10.1016/j.foodhyd.2012.01.004

Murray, B. S., & Dickinson, E. (1996). Interfacial Rheology and the Dynamic Properties of Adsorbed Films of Food Proteins and Surfactants. *Food Science and Technology International*, *2*(3), 131–145.

Ng, T. S. K., McKinley, G. H., & Ewoldt, R. H. (2011). Large amplitude oscillatory shear flow of gluten dough: A model power-law gel. *Journal of Rheology*, *55*(3), 627–654. https://doi.org/10.1122/1.3570340

Nieto-Nieto, T., Wang, Y., Ozimek, L., & Chen, L. (2014). Effects of partial hydrolysis on structure and gelling properties of oat globular proteins. *Food Research International*, *55*, 418–425. https://doi.org/10.1016/j.foodres.2013.11.038

Nishinari, K., Fang, Y., Guo, S., & Phillips, G. O. (2014). Soy proteins: A review on composition, aggregation and emulsification. *Food Hydrocolloids*, *39*, 301–318. https://doi.org/10.1016/j.foodhyd.2014.01.013

O'Kane, F. (2004). *Molecular Characterisation and Heat - Induced Gelation of Pea Vicilin and Legumin*. Wageningen University and Research.

O'Kane, F., Happe, R., Vereijken, J., Gruppen, H., & Van Boekel, M. (2004a). Characterization of Pea Vicilin. 1. Denoting Convicilin as the α-Subunit of the Pisum Vicilin Family. *Journal of Agricultural and Food Chemistry*, *52*(10), 3141–3148. https://doi.org/10.1021/jf035104i

O'Kane, F., Happe, R., Vereijken, J., Gruppen, H., & Van Boekel, M. (2004b). Characterization of Pea Vicilin. 2. Consequences of Compositional Heterogeneity on Heat-Induced Gelation Behavior. *Journal of Agricultural and Food Chemistry*, *52*(10), 3149–3154. https://doi.org/10.1021/jf035105a

O'Kane, F., Happe, R., Vereijken, J., Gruppen, H., & Van Boekel, M. (2004c). Heat-induced gelation of pea legumin: Comparison with soybean glycinin. *Journal of Agricultural and Food Chemistry*, *52*(16), 5071–5078. https://doi.org/10.1021/jf035215h

O'Kane, F., Vereijken, J., Gruppen, H., & van Boekel, M. (2005). Gelation behavior of protein isolates extracted from 5 cultivars of Pisum sativum L. *Journal of Food Science*, *70*(2), C132-137. https://doi.org/10.1111/j.1365-2621.2005.tb07073.x

Ochenduszko, A., & Buckin, V. (2010). Real-time monitoring of heat-induced aggregation of β-lactoglobulin in aqueous solutions using high-resolution ultrasonic spectroscopy. *International Journal of Thermophysics*, *31*(1), 113–130. https://doi.org/10.1007/s10765-010-0705-0

Ochiai, K., Kamata, Y., & Shibasaki, K. (1982). Effect of tryptic digestion on emulsifying properties of soy protein. *Agricultural and Biological Chemistry*, *46*(1), 91–96. https://doi.org/10.1080/00021369.1982.10865031

Panyam, D., & Kilara, A. (1996). Enhancing the functionality of food proteins by enzymatic modification. *Trends in Food Science and Technology*, *7*(4), 120–125. https://doi.org/10.1016/0924-2244(96)10012-1

Papalamprou, E. M., Doxastakis, G. I., Biliaderis, C. G., & Kiosseoglou, V. (2009). Influence of preparation methods on physicochemical and gelation properties of chickpea protein isolates. *Food Hydrocolloids*, *23*(2), 337–343. https://doi.org/10.1016/j.foodhyd.2008.03.006

Park, J. D., & Ahn, K. H. (2013). Structural evolution of colloidal gels at intermediate volume fraction under start-up of shear flow. *Soft Matter*, *9*(48), 11650–11662. https://doi.org/10.1039/c3sm52090k

Park, J. D., Ahn, K. H., & Lee, S. J. (2015). Structural change and dynamics of colloidal gels under oscillatory shear flow. *Soft Matter*, *11*(48), 9262–9272. https://doi.org/10.1039/c5sm01651g

Peng, W., Kong, X., Chen, Y., Zhang, C., Yang, Y., & Hua, Y. (2016). Effects of heat treatment on the emulsifying properties of pea proteins. *Food Hydrocolloids*, *52*, 301–310. https://doi.org/10.1016/j.foodhyd.2015.06.025

Peng, X., & Guo, S. (2015). Texture characteristics of soymilk gels formed by lactic fermentation: A comparison of soymilk prepared by blanching soybeans under different temperatures. *Food Hydrocolloids*, *43*, 58–65. https://doi.org/10.1016/j.foodhyd.2014.04.034

Peters, J. P. C. M., Vergeldt, F. J., Boom, R. M., & van der Goot, A. J. (2017). Water-binding capacity of protein-rich particles and their pellets. *Food Hydrocolloids*, *65*, 144–156. https://doi.org/10.1016/j.foodhyd.2016.11.015

Petruccelli, S., & Añón, M. C. (1995). Thermal Aggregation of Soy Protein Isolates. *Journal of Agricultural and Food Chemistry*, *43*(12), 3035–3041. https://doi.org/10.1021/jf00060a009

Piorkowski, D. T., & McClements, D. J. (2014). Beverage emulsions: Recent developments in formulation, production, and applications. *Food Hydrocolloids*, *42*, 5–41. https://doi.org/10.1016/j.foodhyd.2013.07.009

Plumb, G. W., Carr, H. J., Newby, V. K., & Lambert, N. (1989). A study of the trypsinolysis of pea 11 S globulin. *Biochimica et Biophysica Acta (BBA)/Protein Structure and Molecular*, *999*(3), 281–288. https://doi.org/10.1016/0167-4838(89)90010-1

Plumb, G. W., & Lambert, N. (1990). A comparison of the trypsinolysis products of nine 11S globulin species. *Topics in Catalysis*, *3*(6), 465–473. https://doi.org/10.1016/S0268-005X(09)80224-5

Precha-Atsawanan, S., Uttapap, D., & Sagis, L. M. C. (2018). Linear and nonlinear rheological behavior of native and debranched waxy rice starch gels. *Food Hydrocolloids*, *85*(June), 1–9. https://doi.org/10.1016/j.foodhyd.2018.06.050

Rao, C. S., & Damodaran, S. (2000). Is surface pressure a measure of interfacial water activity? Evidence from protein adsorption behavior at interfaces. *Langmuir*, *16*(24), 9468–9477. https://doi.org/10.1021/la0007168

Razumovsky, L., & Damodaran, S. (1999). Surface Activity - Compressibility Relationship of Proteins at the Air - Water Interface. *Langmuir*, *9*, 1392–1399.

Renkema, J., Knabben, J., & van Vliet, T. (2001). Gel formation by b -conglycinin and glycinin and their mixtures. *Food Hydrocolloids*, *15*, 407–414.

Ringgenberg, E., Alexander, M., & Corredig, M. (2013). Effect of concentration and incubation temperature on the acid induced aggregation of soymilk. *Food Hydrocolloids*, *30*(1), 463–469. https://doi.org/10.1016/j.foodhyd.2012.05.011

Robins, M. M., Watson, A. D., & Wilde, P. J. (2002). Emulsions - Creaming and rheology. *Current Opinion in Colloid and Interface Science*, *7*(5–6), 419–425. https://doi.org/10.1016/S1359-0294(02)00089-4

Ross-Murphy, S. B. (1995). Rheological Characterisation of Gels. *Journal of Texture Studies*, *26*(4), 391–400. https://doi.org/10.1111/j.1745-4603.1995.tb00979.x

Ross-Murphy, S. B., & Shatwell, K. P. (1993). Polysaccharide strong and weak gels. *Biorheology*, *30*(3–4), 217–227. https://doi.org/10.3233/BIR-1993-303-407

Ruiz, G. A., Xiao, W., Van Boekel, M., Minor, M., & Stieger, M. (2016). Effect of extraction pH on heat-induced aggregation, gelation and microstructure of protein isolate from quinoa (Chenopodium quinoa Willd). *Food Chemistry*, *209*, 203–210. https://doi.org/10.1016/j.foodchem.2016.04.052

Sah, B. N. P., Vasiljevic, T., McKechnie, S., & Donkor, O. N. (2016). Physicochemical, textural and rheological properties of probiotic yogurt fortified with fibre-rich pineapple peel powder during refrigerated storage. *LWT - Food Science and Technology*, *65*, 978–986. https://doi.org/10.1016/j.lwt.2015.09.027

Sanz, T., Salvador, A., Jiménez, A., & Fiszman, S. M. (2008). Yogurt enrichment with functional asparagus fibre. Effect of fibre extraction method on rheological properties, colour, and sensory acceptance. *European Food Research and Technology*, *227*(5), 1515–1521. https://doi.org/10.1007/s00217-008-0874-2

Schneider, C. A., Rasband, W. S., & Eliceiri, K. W. (2012). NIH Image to ImageJ: 25 years of image analysis. *Nature America*, *9*, 671–675.

Schroeder, H. E. (1982). Quantitative studies on the cotyledonary proteins in the genus Pisum. *Journal of the Science of Food and Agriculture*, *33*(7), 623–633. https://doi.org/10.1002/jsfa.2740330707

Schwenke, K. D. (2001). Reflections about the functional potential of legume proteins: A review. *Nahrung - Food*, *45*(6), 377–381. https://doi.org/10.1002/1521-3803(20011001)45:6<377::AID-FOOD377>3.0.CO;2-G

Schwenke, K. D., Henning, T., Dudek, S., Dautzenberg, H., Danilenko, A., Kozhevnikov, G., & Braudo, E. (2001). Limited tryptic hydrolysis of pea legumin: Molecular mass and conformational stability of legumin-T. *International Journal of Biological Macromolecules*, *28*(2), 175–182. https://doi.org/10.1016/S0141-8130(00)00167-7

Sendra, E., Kuri, V., Fernández-López, J., Sayas-Barberá, E., Navarro, C., & Pérez-Alvarez, J. A. (2010). Viscoelastic properties of orange fiber enriched yogurt as a function of fiber dose, size and thermal treatment. *LWT - Food Science and Technology*, *43*(4), 708–714. https://doi.org/10.1016/j.lwt.2009.12.005

Sengupta, T., Razumovsky, L., & Damodaran, S. (1999). Energetics of protein-interface interactions and its effect on protein adsorption. *Langmuir*, *15*(20), 6991–7001. https://doi.org/10.1021/la990235s

Shand, P. J., Ya, H., Pietrasik, Z., & Wanasundara, P. K. J. P. D. (2007). Physicochemical and textural properties of heat-induced pea protein isolate gels. *Food Chemistry*, *102*(4), 1119–1130. https://doi.org/10.1016/j.foodchem.2006.06.060

Sijtsma, L., Tezera, D., Hustinx, J., & Vereijken, J. M. M. (1998). Improvement of pea protein quality by enzymatic modification. *Nahrung - Food*, *42*(3–4), 215–216. https://doi.org/10.1002/(sici)1521-3803(199808)42:03/04<215::aid-food215>3.3.co;2-1

Soral-Smietana, M., Swigon, A., Amarowicz, R., & Sijtsama, L. (1998). The solubility of trypsin pea protein hydrolysates (Short communication). *Nahrung*, *42*(03–04), 217–218. https://doi.org/10.1002/(SICI)1521-3803(199808)4210.1002/(SICI)1521-3803(199808)42:03/04<217::AID-FOOD217>3.0.CO;2-2

Sosulski, F. W., & McCurdy, A. R. (1987). Functionality of Flours, Protein Fractions and Isolates from Field Peas and Faba Bean. *Journal of Food Science*, *52*(4), 1010–1014. https://doi.org/10.1111/j.1365-2621.1987.tb14263.x

Stone, A. K., Karalash, A., Tyler, R. T., Warkentin, T. D., & Nickerson, M. T. (2015). Functional attributes of pea protein isolates prepared using different extraction methods and cultivars. *Food Research International*, *76*(P1), 31–38. https://doi.org/10.1016/j.foodres.2014.11.017

Subirade, M., Gueguen, J., & Pézolet, M. (1994). Conformational changes upon dissiciation of a globular protein from pea: a Fourier transform infrared spectroscopy study. *Biochimica et Biophysica Acta*, *1205*, 239–247.

Sun, X. D., & Arntfield, S. D. (2010). Gelation properties of salt-extracted pea protein induced by heat treatment. *Food Research International*, *43*(2), 509–515. https://doi.org/10.1016/j.foodres.2009.09.039

Sun, X. D., & Arntfield, S. D. (2011a). Dynamic oscillatory rheological measurement and thermal properties of pea protein extracted by salt method: Effect of pH and NaCl. *Journal of Food Engineering*, *105*(3), 577–582. https://doi.org/10.1016/j.jfoodeng.2011.03.008

Sun, X. D., & Arntfield, S. D. (2011b). Gelation properties of salt-extracted pea protein isolate catalyzed by microbial transglutaminase cross-linking. *Food Hydrocolloids*, *25*(1), 25–31. https://doi.org/10.1016/j.foodhyd.2010.05.002

Sun, X. D., & Arntfield, S. D. (2012). Molecular forces involved in heat-induced pea protein gelation: Effects of various reagents on the rheological properties of salt-extracted pea protein gels. *Food Hydrocolloids*, *28*(2), 325–332. https://doi.org/10.1016/j.foodhyd.2011.12.014

Swanson, B. G. (1990). Pea and Lentil Protein Extraction and Functionality. *Journal of the American Oil Chemists' Society*, *67*(5), 276–280.

Tamm, F., Gies, K., Diekmann, S., Serfert, Y., Strunskus, T., Brodkorb, A., & Drusch, S. (2015). Whey protein hydrolysates reduce autoxidation in microencapsulated long chain polyunsaturated fatty acids. *European Journal of Lipid Science and Technology*, *117*(12), 1960–1970. https://doi.org/10.1002/ejlt.201400574

Tamm, F., Herbst, S., Brodkorb, A., & Drusch, S. (2016). Functional properties of pea protein hydrolysates in emulsions and spray-dried microcapsules. *Food Hydrocolloids*, *58*, 204–214. https://doi.org/10.1016/j.foodhyd.2016.02.032

Tan, S. H., Mailer, R. J., Blanchard, C. L., Agboola, S. O., & Day, L. (2014). Gelling properties of protein fractions and protein isolate extracted from Australian canola meal. *Food Research International*, *62*(October 2016), 819–828. https://doi.org/10.1016/j.foodres.2014.04.055

Tang, C. H., Chen, L., & Foegeding, E. (2011). Mechanical and water-holding properties and microstructures of soy protein isolate emulsion gels induced by CaCl2, glucono-δ-lactone (GDL), and transglutaminase: Influence of thermal treatments before and/or after emulsification. *Journal of Agricultural and Food Chemistry*, *59*(8), 4071–4077. https://doi.org/10.1021/jf104834m

Tang, C. H., & Liu, F. (2013). Cold, gel-like soy protein emulsions by microfluidization: Emulsion characteristics, rheological and microstructural properties, and gelling mechanism. *Food Hydrocolloids*, *30*(1), 61–72. https://doi.org/10.1016/j.foodhyd.2012.05.008

Thanh, V. H., & Shibasaki, K. (1976). Major Proteins of Soybean Seeds. A Straightforward Fractionation and Their Characterization. *Journal of Agricultural and Food Chemistry*, *24*(6), 1117–1121. https://doi.org/10.1021/jf60208a030

Tsoukala, A., Papalamprou, E., Makri, E., Doxastakis, G., & Braudo, E. E. (2006). Adsorption at the air-water interface and emulsification properties of grain legume protein derivatives from pea and broad bean. *Colloids and Surfaces B: Biointerfaces*, *53*(2), 203–208. https://doi.org/10.1016/j.colsurfb.2006.08.019

Tsumura, K., Saito, T., Tsuge, K., Ashida, H., Kugimiya, W., & Inouye, K. (2005). Functional properties of soy protein hydrolysates obtained by selective proteolysis. *LWT - Food Science and Technology*, *38*(3), 255–261. https://doi.org/10.1016/j.lwt.2004.06.007

Tzitzikas, E. N., Vincken, J. P., De Groot, J., Gruppen, H., & Visser, R. G. F. (2006). Genetic variation in pea seed globulin composition. *Journal of Agricultural and Food Chemistry*, *54*(2), 425–433. https://doi.org/10.1021/jf0519008

Utsumi, S., & Kinsella, J. E. (1985). Forces Involved in Soy Protein Gelation: Effects of Various Reagents on the Formation, Hardness and Solubility of Heat-Induced Gels Made from 7S, 11S, and Soy Isolate. *Journal of Food Science*, *50*(5), 1278–1282. https://doi.org/10.1111/j.1365-2621.1985.tb10461.x

Wan, Z., Yang, X., & Sagis, L. M. C. (2016). Nonlinear Surface Dilatational Rheology and Foaming Behavior of Protein and Protein Fibrillar Aggregates in the Presence of Natural Surfactant. *Langmuir*, *32*(15), 3679–3690. https://doi.org/10.1021/acs.langmuir.6b00446

Wang, B., Wang, L., Li, D., Wei, Q., & Adhikari, B. (2012). The rheological behavior of native and high-pressure homogenized waxy maize starch pastes. *Carbohydrate Polymers*, *88*(2), 481–489. https://doi.org/10.1016/j.carbpol.2011.12.028

Wang, C. H., & Damodaran, S. (1990). Thermal Gelation of Globular Proteins: Weight-Average Molecular Weight Dependence of Gel Strength. *Journal of Agricultural and Food Chemistry*, *38*(5), 1157–1164. https://doi.org/10.1021/jf00095a001

Wang, H. L., Kraidej, L., & Hesseltine, C. W. (1974). Lactic acid fermentation of soybean milk. *J.Milk Food Technol.*, *37*(2), 71–73. https://doi.org/10.4315/0022-2747-37.2.71

Wang, J., Zhao, M., Yang, X., & Jiang, Y. (2006). Improvement on functional properties of wheat gluten by enzymatic hydrolysis and ultrafiltration. *Journal of Cereal Science*, *44*(1), 93–100. https://doi.org/10.1016/j.jcs.2006.04.002

WHO. (2013). Draft action plan for the prevention and control of noncommunicable diseases 2013 – 2020 Report by the Secretariat. *Report by the Secretariat*, *April*, 1–50.

Wilde, P., Mackie, A., Husband, F., Gunning, P., & Morris, V. (2004). Proteins and emulsifiers at liquid interfaces. *Advances in Colloid and Interface Science*, *108–109*, 63–71. https://doi.org/10.1016/j.cis.2003.10.011

Yamagishi, T., Miyakawa, A., Noda, N., & Yamauchi, F. (1983). Isolation and Electrophoretic Analysis of Heat-induced Products of Mixed Soybean 7S and 11S Globulins. *Agricultural and Biological Chemistry*, *47*(6), 1229–1237. https://doi.org/10.1271/bbb1961.47.1229

Yang, C., Wang, Y., & Chen, L. (2017). Fabrication, characterization and controlled release properties of oat protein gels with percolating structure induced by cold gelation. *Food Hydrocolloids*, *62*, 21–34. https://doi.org/10.1016/j.foodhyd.2016.07.023

Yang, C., Wang, Y., Vasanthan, T., & Chen, L. (2014). Impacts of pH and heating temperature on formation mechanisms and properties of thermally induced canola protein gels. *Food Hydrocolloids*, *40*, 225–236. https://doi.org/10.1016/j.foodhyd.2014.03.011

Yarranton, H. W., Sztukowski, D. M., & Urrutia, P. (2007). Effect of interfacial rheology on model emulsion coalescence. I. Interfacial rheology. *Journal of Colloid and Interface Science*, *310*(1), 246–252. https://doi.org/10.1016/j.jcis.2007.01.071

Yazici, F., Alvarez, V. B., & Hansen, P. M. T. (1997). Fermentation and properties of calcium-fortified soy milk yogurt. *Journal of Food Science*, *62*(3), 457–461. https://doi.org/10.1111/j.1365-2621.1997.tb04406.x

Yousseef, M., Lafarge, C., Valentin, D., Lubbers, S., & Husson, F. (2016). Fermentation of cow milk and/or pea milk mixtures by different starter cultures: Physico-chemical and sensorial properties. *LWT - Food Science and Technology*, *69*, 430–437. https://doi.org/10.1016/j.lwt.2016.01.060

Zannini, E., Jeske, S., Lynch, K., & Arendt, E. K. (2018). Development of novel quinoa-based yoghurt fermented with dextran producer Weissella cibaria MG1. *International Journal of Food Microbiology*, *268*(January), 19–26. https://doi.org/10.1016/j.ijfoodmicro.2018.01.001

Zare, F., Boye, J. I., Champagne, C. P., Orsat, V., & Simpson, B. K. (2013). Probiotic Milk Supplementation with Pea Flour: Microbial and Physical Properties. *Food and Bioprocess Technology*, *6*(5), 1321–1331. https://doi.org/10.1007/s11947-012-0828-3

Zhai, J., Miles, A. J., Pattenden, L. K., Lee, T. H., Augustin, M. A., Wallace, B. A., Aguilar, M. I., & Wooster, T. J. (2010). Changes in β-lactoglobulin conformation at the oil/water interface of emulsions studied by synchrotron radiation circular dichroism spectroscopy. *Biomacromolecules*, *11*(8), 2136–2142. https://doi.org/10.1021/bm100510j

Appendix

Supplementary material to Manuscript II

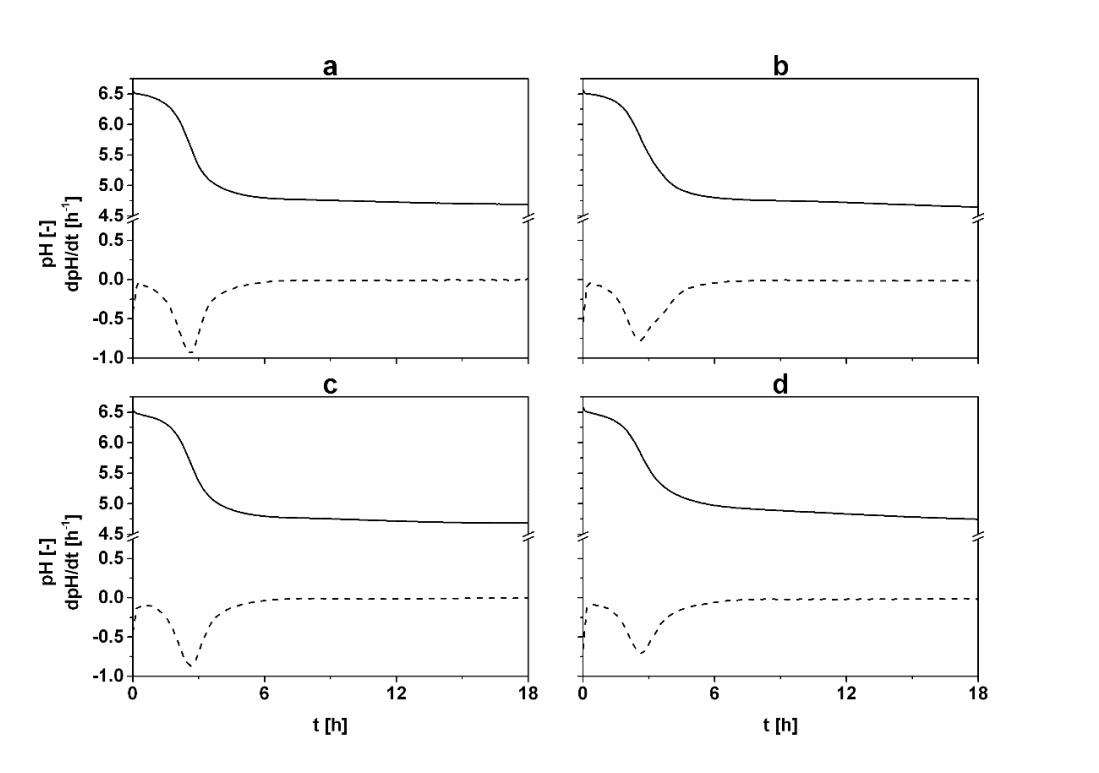

Fig A 1 development of pH (a) over time during the fermentation process of samples containing protein only (a), protein and oil (b), protein and fibre (c) and protein, oil and fibre (d). Development of the parameters (closed lines) is shown alongside their first derivations (dashed lines).

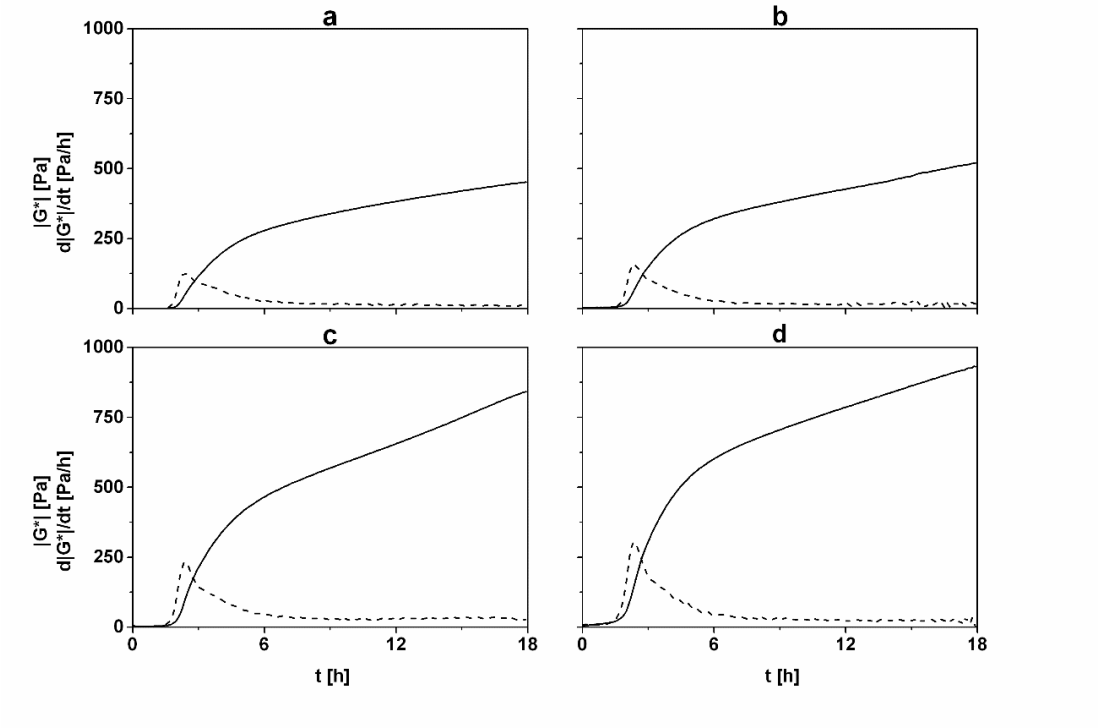

Fig A 2 development of complex shear modulus |G| over time during the fermentation process of samples containing protein only (a), protein and oil (b), protein and fibre (c) and protein, oil and fibre (d). Development of the parameters (closed lines) is shown alongside their first derivations (dashed lines).*

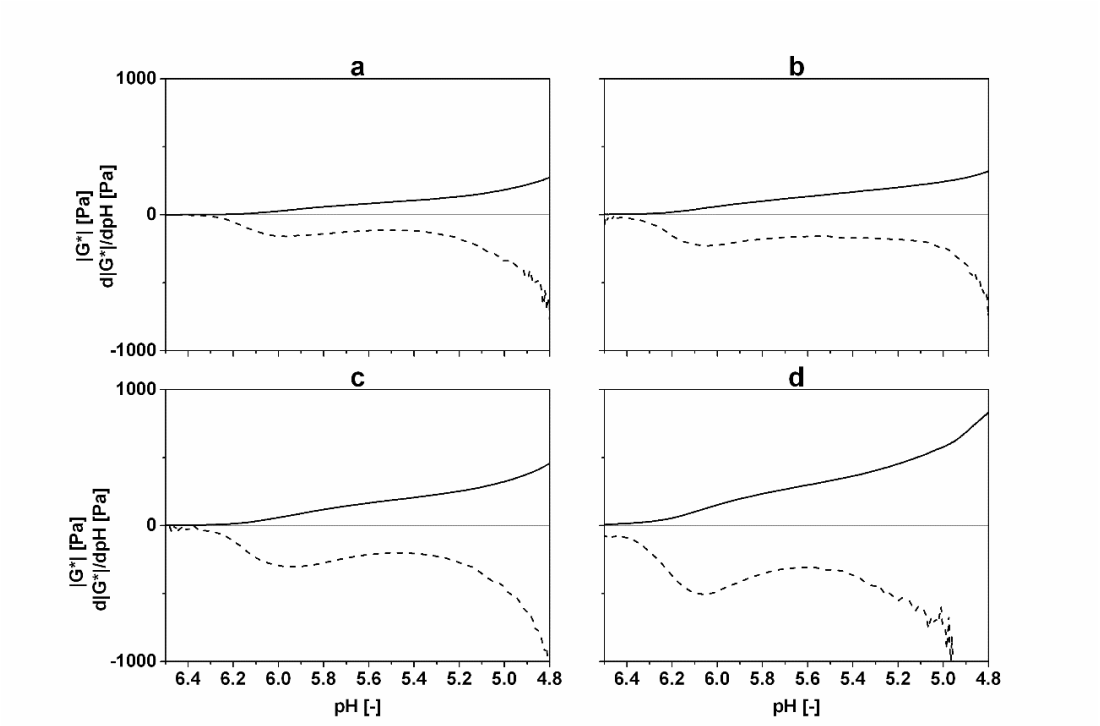

Fig A 3 development of |G| over pH during the fermentation process of samples containing protein only (a), protein and oil (b), protein and fibre (c) and protein, oil and fibre (d). Development of the parameters (closed lines) is shown alongside their first derivations (dashed lines).*

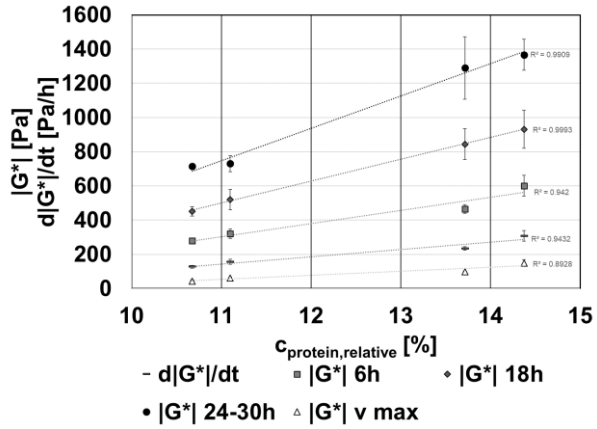

Fig A 4 correlation between relative protein concentration and $d|G^*|/dt_{max}$ as well as $|G^*|$ at different times of fermentation and resting.

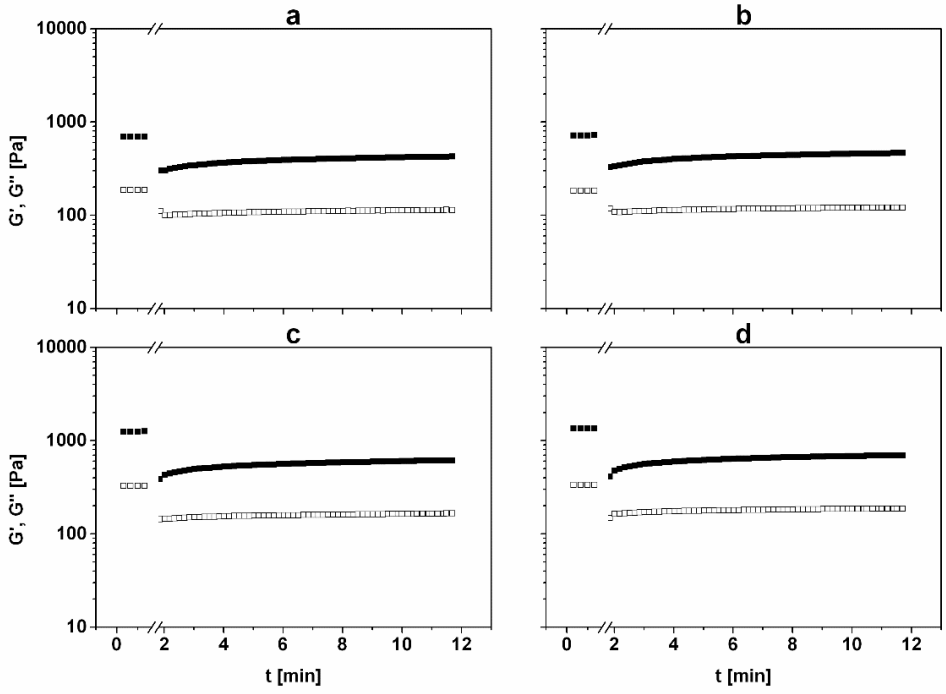

Fig A 5 Thixotropy test of fermented of samples containing protein only (a), protein and oil (b), protein and fibre (c) and protein, oil and fibre (d)after 24-30 h storage (6 °C)., (■ G', □ G'').

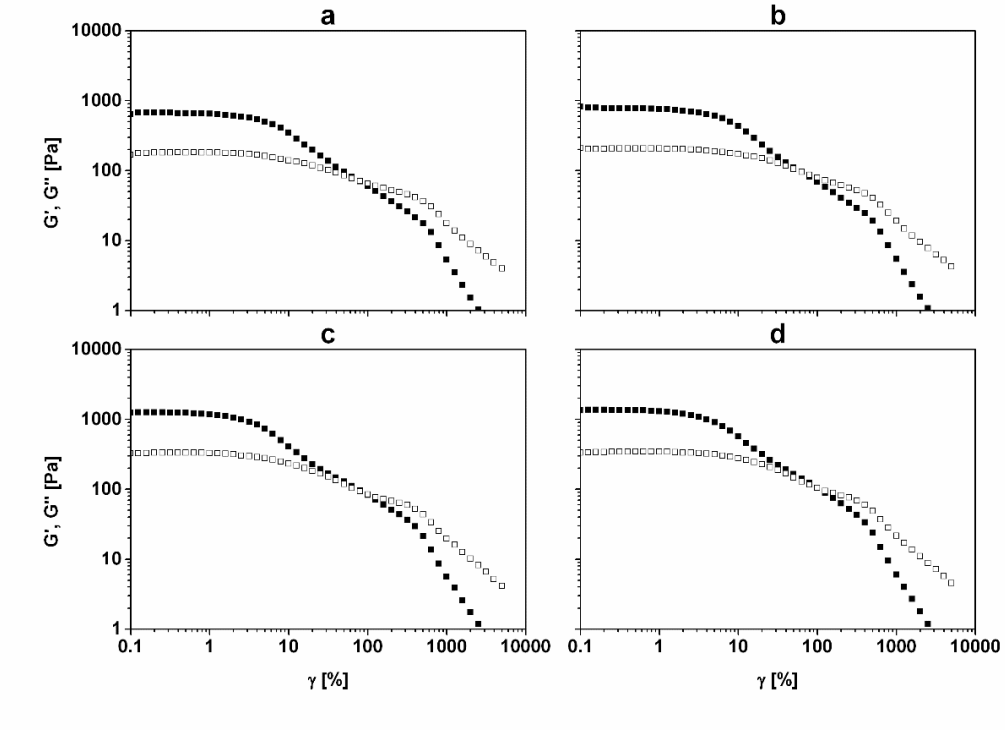

Fig A 6 amplitude sweeps of fermented of samples containing protein only (a), protein and oil (b), protein and fibre (c) and protein, oil and fibre (d)after 24-30 h storage (6 °C)., (■G', □G'').

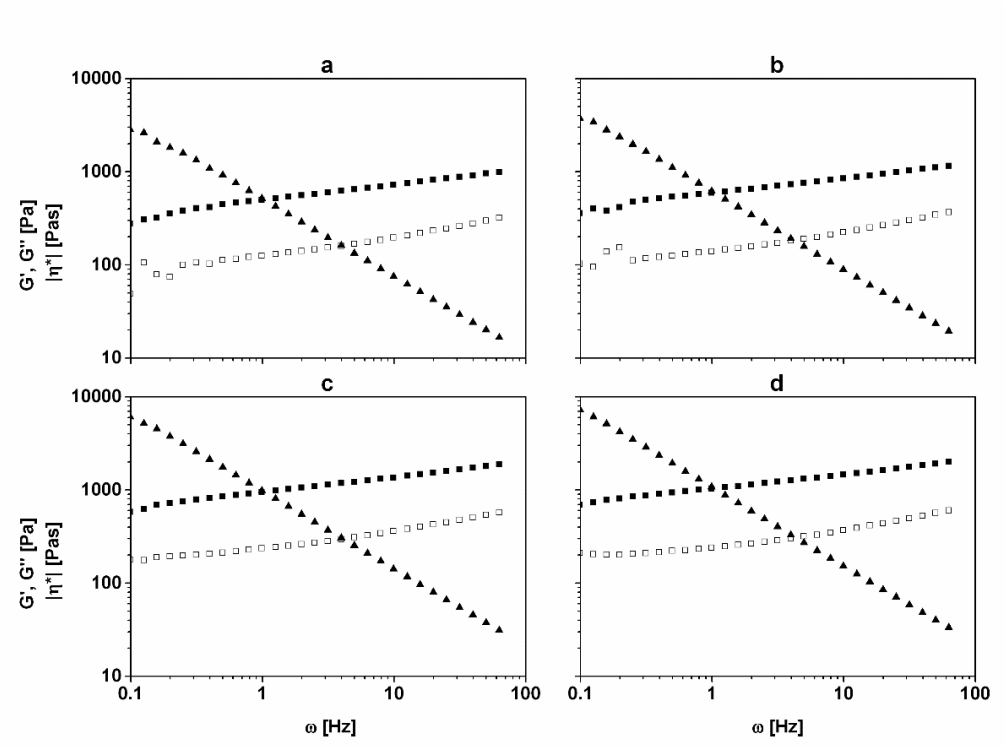

Fig A 7 frequency sweeps of fermented of samples containing protein only (a), protein and oil (b), protein and fibre (c) and protein, oil and fibre (d)after 24-30 h storage (6 °C)., (■G', □G'' ▲ |η|).*

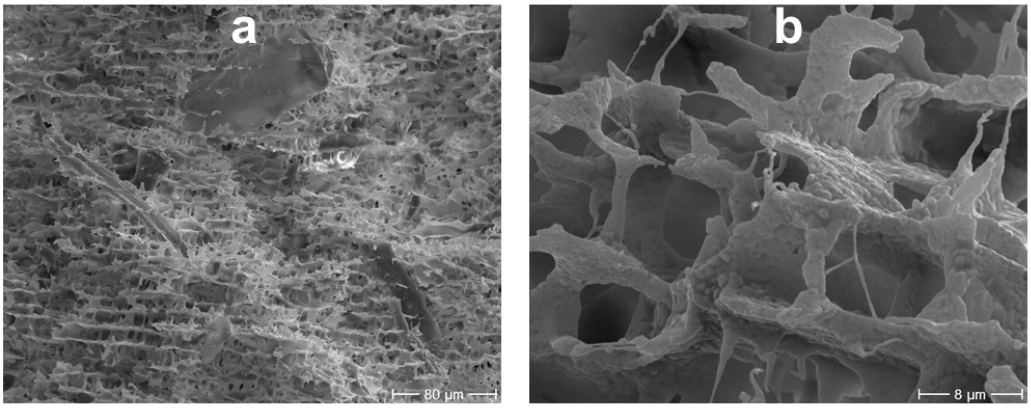

Fig A 8 SEM images of samples containing oil and fibre at 300-fold (a) and 3000-fold (b) magnification.

Supplementary material to Manuscript IV

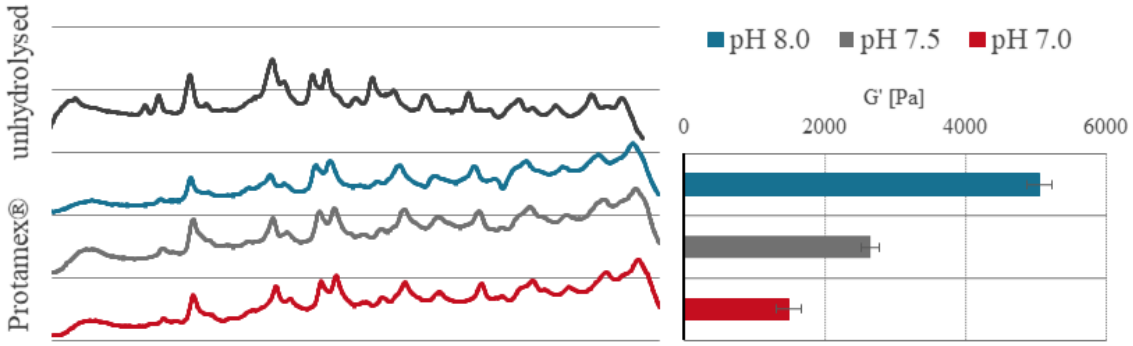

Fig A 9 molecular weight profile of pea protein (black) and pea protein hydrolysed with Protamex® under different pH conditions (blue: pH 8.0, grey: pH 7.5, red: pH 7.0) and storage moduli of the corresponding fermentation induced gels

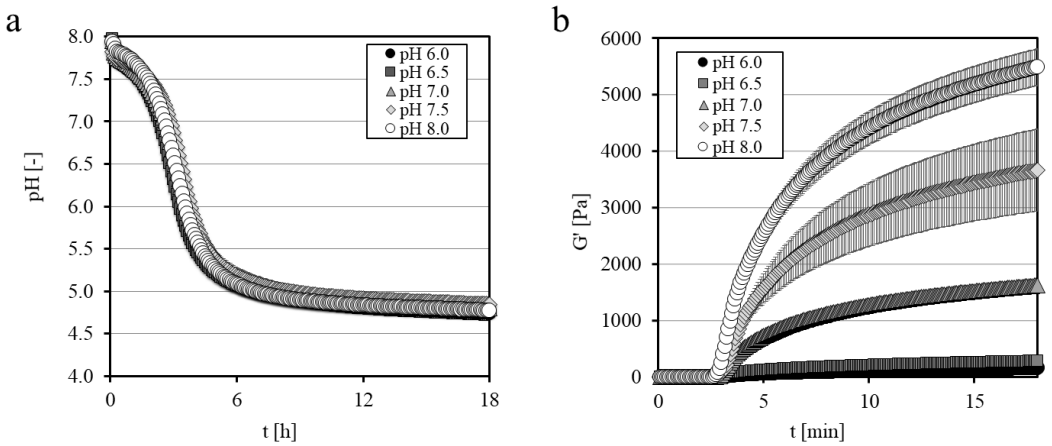

Fig A 10 pH-drop (a) and increase of G' (b) during fermentation of pea protein preheated at different pH-values.

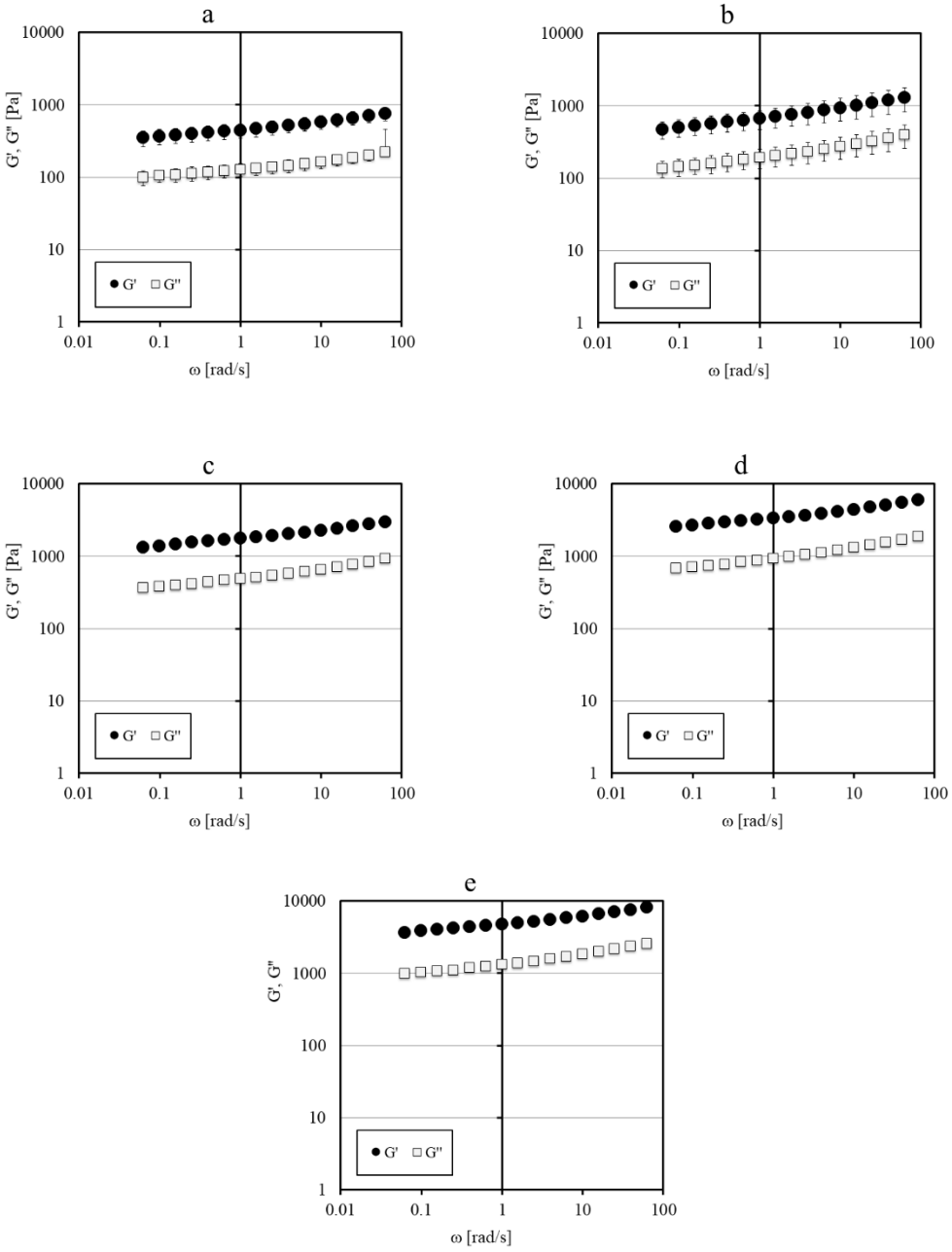

Fig A 11 G' and G'' in frequency sweeps pH 6.0 (a), pH 6.5 (b), pH 7.0 (c), pH 7.5 (d), pH 8.0 (e)

Unpublished data from Manuscript III

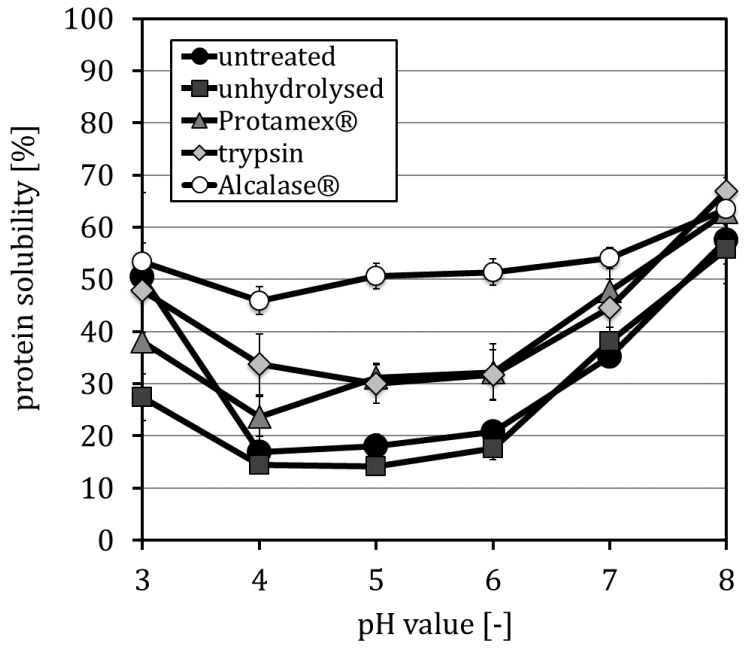

Fig A 12 protein solubility of untreated, unhydrolysed pea protein and pea protein hydrolysed with different enzymes (Protamex®, trypsin® and Alcalase®).

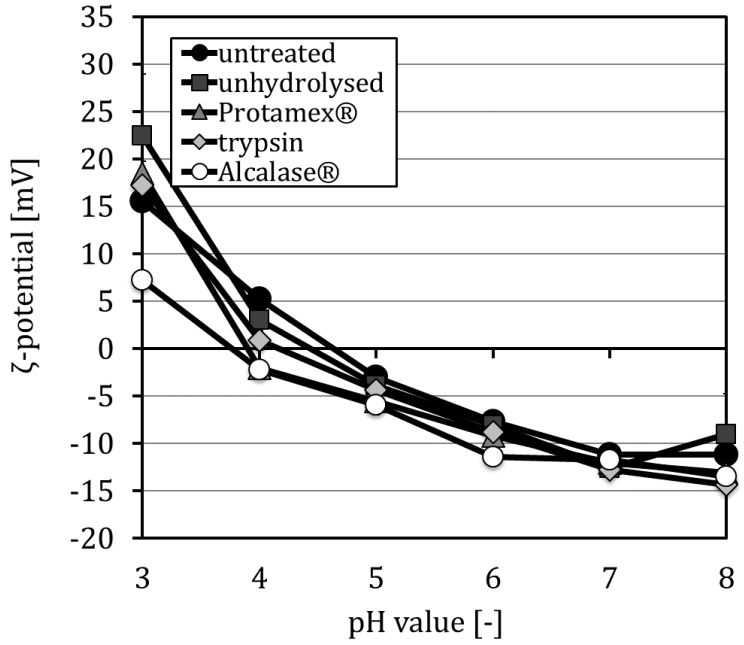

Fig A 13 ζ-potential of untreated or unhydrolysed pea protein and pea protein hydrolysed with different enzymes (Protamex®, trypsin® and Alcalase®).